...To become a star you need to be good, ambitious
and consider the "constrictions" of your life...

Stephen C. Woods

International Doctorate Program in Molecular Oncology and Endocrinology
Doctorate School in Molecular Medicine

XXII cycle - 2006–2009
Coordinator: Prof. Giancarlo Vecchio

"The transcription complex Prep1-Pbx1 regulates the gene expression of tyrosine phosphatases and impairs insulin action in liver cells"

Salvatore Iovino

University of Naples Federico II
Dipartimento di Biologia e Patologia Cellulare e Molecolare
"L. Califano"

Administrative Location

Dipartimento di Biologia e Patologia Cellulare e Molecolare "L. Califano"
Università degli Studi di Napoli Federico II

Partner Institutions

Italian Institutions

Università degli Studi di Napoli "Federico II", Naples, Italy
Istituto di Endocrinologia ed Oncologia Sperimentale "G. Salvatore", CNR, Naples, Italy
Seconda Università di Napoli, Naples, Italy
Università degli Studi di Napoli "Parthenope", Naples, Italy
Università del Sannio, Benevento, Italy
Università di Genova, Genoa, Italy
Università di Padova, Padua, Italy
Università degli Studi "Magna Graecia", Catanzaro, Italy
Università degli Studi di Firenze, Florence, Italy
Università degli Studi di Bologna, Bologna, Italy
Università degli Studi del Molise, Campobasso, Italy
Università degli Studi di Torino, Turin, Italy
Università di Udine, Udine, Italy

Foreign Institutions

Université Libre de Bruxelles, Brussels, Belgium
Universidade Federal de Sao Paulo, Brazil
University of Turku, Turku, Finland
Université Paris Sud XI, Paris, France
University of Madras, Chennai, India
University Pavol Jozef Šafàrik, Kosice, Slovakia
Universidad Autonoma de Madrid, Centro de Investigaciones Oncologicas (CNIO), Spain
Johns Hopkins School of Medicine, Baltimore, MD, USA
Johns Hopkins Krieger School of Arts and Sciences, Baltimore, MD, USA
National Institutes of Health, Bethesda, MD, USA
Ohio State University, Columbus, OH, USA
Albert Einstein College of Medicine of Yeshiwa University, N.Y., USA

Supporting Institutions

Ministero dell'Università e della Ricerca
Associazione Leonardo di Capua, Naples, Italy
Dipartimento di Biologia e Patologia Cellulare e Molecolare "L. Califano", Università degli Studi di Napoli "Federico II", Naples, Italy
Istituto Superiore di Oncologia (ISO), Genoa, Italy
Università Italo-Francese, Torino, Naples, Italy
Università degli Studi di Udine, Udine, Italy
Agenzia Spaziale Italiana
Istituto di Endocrinologia ed Oncologia Sperimentale "G. Salvatore", CNR, Naples, Italy

Italian Faculty

Giancarlo Vecchio, MD, Co-ordinator
Salvatore Maria Aloj, MD
Francesco Saverio Ambesi Impiombato, MD
Francesco Beguinot, MD
Maria Teresa Berlingieri, MD
Angelo Raffaele Bianco, MD
Bernadette Biondi, MD
Francesca Carlomagno, MD
Gabriella Castoria, MD
Angela Celetti, MD
Mario Chiariello, MD
Lorenzo Chiariotti, MD
Vincenzo Ciminale, MD
Annamaria Cirafici, PhD
Annamaria Colao, MD
Alma Contegiacomo, MD
Sabino De Placido, MD
Gabriella De Vita, MD
Monica Fedele, PhD
Pietro Formisano, MD
Alfredo Fusco, MD
Michele Grieco, MD
Massimo Imbriaco, MD
Paolo Laccetti, PhD
Antonio Leonardi, MD
Paolo Emidio Macchia, MD
Barbara Majello, PhD
Rosa Marina Melillo, MD
Claudia Miele, PhD
Francesco Oriente, MD
Roberto Pacelli, MD
Giuseppe Palumbo, PhD
Silvio Parodi, MD
Nicola Perrotti, MD
Giuseppe Portella, MD
Giorgio Punzo, MD
Antonio Rosato, MD
Guido Rossi, MD
Giuliana SalvatoreMD,
Massimo Santoro, MD
Giampaolo Tortora, MD
Donatella Tramontano, PhD
Giancarlo Troncone, MD
Giuseppe Viglietto, MD
Roberta Visconti, MD
Mario Vitale, MD

Foreign Faculty

Université Libre de Bruxelles, Belgium
Gilbert Vassart, MD
Jacques E. Dumont, MD

Universidade Federal de Sao Paulo, Brazil
Janete Maria Cerutti, PhD
Rui Monteiro de Barros Maciel, MD PhD

University of Turku, Turku, Finland
Mikko Laukkanen, PhD

Université Paris Sud XI, Paris, France
Martin Schlumberger, MD
Jean Michel Bidart, MD

University of Madras, Chennai, India
Arasambattu K. Munirajan, PhD

University Pavol Jozef Šafàrik, Kosice, Slovakia
Eva Cellárová, PhD
Peter Fedoročko, PhD

Universidad Autonoma de Madrid - Instituto de Investigaciones Biomedicas, Spain
Juan Bernal, MD, PhD
Pilar Santisteban, PhD

Centro de Investigaciones Oncologicas, Spain
Mariano Barbacid, MD

Johns Hopkins School of Medicine, USA
Vincenzo Casolaro, MD
Pierre A. Coulombe, PhD
James G. Herman MD
Robert P. Schleimer, PhD

Johns Hopkins Krieger School of Arts and Sciences, USA
Eaton E. Lattman, MD

National Institutes of Health, Bethesda, MD, USA
Michael M. Gottesman, MD
J. Silvio Gutkind, PhD
Genoveffa Franchini, MD
Stephen J. Marx, MD
Ira Pastan, MD
Phillip Gorden, MD

Ohio State University, Columbus, OH, USA
Carlo M. Croce, MD
Ginny L. Bumgardner, MD PhD

Albert Einstein College of Medicine of Yeshiwa University, N.Y., USA
Luciano D'Adamio, MD
Nancy Carrasco, MD

“The transcription complex Prep1-Pbx1 regulates the gene expression of tyrosine phosphatases and impairs insulin action in liver cells”

TABLE OF CONTENTS

LIST OF PUBLICATIONS

This dissertation is based upon the following publications:

Perfetti A, Oriente F, Iovino S, Alberobello AT, Barbagallo APM, Esposito I, Fiory F, Teperino R, Ungaro P, Miele C, Formisano P, Begiunot F. Phorbol esters induce intracellular accumalation of the antiapoptotic protein PED/PEA-15 by preventing ubiquitinylation and proteasomal degradation. J Biol Chem 2007 Mar 23;282:8648-57

Oriente F, Fernandez Diaz LC, Miele C, Iovino S, Mori S, Diaz VE, Troncone G, Cassese A., Formisano P, Blasi F, Beguinot F. Prep1 deficiency induces protection from diabetes and increased insulin sensitivity through a p160-mediated mechanism. Mol Cel Biol. 2008 Sep;28:5634-45.

Oriente F*. Iovino S.*, Cassese A., Romano C., Miele C., Troncone G., Balletta M., Perfetti A., Santulli G., Iaccarino G., Valentino R., Beguinot F., Formisano P. Overexpression of PED/PEA-15 induces mesangial expansion and up-regulates Protein kinase C-beta activity and Transforming Growth Factor-beta 1 expression. Diabetologia. 2009 Dec;52:2642–2652
* Equally contributed to the study.

ABSTRACT

Prep1 is an homeodomain transcription factor belonging to the MEINOX subfamily of the TALE (three amino acid loop extension) proteins. Prep1 forms DNA-independent dimeric complexes with all isoforms of the Pbx homeodomain transcription factor, enhancing target specificity and regulatory function. Recently, we have shown that Prep1 deficiency in mice induces protection from diabetes and increased insulin sensitivity in muscle tissue through a mechanism which involves increased protein and mRNA levels of the glucose transporter (GLUT)-4 and the PPAR gamma coactivator-1 alpha (PGC-1α). Since PGC-1α promotes the gluconeogenesis in hepatic tissue, I have studied the role of Prep1 in regulating insulin signaling in liver of Prep1 hypomorphic (Prep1i/i, Prep1i/+) mice, which expressed respectively only 5-7% and 55-57% of protein. Despite the results obtained in muscle tissue, Prep1i/i and Prep1i/+ mice did not show changes in PGC-1α protein and mRNA levels, but surprisingly they have an improved insulin-stimulated phosphorylation of IR and IRS-1/2. This is paralleled by an increase of glycogen content and a reduction of Glucose-6-phosphatase and PEPCK expression. Western blot analysis and qRT-PCR experiments displayed a gene-dosage dependent reduction of protein and mRNA levels of *SHP1* and *SYP* tyrosine phosphatases in liver extracts of Prep1i/i, Prep1i/+ mice. In parallel, the overexpression of Prep1 and Pbx1 in and HepG2 (Human Hepatoma cell line) cells induced insulin resistance by increasing the protein content and mRNA expression of *SHP1* and *SYP* phosphatases, which were paralleled by an inhibition of insulin-stimulated phosphorylation of IR, IRS-1/2 and glycogen accumulation. Interestingly, the overexpression of an inactive form of Prep1 (Prep1HR1), lacking of the interaction site between Prep1 and Pbx1, did not impair SHP1 and SYP expression and insulin-signaling in HepG2 cells. Moreover, in Prep1 overexpressing cells, antisense silencing of SHP1 but not that of SYP rescued insulin-dependent IR phosphorylation and glycogen accumulation. Finally, ChIP and Re-Chip experiments pointed out that the dimeric complex Prep1-Pbx1 bound specific sequences upstream the ATG codon of SYP and SHP1 genes (-625bp and -2113bp respectively) suggesting a direct gene regulation. Luciferase assays confirmed that the regions upstream SYP and SHP1 genes, were functionally activated by Prep1 and Pbx1 overexpression. Thus, the dimeric complex Prep1-Pbx1 directly regulates the gene expression of SYP and SHP1 tyrosine phosphatases by promoting insulin-resistance in liver cells.

BACKGROUND

1. Type 2 Diabetes: an overview

Diabetes mellitus, long considered a disease of minor significance to world health, is now taking its place as one of the main threats to human health in the 21st century. The past two decades have seen an explosive increase in the number of people diagnosed with diabetes worldwide. The global figure of people with diabetes is set to rise from the current estimate of 220 million (2010) to 300 million in 2025 (Figure 1).

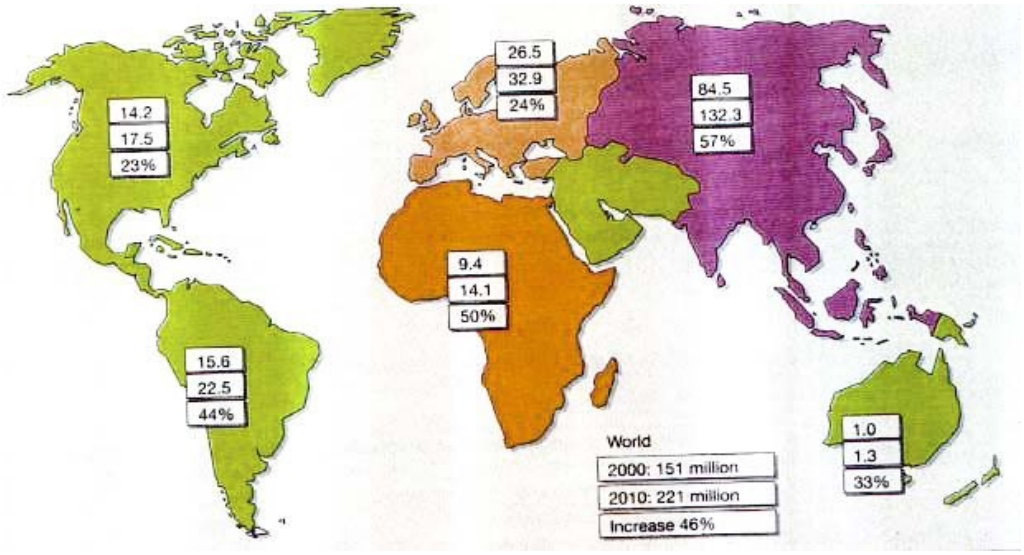

Figure 1. Number of people with diabetes (millions) for 2000 and 2010 (top and middle values respectively), and the percentage increase. Data adapted from the reference Amos et al. 1997.

There are two main forms of diabetes. Type 1 diabetes is due primarily to autoimmune-mediated destruction of pancreatic β–cells, resulting in absolute insulin deficiency. Its frequency is low compared to type 2 diabetes, which accounts for over 90% of cases globally. Type 2 diabetes is characterized by both insulin resistance and impaired insulin secretion. People with type 2 diabetes are not dependent on exogenous insulin, but may require the hormone for the control of glucose homeostasis if this is not achieved with diet alone or with oral hypoglycaemic agents.

2. Glucose homeostasis

Despite periods of feeding and fasting, plasma glucose levels remain in a narrow range between 66 and 110 mg/dl in normal individuals. This tight control is governed by the balance between glucose absorption from the intestine, production by the liver and uptake and metabolism by peripheral tissues such as skeletal muscle and adipose tissue (Saltiel and Kahn 2001).
Carbohydrate metabolism is regulated by several hormone, and also by sympathetic and parasympathetic nervous system (Table 1). The increasing glucose concentration after feeding (80/150 mg/dl) determines an increase of insulin release from pancreatic beta cells and a decrease of glucagon release from pancreatic alpha cells (Kahn 1994). Insulin lowers blood glucose levels both by suppressing glycogenolysis and gluconeogenesis in the liver (thereby decreasing hepatic glucose output), and by stimulating glucose uptake into skeletal muscle and adipose tissue. These actions are opposed by the "counter-regulatory" hormones, which are secreted continuously but whose release is enhanced during physiological "stress" (Pickup 2005).
Thus, the correct efficiency of pancreatic beta cells in insulin synthesis and secretion and its action on the liver, skeletal muscle and adipose tissue represents a key factor in glucose homeostasis maintenance.

	Liver gluconeogenesis	Glycogenolysis	HGO	Pheripheral Glucose Uptake
Insulin	↓↓	↓↓	↓↓	↑↑
Glucagon	↑↑§	↑↑	↑↑	-
Catecholamines	↑↑*§	↑	↑↑	↓
Growth hormone	↑*	-	↑	↓
Cortisol	↑*§	-	↑	↓

Table 1. Main hormones affecting glucose metabolism.
*Indirect enhancement of gluconeogenesis due to increased supply of glycerol and fatty acids by enhanced lypolisis.
§Increased gluconeogenesis by effects on hepatic enzymes and increased supply of glucogenic amino acids.

3. Insulin

Insulin is the most potent anabolic hormone known. Secreted by pancreatic beta cells in response to increase of plasmatic glucose and amino acids levels after feeding, insulin promotes the synthesis and storage of carbohydrates, lipid, proteins and inhibits their degradation and release into the circulation. Insulin

stimulates the uptake of glucose, amino acids and fatty acids into cells, and increases the expression and activity of enzymes that catalyse glycogen, lipid and protein synthesis (Saltiel and Kahn 2001).
Insulin increases glucose uptake in muscle and fat, and inhibits hepatic glucose production (glycogenolysis and gluconeogenesis), thus serving as primary regulator of blood glucose concentration. Insulin also stimulates cell growth and differentiation, promotes the storage of substrates in fat, liver and muscle by stimulating lipogenesis, glycogen and protein synthesis, and inhibiting lipolysis, glycogenolysis and protein breakdown (Figure 2) (Saltiel and Kahn 2001).

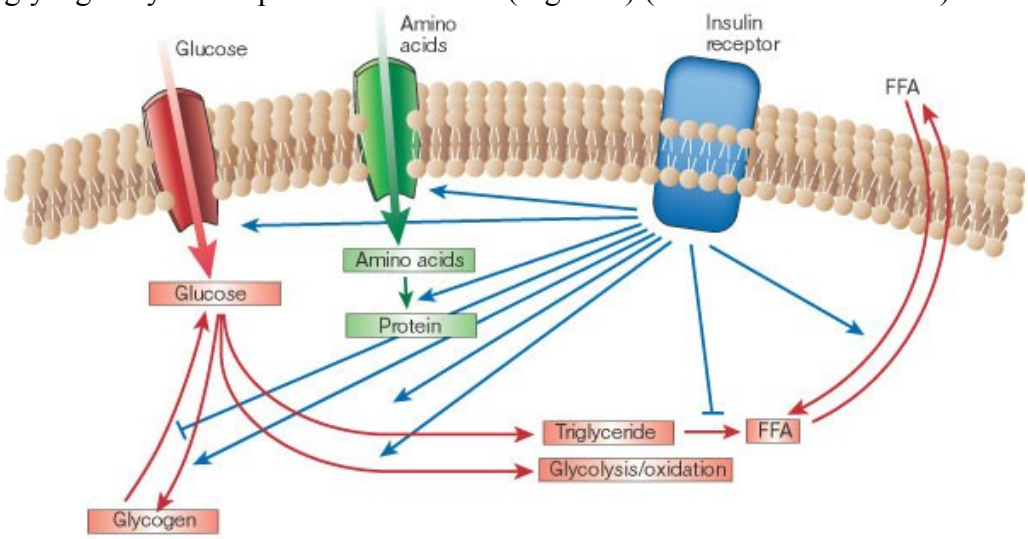

Figure 2. The regulation of metabolism by the insulin.
Insulin promotes the synthesis and storage of carbohydrates, lipids and proteins. Indeed, insulin stimulates the uptake of glucose, amino acids and fatty acids into cells, and increases the expression or activity of enzymes that catalyse glycogen, lipid and protein synthesis, while inhibiting the activity or expression of those that catalyse degradation.

4. Insulin signaling system

Insulin action is mediated through the insulin receptor (IR), a transmembrane glycoprotein with intrinsic protein tyrosine kinase activity. The insulin receptor belongs to a subfamily of receptor tyrosine kinases that includes the insulin-like growth factor (IGF)-I receptor and the insulin receptor-related receptor (IRR). These receptors are tetrameric proteins consisting of two α- and two β-subunits that function as allosteric enzymes where the α-subunit inhibits the tyrosine kinase activity of the β-subunit. Insulin binding to the α-subunit leads to derepression of the kinase activity of the β-subunit followed by trans-phosphorylation of the β-

subunits and conformational change of the α subunits that further increases kinase activity (Patti and Kahn 1998). Several intracellular substrates of the insulin receptor kinases have been identified (Figure 3). Four of these belong to the family of insulin-receptor substrate (IRS) proteins (White et al. 1998). Other substrates include Gab-1 and isoforms of Shc10 (Pessin and Saltiel 2000). The phosphorylated tyrosines in these substrates act as "docking sites" for proteins that contain SH2 (Srchomology-2) domains. Many of these SH2 proteins are adaptor molecules, such as the p85 regulatory subunit of PI(3)K and Grb2, or CrkII, which activate small G proteins by binding to nucleotide exchange factors. Others are themselves enzymes, including the phosphotyrosine phosphatase SYP and the cytoplasmic tyrosine kinase Fyn. PI(3)K has a pivotal role in the metabolic and mitogenic actions of insulin (Shepherd et al. 1995). It consists of a p110 catalytic subunit and a p85 regulatory subunit that possesses two SH2 domains that interact with tyrosinephosphorylated motifs in IRS proteins (Myers MG Jr et al. 1992). PI(3)K catalyses the phosphorylation of phosphoinositides on the 3-position to produce phosphatidylinositol-3-phosphates, especially PtdIns(3,4,5)P3, which bind to the pleckstrin homology (PH) domains of a variety of signaling molecules thereby altering their activity, and subcellular localization (Lietzke et al. 2000). Phosphotidylinositol-3-phosphates regulate three main classes of signaling molecules: the AGC family of serine/threonine protein kinases, the Rho family of GTPases, and the TEC family of tyrosine kinases. PI(3)K also might be involved in regulation of phospholipase D, leading to hydrolysis of phosphatidylcholine and increases in phosphatidic acid and diacylglycerol. The best characterized of the AGC kinases is phosphoinositide-dependent kinase 1 (PDK1), one of the serine kinases that phosphorylates and activates the serine/threonine kinase Akt/PKB (Alessi et al. 1997). Akt/PKB has a PH domain that also interacts directly with PtdIns(3,4,5)P3, promoting membrane targeting of the protein and catalytic activation. Akt/PKB has a pivotal role in the transmission of the insulin signal, by phosphorylating the enzyme GSK-3, the forkhead transcription factors and cAMP response element-binding protein.

Other AGC kinases that are downstream of PI(3)K signaling include the atypical PKCs, such as PKC-ζ. Akt/PKB and/or the atypical PKCs are required for insulin stimulated glucose transport (Standaert et al. 1997).

As is the case for other growth factors, insulin stimulates the mitogen activaed protein (MAP) kinase extracellular signal regulated kinase (ERK) (Figure 3). This pathway involves the tyrosine phosphorylation of IRS proteins and/or Shc, which in turn interact with the adapter protein Grb2, recruiting the Son-of-sevenless (SOS) exchange protein to the plasma membrane for activation of Ras. The activation of Ras also requires stimulation of the tyrosine phosphatase SYP, through its interaction with receptor substrates such as Gab-1 or IRS-1/2. Once activated, Ras operates as a molecular switch, stimulating a serine kinase cascade

through the stepwise activation of Raf, MEK and ERK. Activated ERK can translocate into the nucleus, where it catalyses the phosphorylation of transcription factors such as p62TCF, initiating a transcriptional programme that leads to cellular proliferation or differentiation (Boulton et al. 1991).

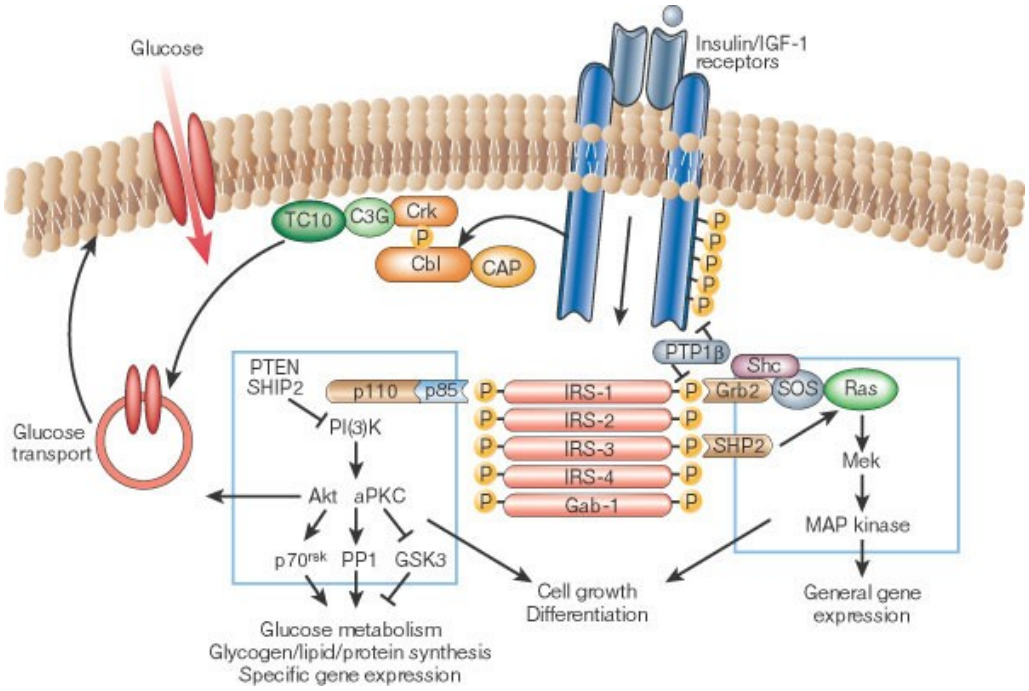

Figure 3. Signal transduction in insulin action.
The insulin receptor is a tyrosine kinase that undergoes autophosphorylation, and catalyses the phosphorylation of cellular proteins such as members of the IRS family, Shc and Cbl. Upon tyrosine phosphorylation, these proteins interact with signaling molecules through their SH2 domains, resulting in a diverse series of signaling pathways, including activation of PI(3)K and downstream PtdIns(3,4,5)P3-dependent protein kinases, Ras and the MAP kinase cascade. These pathways act in a concerted fashion to coordinate the regulation of vesicle trafficking, protein synthesis, enzyme activation and inactivation, and gene expression, which results in the regulation of glucose, lipid and protein metabolism.

4.1 Regulation of glycogen synthesis

Insulin stimulates glycogen accumulation through a coordinated increase in glucose transport and glycogen synthesis. The hormone activates glycogen synthase by promoting its dephosphorylation, through the inhibition of kinases such as PKA or GSK-3 and activation of protein phosphatase 1 (PP1) (Cross et al. 1994). Upon its activation downstream of PI(3)K, Akt phosphorylates and inactivates GSK-3, decreasing the rate of phosphorylation of glycogen synthase, thus increasing its activity state (Cross et al. 1994). Insulin does not activate PP1

globally, but rather specifically targets discrete pools of the phosphatase, primarily increasing PP1 activity localized at the glycogen particle. The compartmentalized activation of PP1 by insulin is due to glycogen-targeting subunits, which serve as 'molecular scaffolds', bringing together the enzyme directly with its substrates glycogen synthase and phosphorylase in a macromolecular complex, and in the process exerting profound effects on PP1 substrate-specific activity (Newgard et al. 2000).
Four different proteins have been reported to target PP1 to the glycogen particle. Despite a proposed common function, no two targeting subunits share more than 50% sequence homology, and this is largely confined to the PP1- and glycogen-binding regions. Overexpression of these scaffolding proteins in cells or *in vivo* results in a marked increase in cellular glycogen levels (Newgard et al. 2000). Although the mechanism by which insulin activates glycogen-associated PP1 remains unknown, inhibitors of PI(3)K block this effect, suggesting that PtdIns(3,4,5)P_3-dependent protein kinases are involved. These scaffolding proteins have a critical permissive role in the hormonal activation of the enzyme, perhaps interacting with additional proteins that regulate the interaction of PP1 with glycogen synthase and phosphorylase

4.2 Regulation of gluconeogenesis

Insulin inhibits the production and release of glucose by the liver by blocking gluconeogenesis and glycogenolysis (Figure 4). This occurs through a direct effect of insulin on the liver (Micheal et al. 2000), as well as by indirect effects of insulin on substrate availability (Bergman and Ader 2000). Insulin can also influence glucose metabolism indirectly by changes in free fatty acids generated from visceral fat, the so called “single gateway” hypothesis (Bergman 1997). Because visceral fat is less sensitive to insulin than subcutaneous fat, even after a meal there is little suppression of lipolysis by the hormone in this fat depot. The resulting direct flux of fatty acids derived from these fat cells through the portal vein to the liver can stimulate glucose production, thus providing a signal for both insulin action and insulin resistance in the liver.
Insulin directly controls the activities of a set of metabolic enzymes by phosphorylation or dephosphorylation and also regulates the expression of genes encoding hepatic enzymes of gluconeogenesis and glycolysis (Pilkis and Granner 1992). It inhibits the transcription of the gene encoding phosphoenolpyruvate carboxykinase, the rate-limiting step in gluconeogenesis (Sutherland et al. 1996). The hormone also decreases transcription of the genes encoding fructose-1,6-bisphosphatase and glucose-6-phosphatase, and increases transcription of glycolytic enzymes such as glucokinase and pyruvate kinase, and lipogenic enzymes such as fatty acid synthase and acetyl-CoA carboxylase. Although the transcription factors that control the expression of these genes have remained

elusive, new data suggest a potential role for the forkhead family of transcription factors through phosphorylation by Akt-related protein kinases (Nakae et al. 1999), and the PPARγ co-activator PGC-1α (Yoon et al. 2001).

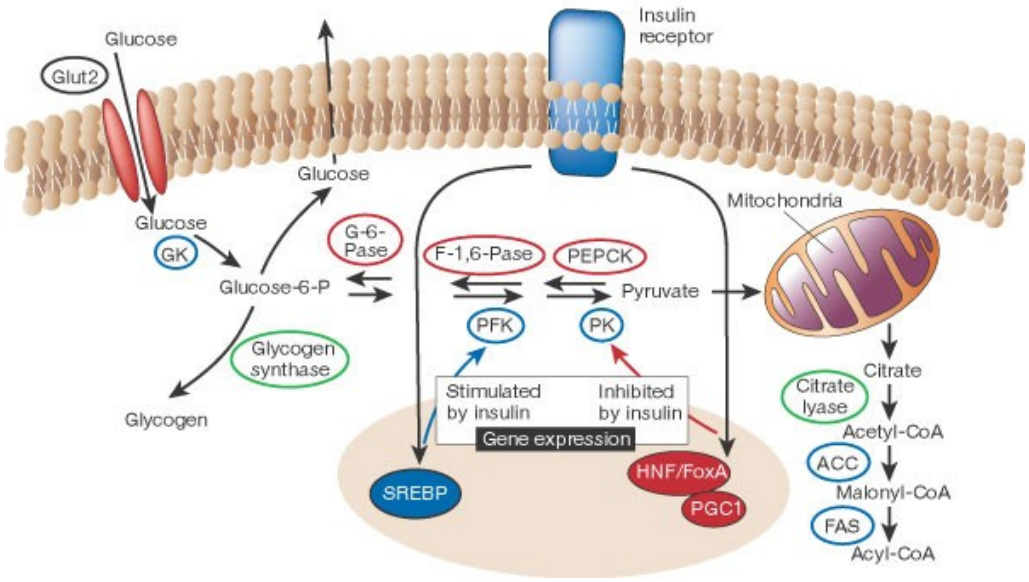

Figure 4. The regulation of glucose metabolism in the liver.
In the hepatocyte, insulin stimulates the utilization and storage of glucose as lipid and glycogen, while repressing glucose synthesis and release. This is accomplished through a coordinated regulation of enzyme synthesis and activity. Insulin stimulates the expression of genes encoding glycolytic and fatty-acid synthetic enzymes (in blue), while inhibiting the expression of those encoding gluconeogenic enzymes (in red). These effects are mediated by a series of transcription factors and co-factors, including sterol regulatory element-binding protein (SREBP)-1, hepatic nuclear factor (HNF)-4, the forkhead protein family (Fox) and PPARγ co-activator 1 (PGC1). The hormone also regulates the activities of some enzymes, such as glycogen synthase and citrate lyase (in green), through changes in phosphorylation state. GK, glucokinase; Glucose-6-P, glucose-6-phosphate; G6Pase, glucose-6-phosphatase; F-1,6-Pase, fructose-1,6-bisphosphatase; PEPCK, phosphoenolpyruvate carboxykinase; PFK, phosphofructokinase; PK, pyruvate kinase; ACC, acetyl-CoA carboxylase; FAS, fatty-acid synthase.

5. Inhibition of insulin signaling: the tyrosine phosphatases

Insulin signaling cascade may be attenuated by several enzymes, one of the most important are the protein tyrosine phosphatases (PTPases), which catalyse the rapid dephosphorylation of the receptor and its substrates. A number of PTPases have been identified that catalyse dephosphorylation of the insulin receptor *in vitro*, some of which are expressed in insulin-responsive cells, or up-regulated in

states of insulin resistance. Most attention has focused on the cytoplasmic phosphatases PTP-1B, SYP and SHP1.

PTP-1B was the first mammalian PTP identified and purified to homogeneity. This phosphatase is widely expressed and localizes predominantly to the ER through a cleavable proline-rich C-terminal segment (Frangioni et al. 1992).

In addition to the IR, IRS-1 might also be a substrate of PTP-1B because in the presence of Grb2, IRS-1 dephosphorylation by PTP-1B is accelerated (Goldstein et al. 2000).

Knockout of PTP-1B leads to increased insulin induced IR phosphorylation in liver and muscle but not adipose tissue. IRS-1 phosphorylation was also increased in muscle, but it is unclear whether this is because IRS-1 is a substrate of PTP-1B, or an increased IR activity in knockout mice. Furthermore, PTP-1B-deficient mice are hypersensitive as assayed by oral glucose tolerance tests, intraperitoneal insulin tolerance tests, and blood levels of glucose and insulin (Elchebly et al. 1999). Importantly, PTP-1B–/– mice are also resistant to diet-induced obesity, due in part to a decrease in fat cell mass and increased energy expenditure (Klaman et al. 2000).

SYP is a widely expressed PTP that contains two N-terminal SH2 domains, a C-terminal catalytic domain and a C-terminal segment containing two tyrosyl phosphorylation sites (Feng 1999). In contrast to many other growth factor receptor associated PTPs, SYP does not seem to dephosphorylate the receptor. However, Kuhne et al. proposed that the binding of IRS-1 to SYP enhances its phosphatase activity toward IRS-1, resulting in its dephosphorylation in vivo. Genetic studies in mice indicate that SYP is required for embryonic development (Saxton et al. 1997). SYP heterozygous knockout mice are viable, and in these mice, plasma insulin and glucose uptake were normal (Arrandale et al. 1996). Moreover tyrosine phosphorylation of IR and IRS-1 from muscle tissue was similar to that of wild-type controls. These results suggest that SYP might play a minor role in the metabolic effects of insulin. In another approach, when SYP is expressed in a transgenic mouse model, an insulin-resistant phenotype is observed that implicates the PTP as a negative regulator of insulin signaling (Maegawa et al. 1999).

Another PTP recently linked to insulin signaling and glucose metabolism is SHP1. Insulin may stimulate the phosphorylation and activation of SHP1, presumably by a direct association between SHP1 and the insulin receptor (Uchida et al. 1994, Bousquet et al. 1998). Mice expressing a catalytically defective SHP1 ($Ptpn6^{me-v/me-v}$) are markedly glucose tolerant and insulin sensitive compared to wild-type controls, as a result of enhanced insulin receptor signaling to IRS-PI3K-Akt in liver and muscle and increased phosphorylation of CEACAM1 (Dubois et al. 2006). This metabolic phenotype of $Ptpn6^{me-v/me-v}$ mice is recapitulated in normal mice through adenoviral expression of a dominant-negative inactive form of SHP1

in the liver or hepatic knockdown of SHP1 by small hairpin (sh)RNA mediated gene silencing, confirming a crucial role for SHP1 in negatively modulating insulin action and clearance in the liver, thereby regulating whole-body glucose homeostasis (Dubois et al. 1996).
Thus, the combination of these effects implicate PTP-1B, SYP and SHP1 as crucial therapeutic targets in diabetes and obesity.

6. Type 2 diabetes and insulin-resistance

T2D accounts for 90% of all forms of diabetes and is most common in people older than 45 who are overweight. However, as a consequence of increased obesity among young people, it is becoming more common in children and young adults. T2D is a heterogeneous syndrome with many possible causes. This is due to the interaction of environmental factors with a genetic susceptibility to the disease (Table 3), and it is becoming more and more evident that the relative contribution of genes and environment can differ considerably, even among individual whose clinical phenotype is similar (Diabetes Atlas 2006). The maintenance of normal glucose homeostasis depends on a precisely balanced and dynamic interaction between tissue sensitivity to insulin and insulin secretion. Type 2 diabetes develops because of defects in both insulin secretion and action, both of these with a genetic as well as an acquired component. Thus, T2D is made up of different forms each of which is characterized by variable degrees of insulin- resistance and beta cell dysfunction, and which together lead to hyperglycaemia. Insulin resistance, typically, is an early feature of T2D. It results from a genetically determined reduction in insulin sensitivity, compounded by exposure to the environmental factors, which further impair insulin action. Major sites of insulin resistance include liver and the peripheral tissues, skeletal muscle and fat. In muscle and fat, insulin resistance is manifested by decreased glucose uptake; in muscle, it impaired utilization of glucose by non-oxidative pathways as well as by decrease in glucose oxidation; in the liver, insulin resistance leads to failure of insulin to suppress hepatic glucose production, which is followed by glycogen breakdown and particularly by gluconeogenesis (Pickup 2005) (Figure 4).

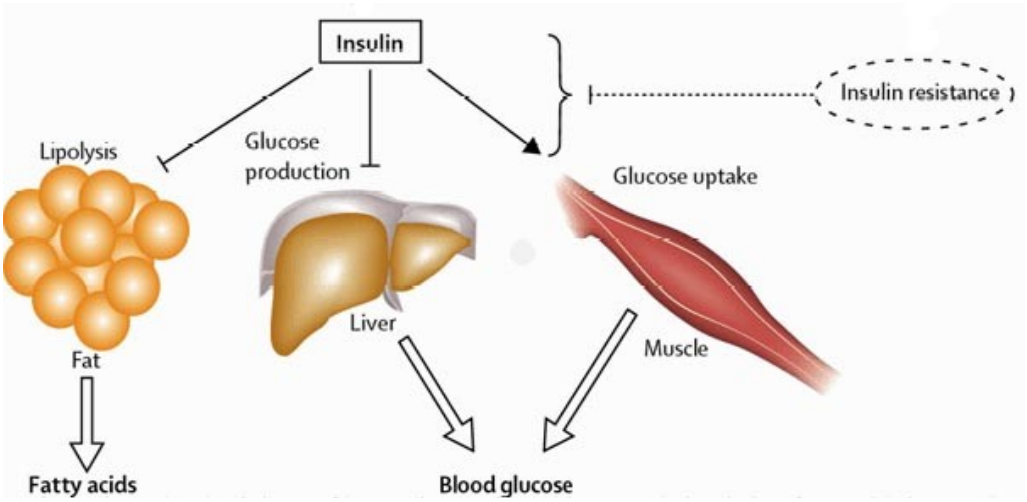

Figure 4. Insulin resistance on tissue targets.
The main sites of insulin resistance are liver and the peripheral tissue, skeletal muscle and fat. insulin resistance is manifested by decreased glucose uptake in muscle and fat, and by failure of insulin to suppress hepatic glucose production in the liver.

The beta cell dysfunction, the other key component of T2D pathophysiology, involves a relatively selective defect in the ability of glucose to provoke insulin secretion by beta cells, a temporal irregularity in the pulse and oscillations of insulin secretion, and a loss of the tight coupling between pulses of insulin secretion and pulse in glucose. This defect accounts for the failure of beta cells to compensate for increasing insulin-resistance and for the ultimate development of overt hyperglycaemia. The disease often remains asymptomatic and undetected for years. People with type 2 diabetes are not completely dependent on exogenous insulin, but may require the hormone for the control of blood glucose levels if this is not achieved with diet alone, regular exercise or with oral hypoglycaemic agents.
But if T2 diabetic people are not diagnosed or successfully treated, may develop "diabetic complications", such as micro-vascular complications (disease of the small blood vessels) including retinopathy, neuropathy and nephropathy, and macro-vascular complications (disease of the large blood vessels) including coronary heart disease, myocardial infarction and stroke.

7. Genes in type 2 diabetes

As mentioned above, insulin resistance and impaired beta cell function are the prominent features of T2D, and they are contributed by genetic and environmental factors. These factors might affect either the process of insulin signal transmission

across the plasma membrane and/or the biochemical pathways allowing glucose uptake and metabolism by the cells, or might affect the pathways regulating beta cell function, including those for beta cell compensation. While several environmental factors have been identified, discovery and characterization of the genes involved in T2D has been an arduous task and has proceeded slowly. In the past 10 years, indeed, geneticists have devoted a large amount of effort to finding T2D genes. These efforts have included many candidate-gene studies, extensive efforts to fine map linkage signals, and an international linkage consortium that was perhaps the best example of a multi-centre collaboration in common-disease genetics (Genome Wide Association Studies, GWAS). Of these efforts, only the candidate-gene studies produced unequivocal evidence for common variants involved in T2D. These are the E23K variant in the potassium inwardly-rectifying channel, subfamily J, member 11 (*KCNJ11*) gene (Nielsen, et al. 2003), the P12A variant in the peroxisome proliferator-activated receptor-γ (*PPARG*) gene (Altshuler, et al. 2000), and common variation in the transcription factor 2, hepatic (*TCF2*) (Gudmundsson, et al. 2007) and the Wolfram syndrome 1 (*WFS1)*10 genes (Sandhu, et al. 2007). All of these genes encode proteins that have strong biological links to diabetes. Rare, severe mutations in these four genes cause monogenic forms of diabetes, and two of them are targets of antidiabetic therapies: *KCNJ11* encodes a component of a potassium channel with a key role in beta cell physiology and it is targeted by the sulphonylurea class of drugs; *PPARG* encodes a transcription factor involved in adipocyte differentiation and it is targeted by the thiazolidinedione class of drugs (Figure 5). A common amino-acid polymorphism (Pro12Ala) in peroxisome proliferator activated receptor-γ (PPARγ) has been associated with T2D. People homozygous for the Pro12 allele are more insulin resistant than those having one Ala12 allele and have a 1.25-fold increased risk of developing diabetes. Moreover, there is also evidence for interaction between this polymorphism and fatty acids, thereby linking this locus with diet (Altshuler, et al. 2000). In 2006, by far the most spectacular recent development in the field of multifactorial T2D genetics has been the identification of TCF7L2 (encoding transcription factor 7-like 2) as the most important T2D-susceptibility gene to date (Owen and McCarthy 2007). The estimate of effect size (an odds ratio for T2D of 1.4-fold per allele) was identified in an intronic SNP with uncertain functional credentials (rs7903146). TCF7L2 variation is strongly associated with rates of progression from impaired glucose tolerance to diabetes (with a hazard ratio of 1.55 between homozygote groups). TCF7L2 is widely expressed and involved in the Wnt signaling cascade. Most studies suggest that the predominant intermediate phenotype associated with TCF7L2 variation is impaired insulin secretion, consistent with the replicated observation that the TCF7L2 association is greater among lean than obese T2D subjects. Early mechanistic hypotheses have focused on the known role of TCF7L2 in the gut, postulating the involvement of impaired

release of glucagon-like peptide-1 (an important islet secretagogue), reduced beta cell mass or intrinsic beta cell dysfunction. Body mass index data and some preliminary associations with leptin and ghrelin levels, however, could point towards a central mechanism. TCF7L2 result was encouraging for two reasons. First, this study analysed more than 200 markers across a region of linkage on chromosome 10q, but the variants that were found to alter risk did not explain the linkage signal, suggesting that a non-candidate-gene or region-based association effort (such as a GWAS) could work. Second, *TCF7L2* was a completely unexpected gene showing that a genome-wide approach could uncover previously unexpected disease pathways.

IPF-1/PDX-1 (Insulin Promoter Factor-1/Pancreatic and Duodenal Homeobox-1) is an homeodomain-containing transcription factor involved in pancreatic development, transcriptional regulation of a number of beta cell genes including insulin, glucokinase, islet amyloid polypeptide and GLUT2, and mediation of glucose-stimulated insulin gene transcription. Mutations in the heterozygous state are associated with MODY4 (Maturity Onset Diabetes in the Young 4), a non-ketotic monogenic form of diabetes mellitus, characterized by an autosomal dominant mode of inheritance, onset usually before 25 years of age and a primary defect in pancreatic beta cell function. IPF-1 mutations have also been discovered in a small fraction of patients with typical adult-onset type 2 diabetes. Subjects with heterozygous mutations in IPF-1 demonstrated reduced insulin secretory responses to glucose and glucagon-like peptide-1, consistent with a defect in the signaling pathways that regulate secretion in the beta cell and/or a defect in beta cell mass.

Functional and cooperative interactions between IPF-1 and another family of homeodomain-containing transcription factors named TALE (Three Aminoacid Loop Extension) is required for several genes regulation. Recently, TALE homeoproteins have been related to diabetes and insulin-resistance (Kim et al. 2002, Oriente et al 2008).

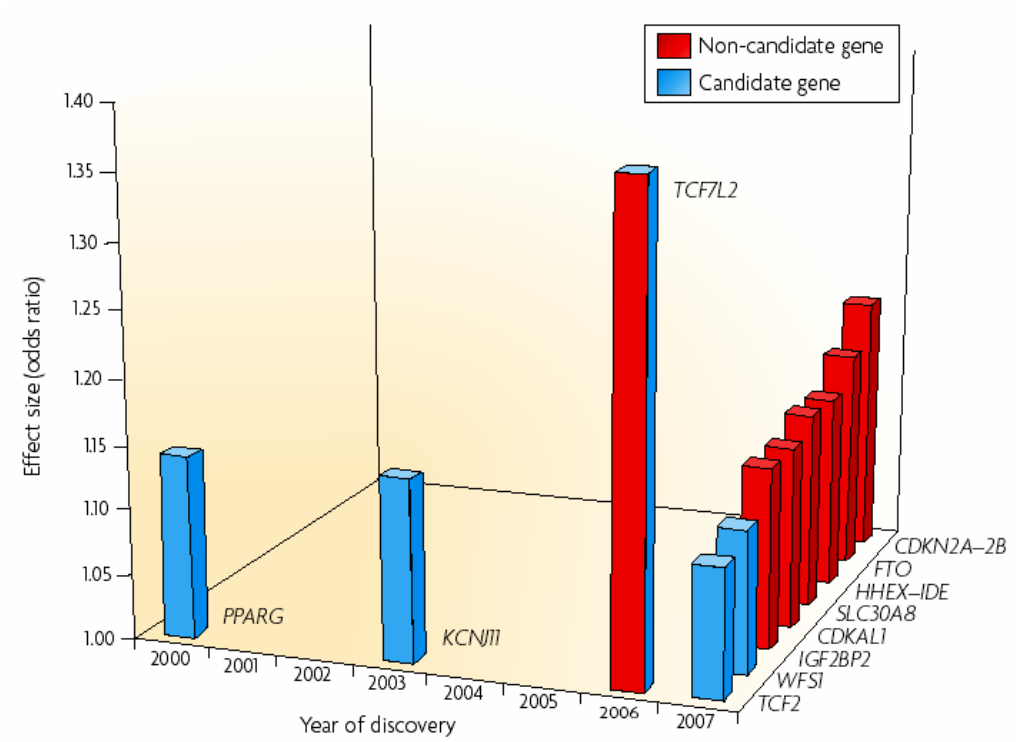

Figure 5. Effect sizes of the 11 common variants confirmed to be involved in type 2 diabetes risk.
The x axis shows the year when published evidences reached the levels of statistical confidence that are now accepted as necessary for genetic association studies. CDKAL1, CDK5 regulatory subunit associated protein 1-like 1; CDKN2, cyclin-dependent kinase inhibitor 2A; FTO, fat mass and obesity-associated; HHEX, haematopoietically expressed homeobox; IDE, insulin-degrading enzyme; IGF2BP2, insulin-like growth factor 2 mRNA-binding protein 2; KCNJ11, potassium inwardly-rectifying channel, subfamily J, member 11; PPARG, peroxisome proliferator-activated receptor-γ gene; SLC30A8, solute carrier family 30 (zinc transporter), member 8; TCF2, transcription factor 2, hepatic; TCF7L2, transcription factor 7-like 2 (T-cell specific, HMg-box); WFS1, Wolfram syndrome 1.

8. TALE proteins

TALE proteins are a family of homeodomain transcription factors which play an important role in the regulation of many genes involved in the organogenesis and differentiation of several organs and tissues. In order to promote these events, TALE proteins may cooperate with HOX proteins as multi molecular complexes (Featherstone 2003, Moens and Selleri 2006).
TALE proteins display a well preserved DNA binding structure of approximately 60 amino acids named homeodomain. This region is composed of three alpha

helices and a flexible N-terminal arm. The homeodomain interacts with the DNA through the third helix making base-specific contacts in the major groove of DNA and through the N-terminal arm which contacts the minor groove of DNA. Between the first and the second alpha helices of the homeodomain there is a 3 aminoacid, virtually represented by a proline (P) - tyrosine (Y) - proline (P) in positions 24-26, loop extension (TALE) responsible for the interaction with HOX proteins (Featherstone 2003, Moens and Selleri 2006).

TALE homeodomain proteins are divided into two groups: the PBC family, including the vertebrate Pbx proteins, fly Extradenticle and worm Ceh-20, and the MEIS family, including vertebrate Meis and Prep, fly Homothorax (Hth) and worm Unc-62 (Figure 6) (Moens and Selleri 2006).

Recent papers have shown the molecular mechanisms through Prep1 and Pbx1 TALE proteins may induce insulin-resistance in animal models (Oriente et al. 2008). These studies have confirmed a novel role of these transcription factors in the pathogenesis of the disease.

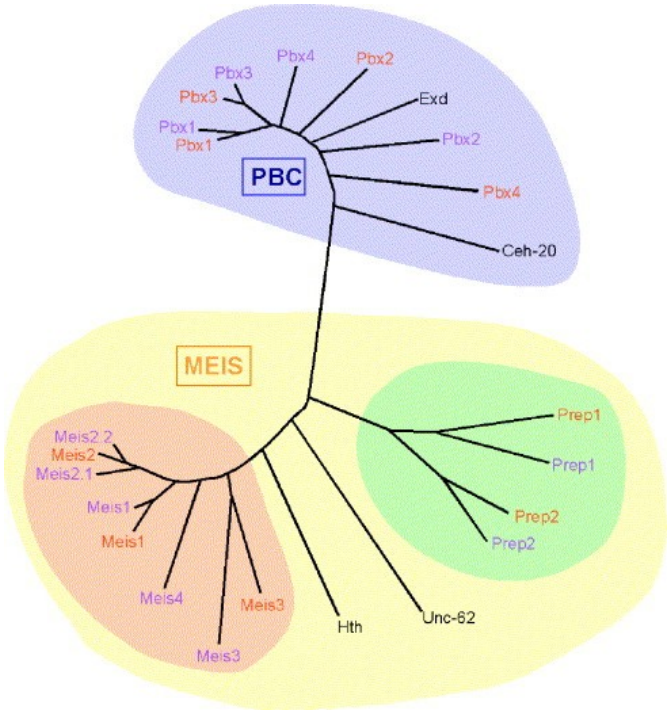

Figure 6. Phylogeny and structure TALE homeodomain proteins.
TALE homeodomain proteins are divided into two groups: the PBC family, including the vertebrate Pbx proteins, fly Extradenticle and worm Ceh-20, and the MEIS family, including vertebrate Meis and Prep, fly Homothorax (Hth) and worm Unc-62. Orange letters indicate mouse proteins, purple lettering indicates their zebrafish orthologs. Although in some cases the orthology assignments are not clear (as for *pbx2* and *pbx4*), genetic rescue experiments in zebrafish have

suggested that the different *pbx* genes are functionally identical. Similar information is not yet available with regard to mammalian *Pbx* genes.

8.1 Pbx1 protein

Pbx1 (pre-B cell leukemia transcription factor) protein is a small ubiquitous molecule which belongs to the PBC family. Pbx1, was identified at the (1;19) chromosomal breakpoint present in 25% of pediatric pre-B cell leukemias. Further studies have shown Pbx1 interact with other transcription factors and play an important role in the embryonic development (Nourse et al. 1990).
Pbx1 protein is characterized by the homeodomain region including the three aminoacid loop extension which interacts with the specific sequences of the HOX transcription factors. Near the amino terminal region there are two highly homologous regions named PBC- A and -B important for the protein-protein interaction (Figure 7) (Burglin 1997, Piper et al. 1999, Moens and Selleri 2006,). The relevance of Pbx1 on glucose metabolism has been underlined by several studies involving knock-out mice. Pbx1−/− mice die during the embryogenesis and show pancreatic hypoplasia and impaired differentiation of endocrine cells. Moreover, Pbx1-/+ mice have low levels of plasma insulin which contributes to the onset of a severe glucose intolerance. In these animals, the levels of PDX-1, a gene involved in the transcription of the insulin gene and the genesis of the pancreas, is strongly reduced, indicating that Pbx1 is important for its expression and most probably assessing the molecular events responsible for the observed phenotype (Selleri et al. 2001, Brendolan et al. 2005, Kim et al. 2002). The different actions of the Pbx class of proteins are also determined by the large numbers of interactors, including homeodomain and non-homeodomain proteins. The affinity of Pbx to the other cofactors or the specific DNA sequences mostly depends on the interaction with another important TALE homeoprotein named Prep1 (Moens and Selleri 2006).

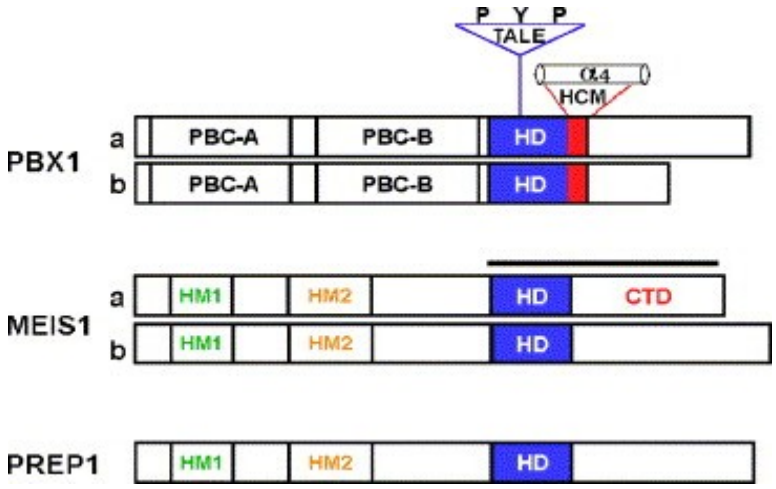

Figure 7. Structure of TALE homeodomain proteins. Prototype members of PBC and MEIS classes are shown here. "a" and "b" refer to splice isoforms of Pbx and Meis proteins. All TALE homeodomain proteins contain a divergent homeodomain (HD) containing a 3 amino acid loop extension (TALE) between the first and second α-helices. The TALE motif virtually always bears a proline (P)–tyrosine (Y)–proline (P) in positions 24–26) and contacts the hexapeptide motif of Hox proteins. Pbx proteins contain an additional DNA-contacting α-helix (α4; HCM) C-terminal to the canonical homeodomain. The PBC-A and PBC-B domains are conserved among Pbx, Exd and Ceh-20, and the PBC-A domain interacts with Meis/Prep proteins. Conversely, the HM1 and HM2 domains conserved among Meis/Prep proteins and are required for interactions with Pbx proteins. Posterior *Hox* genes of the AbdB subclass are unusual in that they can interact directly with Meis proteins via a C-terminal region (CTD) of Meis including the homeodomain; this region is indicated by a black bar.

8.2 Prep1 protein

Prep1 (Pbx regulating protein1) is an ubiquitary homeodomain transcription factor belonging to the MEINOX subfamily of TALE proteins (Berthelsen et al. 1998) mapping on the chromosome 21q.22.3. Prep1 forms DNA-independent dimeric complexes with the Pbx homeodomain trancription factor, enhancing target specificity and regulatory function (Berthelsen et al. 1998). It is a 64kDa protein which can localize both in cytoplasm and in the nucleus (Berthelsen et al. 1998). The protein shows two well-preserved domain named HR (HM in the figure) (homology region) 1 and 2 necessary for interaction with its partners and DNA binding. Near the C-terminus there is the homeodomain region necessary for DNA binding and between the first and the second alpha helices of the homeodomain there is the 3 aminoacid loop extension (TALE) (Figure 7) (Berthelsen et al. 1998). Prep1 can form heterodimers with PBC proteins and, in particular, the HR1 and HR2 domains of Prep bind the PBC-A sequence of Pbx1. Heterodimerization with Pbx appears to be essential to translocate Prep1 into the nucleus. On the other hand, Prep1 dimerization prevents nuclear export and the proteasomal degradation

of Pbx prolonging its half-life (Berthelsen et al. 1999). Heterodimerization of Prep1 with Pbx forms the UEF-3 (urokinase Enhancer factor-3) transcription factor which is important in the regulation of the expression of the interleukin 3 (IL-3), stromelysin and urokinase plasminogen activator (uPA), a protease involved in fibrinolysis, innate and adaptive immunity (Berthelsen et al. 1996). In addition, co-expression of Pbx1-Prep1 inhibits the *glucagon* gene transcription in non-glucagon-producing cells, (Herzig et al. 2000). Prep1 and Pbx1 can form ternary complexes with the pancreatic and duodenal homeobox 1 (PDX-1). Functional and cooperative interactions between PDX-1, Pbx, and Prep1 is required for somatostatin gene transcription (Goudet et al. 1999). Several studies on Prep1 have been conducted in different kind of animals. In mice, a null Prep1 mutation results in early lethality (E7.5) (Fernandez and Blasi, unpublished data), precluding a study of the Prep1 role(s) in later developmental processes. An insertion of a retroviral vector in the first intron of the Prep1 gene results in a hypomorphic mutation (Prep1i/i) that exhibits variable penetrance and expressivity. Most Prep1i/i embryos die between E17.5 and P0, although about 1/4 of these escape embryonic lethality. The mice escaping embryonic lethality show T-cell development anomalies (Penkov). In addition, erythropoiesis and angiogenesis are impaired, with liver hypoplasia, decreased hematocrit, anemia, and delayed erythroid differentiation together with a decrease in capillary formation. Prep1i/i embryos also display major eye anomalies and exhibit decreased levels of Pbx1, Pbx2, and Meis1 proteins as well as decreased expression of cMyb and Pax6, consistent with the hematopoietic and eye phenotype, respectively (Ferretti et al. 2006).

8.2.1 Prep1 and diabetes

In our laboratory we have recently evidenced an important role of Prep1 in pancreas development and in glucose homeostasis (Oriente et al. 2008). Prep1 hypomorphic (Prep1i/i) mice, which expressed only 5-7% of Prep1, show smaller islets consistent with a 35% decrease of both glucagon and insulin secretion. Pbx1 levels are reduced in Prep1i/i mice, emphasizing the idea that Prep1 hierarchically acts upstream in the network regulating pancreas development by controlling the levels of Pbx1. However, Prep1i/i animals exhibit enhanced sensitivity to insulin action in skeletal muscle and are protected from developing streptozotocin-induced diabetes. Measurement of the expression of several proteins playing an important role in insulin sensitivity and glucose disposal, like the insulin receptor (IR), Insulin Receptor Substrate-1 and -2, Akt/PKB, PKC zeta, ERK1/2 and Pbx1, have revealed no significant differences in Prep1i/i and control mice. In contrast, the levels of glucose transporter (GLUT4) and the PPAR gamma coactivator-1 alpha (PGC-1α) are markedly increased, while the p160 Myb-binding protein

(p160), a molecule which is known to inhibit the PGC-1 α-mediated glucose transport and competes with Pbx1 to bind Prep1, is reduced in hypomorphic mice. These findings raises the possibility that, in the skeletal muscle, Prep1 down-regulation results in activation of the glucose transport machinery by decreasing p160 levels. These effects have been confirmed by transfecting Prep1, Pbx1 and p160 cDNA in differentiating L6 skeletal muscle cells. Overexpression of Prep1 reduces the levels of PGC1α and GLUT4 and increases p160 protein expression in these cells, while overexpression of Pbx1 boosts the levels of PGC1α and GLUT4. Thus, Pbx1 and Prep1 have opposite effects on insulin-dependent glucose disposal by muscle. Prep1-mediated p160 expression is, at least in part, post-translational. In addition, a direct delivery of p160 cDNA in the muscle of Prep1 hypomorphic mice mimics the effect of Prep1, decreasing PGC-1α and GLUT4 expression. On the basis of the results, Prep1 might be considered as a new gene involved in the pathogenesis of type 2 diabetes and insulin-resistance.

AIMS OF THE STUDY

This thesis concerns the role of Prep1 homeodomain protein on liver insulin action in animal models and in hepatic cultured cells. In particular, I focused my attention on the effects mediated by the transcription complex Prep1-Pbx1.

Data produced in our lab indicate that Prep1 deficiency may positively modulate the intracellular pool of GLUT4 in muscle tissue by enhancing the transcription of the PPAR gamma coactivator-1 alpha (PGC-1α) gene (Oriente et al. 2008). This molecular effects lead to improvement of insulin sensitivity in this tissue.

As mentioned before, liver gluconeogenesis is a major process determining insulin-regulated glucose metabolism. Expression of the gluconeogenic enzymes G6Pase and PEPCK is regulated not only by the recruitment or modifications of transcription factors but also of co-activator proteins, including PGC-1α (Yoon et al. 2001). Whether and how Prep1 affects glucose metabolism in liver is unknow at the present but important to clarify in order to elucidate how Prep1 regulates insulin-dependent glucose metabolism at the whole-body level.

Thus, my purpose was to investigate whether the deficiency of Prep1 in liver might reproduce the molecular changes in PGC-1α levels observed in muscle tissue and modulate the glucose metabolism in this organ.

To achieve my aim I have studied glucose metabolism and insulin action in liver of Prep1 hypomorphic mice (Prep1i/i) and focused my attention on the possible genes which could have been regulated by the transcription complex Prep1-Pbx1.

Secondly, I have investigated whether the overexpression of Prep1 might induce insulin-resistance in hepatic cells (HepG2) and confirm the molecular mechanism by which Prep1 acts.

MATERIALS AND METHODS

Materials

Media, sera, antibiotics for cell culture and the lipofectamine reagent were from Invitrogen (Grand Island, NY). The Prep1, PGC-1α, actin, IR, Pbx1, SYP, SHP1 and PTP-1B antibodies were from Santa Cruz Biotechnology, Inc. (Santa Cruz, CA). The pY, IRS1, IRS2, antibodies were from Upstate Biotechnolgy (Lake Placid, NY). Protein electrophoresis, Real Time PCR, luciferase assay reagents were purchased from Bio-Rad (Richmond, VA), Western blotting and ECL reagents from Amersham Biosciences (Arlington Heights, IL). All other chemicals were from Sigma (St. Louis, MO).

Generation of Prep1 hypomorphic mice

Prep1 targeted mice were generated by gene trapping by Lexikon Genetics, Inc. (The Woodlands, Texas) and have been previously described (15, 38). In the experiments reported in this paper, heterozygous mice were backcrossed with wild-type (WT) C57BL/6 for 4 generations. All animal handling conformed to regulations of the Ethics Committee on Animal Use of H. S. Raffaele (IACUC permission number 207). Hepatic tissue samples were collected rapidly after mice were sacrificed by pentobarbitone overdose. Tissues were snap frozen in liquid nitrogen and stored at –80°C for subsequent western blotting.

Determination of glycogen content and pyruvate tolerance test

Hepatic tissue samples or HepG2 cells were homogenized in 0.1% SDS (1ml/24mg tissue or 1 ml/culture plate) using a glass-teflon potter and incubated 30' at 37°C. After the incubation, 500 μl of lysates were used for the assay. The glycogen was precipitated by adding ½ vol. (250μl) saturated Na2SO4 and 1.2 vol. (600μl) 95% EtOH and incubating 30' in ice. To isolate the glycogen, the samples were centrifuged at 4°C 20' at 1000rpm. The glycogen pellet was completely dried in vacuum conditions by SPEED VAC centrifugation and resuspended in 1ml dH2O. Finally, the samples were transferred into glass tubes and mixed with 1ml 5% Aqueous Phenol (Sigma-Aldrich) and 5ml 98% H2SO4 to disrupt the molecules of glycogen. The samples were incubated 10' at RT and subsequently 20' at 30° C in agitation. The molecules of glucose derived by the intracellular pool of glycogen were quantified by spectrophotometric analysis (reading 490

nm), compared with a linear standard curve of standard glycogen samples and normalized for the proteins content of the samples. For the pyruvate tolerance test, mice deprived of food for 16 hours were injected intraperitoneally with pyruvate dissolved in saline (2g/Kg) and venous blood glucose was drawn by tail clipping at 0, 30, 60, 90, and 120 min and measured with a glucometer (A. Menarini Diagnostics).

Cell culture procedures and transfection

HepG2 hepatoma cells and NMuLi mouse liver cells were cultured at 37°C in Dulbecco' s modified Eagle' s medium (DMEM) supplemented with 10% fetal bovine serum, 2% L-glutamine, 10,000 units/ml penicillin, 10,000 μg/ml streptomycin. Transient transfection of Prep1, Prep1HR, p160 and Pbx1 plasmid sDNAs or SYP and SHP1 phosphorothioate antisense oligonucleotides were performed by the Lipofectamine reagent according to the manufacturer's instruction. For these studies, 60-80% confluent cells were washed twice with Optimem (Invitrogen) and incubated for 8h with 3-5μg of plasmid construct or with 250nM of oligonucleotides and 45-60 μl of lipofectamine reagent. In transient transfection, the medium was then replaced with DMEM with 10% fetal bovine serum and cells further incubated for 15 h before being assayed. In stably transfection individual G418-resistant clones were selected by the limiting dilution technique (G418 effective dose, 0.8 mg/ml).

Western blot analysis and immunoprecipitation procedures

Tissue samples were homogenized in a Polytron (Brinkman Instruments, N.Y.) in 20 ml T-PER reagent/gram of tissue according to manufacture (Pierce, IL). After centrifugation at 10,000 rpm for 5 minutes, supernatant was collected. Cells were solubilized in lysis buffer (50 mmol/l HEPES, pH 7.5, 150 mmol/l NaCl, 10 mmol/L EDTA, 10 mmol/l Na4P2O7, 2 mmol/L Na3VO4, 100 mmol/L NaF, 10% glycerol, 1% Triton X-100, 1 mmol/L PMSF, 10 mg/ml aprotinin) for 1 h at 4C and lysates were centrifuged at 5,000g for 20 min. Total or immunoprecipitated homogenates were separated by SDS-PAGE and transferred on 0.45 μm Immobilon-P membranes. Upon incubation with primary and secondary antibodies, immunoreactive bands were detected by ECL according to the manufacturer's instructions.

Real-Time RT-PCR analysis

Total cellular RNA was isolated from liver and HepG2 cells by using the RNeasy kit (QIAGEN Sciences, Germany), according to manufacturer's instructions. 1 μg of tissue or cell RNA was reverse-transcribed using Superscript II Reverse Transcriptase (Invitrogen, CA). PCR reactions were analyzed using SYBR Green mix (Invitrogen, CA). Reactions were performed using Platinum SYBR Green qPCR Super-UDG using an iCycler IQ multicolor Real Time PCR Detection System (Biorad, CA). All reactions were performed in triplicate and β-actin was used as an internal standard.

Chromatin immunoprecipitation (ChIP) and Re-ChIP assay

The cross-linking solution, containing 1% formaldehyde, was added directly to cell culture media. The fixation proceeded for 10 min and was stopped by the addition of glycine to a final concentration of 125 mM. nMuLi cells were rinsed twice with cold phosphate buffered saline plus 1 mM phenylmethylsulfonyl fluoride and then scraped. Cells were collected by centrifugation at 800 X g for 5 min at 4 °C. Cells were swelled in cold cell lysis buffer containing 5 mM PIPES (pH 8.0), 85 mM KCl, 0.5% Nonidet P-40, 1 mM phenylmethylsulfonyl fluoride, and inhibitors mixture (Sigma) and incubated on ice for 10 min. Nuclei were precipitated by microcentrifugation at 2000Xg for 5 min at 4 °C, resuspended in nuclear lysis buffer containing 50 mM Tris-HCl (pH 8.0), 10 mM EDTA, 0.8% SDS, 1 mM phenylmethylsulfonyl fluoride and inhibitors mixture (Sigma), and then incubated on ice for 10 min. Samples were broken by sonication into chromatin fragments of an average length of 500/ 1000 bp and then microcentrifuged at 16,000 X g for 10 min at 4 °C. The sonicated cell supernatant was diluted 8-fold in chromatin immunoprecipitation (ChIP) dilution buffer containing 0.01% SDS, 1.1% Triton X-100, 1.2 mM EDTA, 16.7 mM Tris- HCl (pH 8.0), and 167 mM NaCl and precleared by adding salmon sperm and conjugating protein at equimolar concentration for 90 min at 4 °C. Precleared chromatin from 1X106 cells was incubated with 1 μg of polyclonal antibody (anti-Prep1) or no antibody and rotated at 4 °C for 16 h. Immunoprecipitates were washed five times with radioimmune precipitation assay buffer containing 10 mM Tris-HCl (pH 8.0), 1 mM EDTA, 1% Triton X-100, 0.1% sodium deoxycholate, 0.1% SDS, 140 mM NaCl, and 1 mM phenylmethylsulfonyl fluoride, twice with LiCl buffer containing 0.25 M LiCl, 1% Nonidet P-40, 1% sodium deoxycholate, 1 mM EDTA, 10 mM Tris-HCl (pH 8.0), and then 3 times with TE (10 mM Tris-HCl (pH 8.0), 1 mM EDTA). Before the first wash, the supernatant from the

reaction lacking primary antibody was saved as total input of chromatin and was processed with the eluted immunoprecipitates beginning at the cross-link reversal step. Immunoprecipitates were eluted by adding 1% SDS, 0.1 M NaHCO3, and reverse cross-linked by the addition of NaCl to a final concentration of 200 mM and by heating at 65 °C for at least 4 h. Recovered material was treated with proteinase K, extracted with phenol-chloroform-isoamyl alcohol (25:24:1), and precipitated. The pellets were resuspended in 30 μl of TE and analyzed by PCR using specific primers for the analyzed regions. The input sample was resuspended in 30 μl of TE and diluted 1:10 before PCR. For ReChIP assay, immunoprecipitates with the first antibody were eluted in 50 ml of DTT 10 mM, diluted 10-fold in ChIP Dilution Buffer supplemented with protease inhibitors, and immunoprecipitated with the second antibody. Following immunoprecipitation, samples are processed as described above for ChIP assay and eluted DNA amplified by PCR with specific oligos.

Luciferase assay

The mouse genomic region of SHP1 n.2 (-2113/-1778) was amplified by PCR from genomic mouse DNA isolated from murine liver cell line (NmuLi cells). The following primers were used: F: 5'-KpnI- TCGGTGTGAGATCGGTACAA-3' and R:5'-SacI- TCCGAGTTGGTGTCTCAGTG-3' (SHP1 n°2), (where SacI and KpnI indicate the restriction sites added to the sequence). The amplified regions were cloned in *Plg3 promoter vector* (Promega) by SacI and KpnI cloning strategy. To examine the effect of Prep1 and Pbx1 on SHP1 n°2 regions, HeLa cells were cotransfected with 2 μg of SHP1 n.2 promoter vector together with different amounts of Prep1 and Pbx1 expression vectors. Total DNA content (up to 4 μg/plate) was normalized to the empty vector devoid of Prep1 and Pbx1 coding sequence. 48 h after transfection luciferase activity was measured by a commercial luciferase assay kit (Promega). Values were normalized for beta-galactosidase.

Statistical procedures

Data were analysed with the Statview software (Abacus-concepts) by one-factor analysis of variance. P values of less than 0.05 were considered statistically significant.

RESULTS AND DISCUSSION

Prep1 deficiency may positively modulate the intracellular pool of GLUT4 in muscle tissue by enhancing the transcription of the PPAR gamma coactivator-1 alpha (PGC-1α) gene (Oriente et al. 2008). These molecular changes have been observed in Prep1 hypomorphic mice (Prep1i/i) and lead to increase insulin sensitivity in this tissue.

To address the role of PGC-1α in liver of Prep1 hypomorphic mouse, I analyzed the hepatic protein and mRNA levels of PGC-1α in Prep1i/i and i/+ mice. Surprisingly, No significant differences were detected in Prep1 hypomorphic and control littermates (Figure 8a, b).

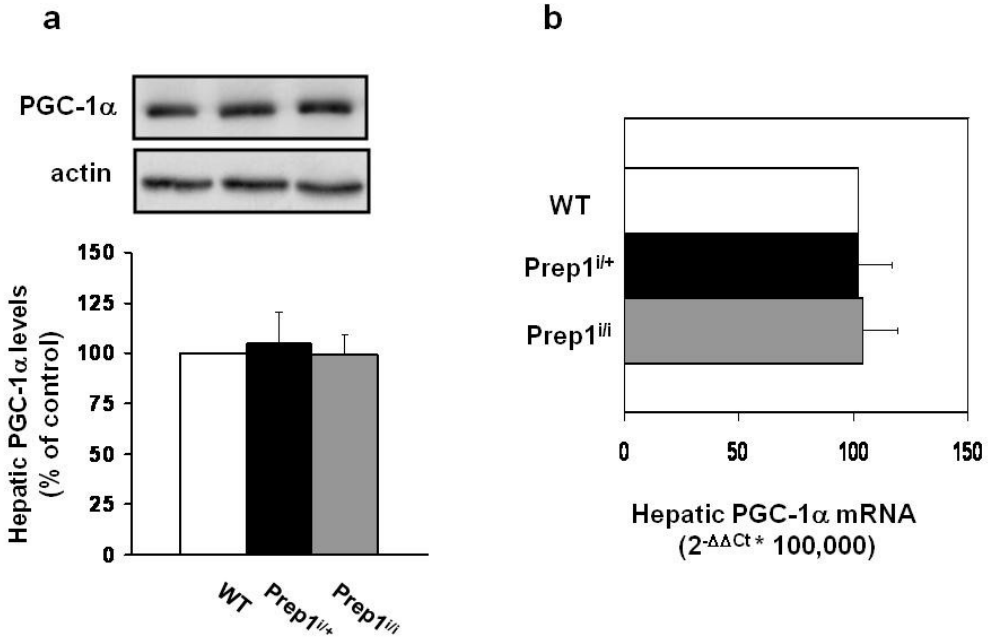

Figure 8. Role of PGC-1α in the liver of the Prep1 hypomorphic mice. Livers from Prep1 hypomorphic and control mice were dissected, solubilized and subjected to Western blot analysis with PGC-1α and actin antibodies. Blots were revealed by ECL and autoradiography and bands quantified by densitometric analysis. Each bar represents the mean ± SD of duplicate determinations in 10 mice/group (a). The abundance of mRNA for PGC-1α was determined by RT-PCR analysis of total RNA isolated from liver of the hypomorphic and control mice, using beta-actin as internal standard. Each bar represents the mean ± SD of four independent experiments performed in 8 mice/genotype (b).

In order to study the hepatic glucose metabolism of Prep1 hypomorphic mice, I profiled the initial steps of the insulin signaling cascade by measuring the protein expression and the activation levels (tyrosine phosphorylation) of the insulin

receptor (IR) and the IRSs proteins (IRS1-2). In particular, I activated the insulin signaling cascade by injecting control and hypomorphic mice intraperitoneally with insulin 0.75mU/g. Subsequently, mice were sacrificed and immunopreciptiation assays were performed with specific antibodies against the phosphorylated tyrosines of IR and IRS1-2 in liver extracts. No change was evidenced in either IR, IRS1 or IRS2 total protein levels, while, tyrosine phosphorylation of all these proteins was significantly increased in Prep1 hypomorphic mice, in a gene dosage-dependent manner, compared to wild type mice (Figure 9).

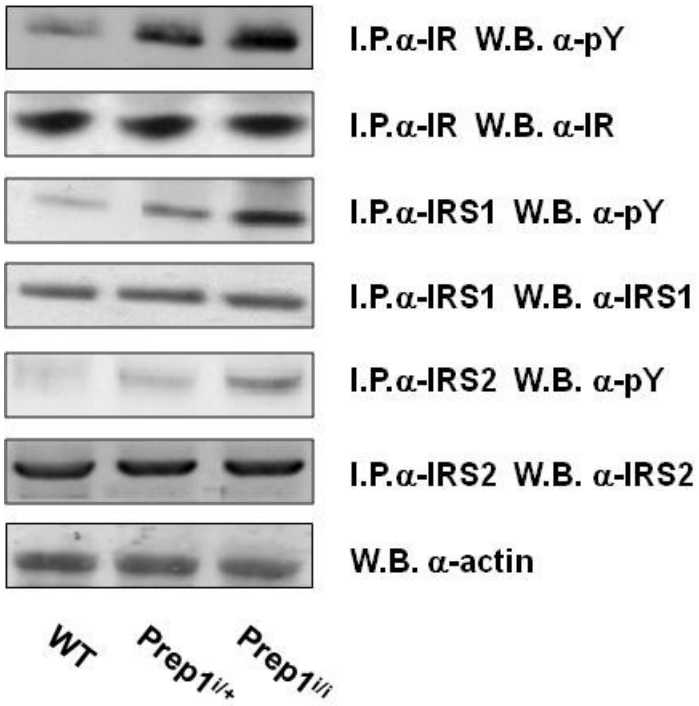

Figure 9. Insulin signaling in liver of Prep1 hypomorphic mice. Protein lysates (250μg) from liver tissue of WT and Prep1 hypomorphic mice, injected with insulin 0.75mU/g, were immunoprecipitated with IR, IRS-1 or IRS-2 antibodies followed by blotting with phosphotyrosine, IR, IRS-1 or IRS-2 antibodies. Actin antibodies were used for the loading control normalization. The autoradiograph is representative of four independent experiments.

It is known that the effect of insulin on liver cells is to block the gluconeogenesis by reducing the expression of *G6Pase* and *PEPCK* and induce glycogen storage. I assessed whether the enhanced insulin signaling might affect the final steps of insulin pathway by measuring the gene expression of *G6Pase* and *PEPCK* and by checking the gluconeogenesis and the glycogen storage after insulin stimulation.

As shown in figure 10a, b, Prep1i/i mice display 2-fold increase in glycogen accumulation and the effect of the insulin on the downregulation of *G6Pase* and *PEPCK* genes is stronger compared to control mice.

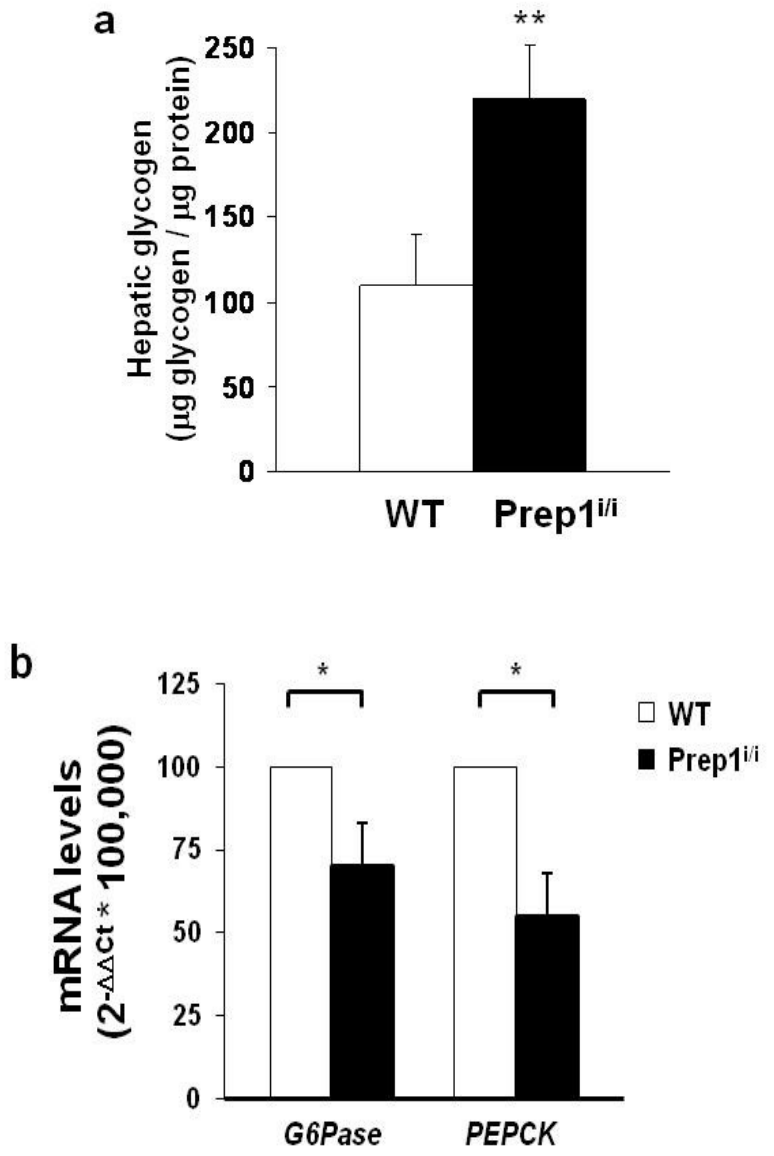

Figure 10. Insulin-stimulated glycogen storage and *G6Pase/PEPCK* gene expression in Prep1 hypomorphic mice. Prep1 hypomorphic and control mice (n = 12 mice/group) were intraperitoneally injected with insulin (0.75 mU/g body weight) for 2 hours, then the liver was isolated and glycogen content was measured as described in material and methods. Bars represent the means ± SD of determinations in 12 mice/group. Asterisks indicate statistically significant differences (**, $p < 0.01$) (a). The abundance of mRNA for *G6Pase* and *PEPCK* was determined by real-time RT-PCR analysis of total RNA isolated from liver of the hypomorphic and control

mice, using beta-actin as internal standard. Each bar represents the mean ± SD of four independent experiments performed in 8 mice/genotype (b).

G6Pase and PEPCK are key enzymes in the hepatic regulation of glucose output and gluconeogenesis respectively. I have evaluated if the reduction of G6Pase and PEPCK observed in the liver of Prep1 hypomorphic mice in response to insulin might have modified the rate of glucose output/gluconeogenesis. One of the test, widely used in literature, to study this aspect of glucose metabolism is the pyruvate tolerance test (PTT), because, pyruvate gets into the hepatic cells and it is quickly converted into glucose. I have measured the blood glucose levels during 2 hours after the Na pyruvate administration. As shown in figure 11 the profile of blood glucose of Prep1i/+ mice indicated that the sensitivity to pyruvate-induced hyperglycemia was significantly lower in Prep1i/+.

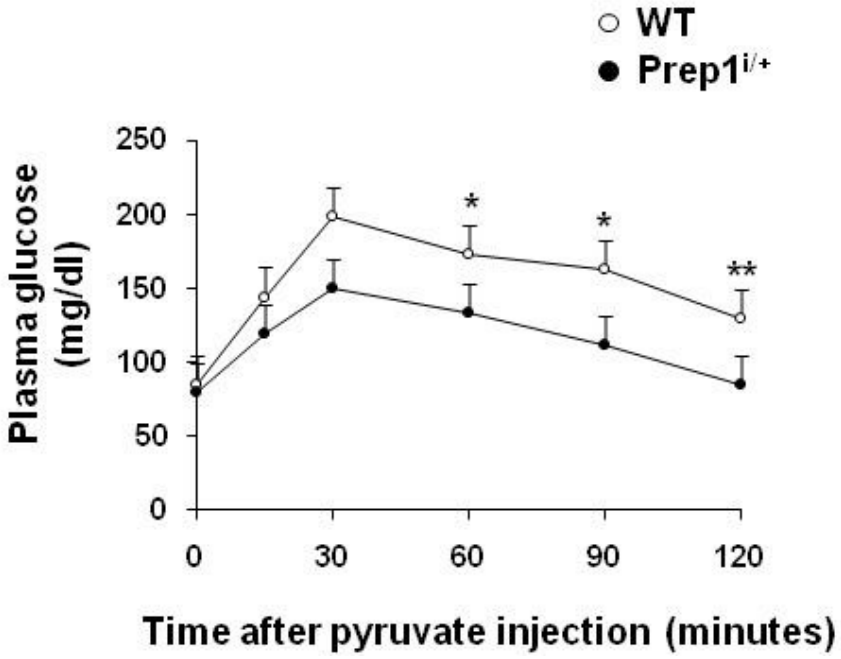

Figure 11. Pyruvate tolerance test in Prep1i/+ mice. B. WT and Prep1i/+ mice (n=12 mice/group) were fasted for 16 hours, injected with pyruvate (2g/Kg) and plasma glucose concentrations were quantified at the indicated times. Data points represent the means ± SD of results obtained from each group of mice. Asterisks denote statistically significant differences (*, $p < 0.05$; **, $p < 0.01$).

Thus, the reduction of *G6Pase* and *PEPCK* expression observed in the liver of Prep1 hypomorphic mice, reflects the lower glycemia observed during the experiment. The enhanced insulin signaling of these mice may contribute to reduce pyruvate-induced hyperglycemia in Prep1 hypomorphic mice compared to WT mice. This last set of results indicate that Prep1 deficiency may significantly

modify insulin action in hepatic tissue by improving either the first steps of the cascade and the functional effects of the hormone. Moreover, the network involved in Prep1 action in liver is completely different from the muscle, since PGC-1α is not involved.

To investigate the molecular mechanisms of this phenotype, I evaluated the activation and the protein levels of several serine/threonine kinase proteins involved in the negative regulation of insulin action. No difference was detected for members of PKC isoforms (α and δ), ERK1/2 and JNK between WT and Prep1 hypomorphic mice (data not shown). Also GRB10, an adapter protein which interact with IR and reduces insulin-stimulated tyrosine phosphorylation of IRS1 and IRS2, was unchanged (data not shown). The insulin-dependent liver glucoregulatory function is also known to be regulated by the tyrosine phosphatases SYP, SHP1 and PTP-1B. Interestingly, protein levels of SYP and SHP1 were reduced, respectively, by 3- and 2-fold in Prep1i/i mice livers and more moderately in Prep1i/+ mice (Figure 11a). This reduction appeared, at least in part, transcriptional, in fact, consistently with this hypotesis, SYP and SHP1 mRNA levels were also decreased in the Prep1i/+ and Prep1i/i mice (Figure 11b). Surprisingly, PTP-1B levels did not change in the Prep1 hypomorphic animals (Figure 11a, b).

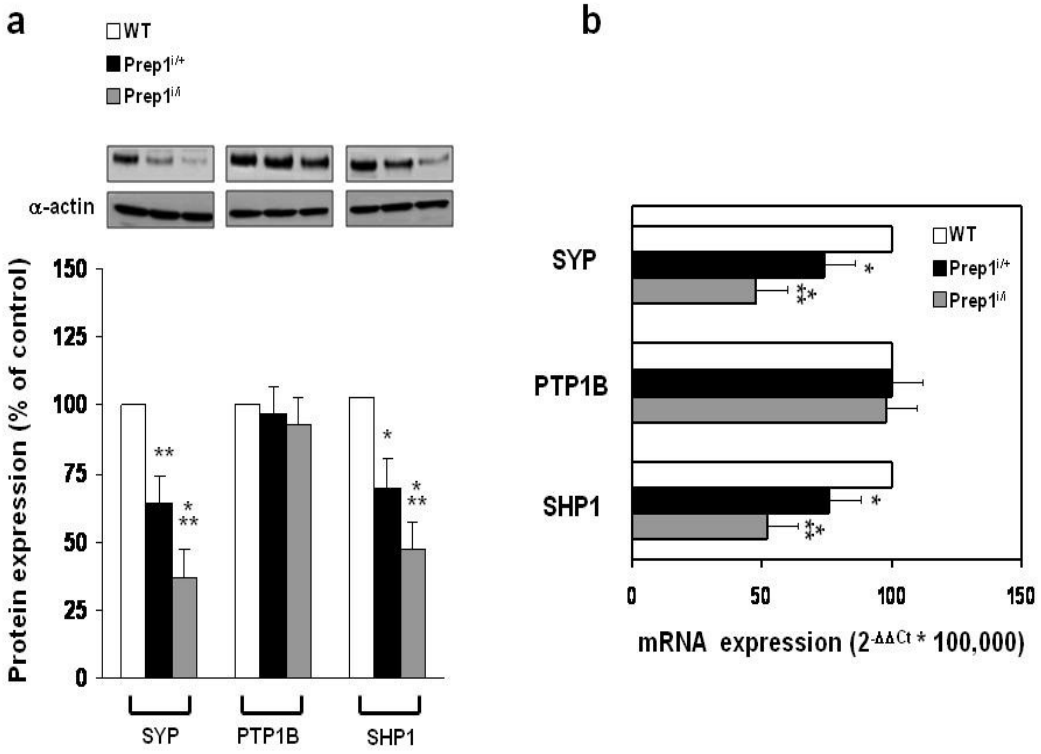

Figure 11. Protein and mRNA levels of SYP, PTP1-B and SHP1 in hepatic tissue of Prep1 hypomorphic mice. SYP, PTP1-B and SHP1 tyrosine phosphatases protein expression was measured by western blot in hepatic tissues from hypomorphic and control mice using anti- SYP, PTP-1B and SHP1 antibodies. Each bar represents the mean ± SD of duplicate determinations in 10 mice/group. Asterisks denote statistically significant differences (**, $p < 0.01$; ***, $p < 0.001$) (a). The abundance of mRNAs of *SYP*, *PTP-1B* and *SHP1* genes was determined by real-time RT-PCR analysis of total RNA isolated from liver tissue of the hypomorphic and control mice, using beta-actin as internal standard. Each bar represents the mean ± SD of four independent experiments performed in 6 mice/genotype (b).

The tyrosine phosphatases PTP-1B, SYP, and SHP1 play a fundamental role in the insulin-dependent liver glucoregulatory function. They are known to negatively modulate insulin action on liver glucose metabolism through tyrosine dephosphorylation of the insulin receptor and/or insulin receptor substrates. The balance in the level of activity of these individual phosphatases represents an important determinant of normal liver glucoregulation. How, at the physiological and molecular levels, this balance is maintained has been only partially elucidated. Prep1 might be a pivotal molecule in the regulation of these phosphatases and it could be a novel candidate in their transcriptional modulation.

To further examine Prep1 action on early tyrosine phosphorylation in the insulin signaling cascade and on the regulation of tyrosine phosphatases, I have transiently

transfected a Prep1 cDNA in the HepG2 hepatoma cells, which represent a good model of liver cells. As shown in figure 12a, the transfection almost completely prevented insulin-induced tyrosine phosphorylation of the insulin receptor as well as that of IRS-1 and IRS-2. No change was evidenced in the abundance of any of these proteins. Furthermore, Prep1 transfection up-regulated SYP and SHP1 expression both at the mRNA and the protein levels but elicited no action on that of PTP-1B (figure 12c, d).

The effects of Prep1 on gene regulation is tightly dependent on many interactors which can recruit it in different transcription networks and modulate the target of its transcription activity. Since one of the main partners of Prep1 is Pbx1, I focused my attention on the transcription complex Prep1-Pbx1 as a possible regulator of the transcription of the *SYP* and *SHP1* genes. To validate this hypothesis, I transfected HepG2 cells with cDNAs of Pbx1 and Prep1HR1 This mutant contains one point mutation in the domain HR1 which is fundamental for the interaction between Prep1 and Pbx1, resulting in an abolishment of the recruitment and function of the transcription complex. Interestingly, the overexpression of a Pbx1 cDNA in HepG2 cells mimicked Prep1 effects on insulin-stimulated tyrosine phosphorylation of the insulin receptor kinase and IRS-1/2 (figure 12b), as well as the effects of Prep1 on SYP and SHP1 gene and protein expression (figure 12c, d). More importantly, Prep1HR1 mutant was unable to exert the biological effects exerted by the overexpression of the WT protein and Pbx1 (Figure 12a,c,d).

Moreover, transfection of the Prep1 cDNA, but not that of the Prep1HR1 mutant, abolished insulin-induced glycogen accumulation in the HepG2 cells (figure 13). As in the case of the insulin signal activation, the effect of Prep1 was mimicked by Pbx1 overexpression.

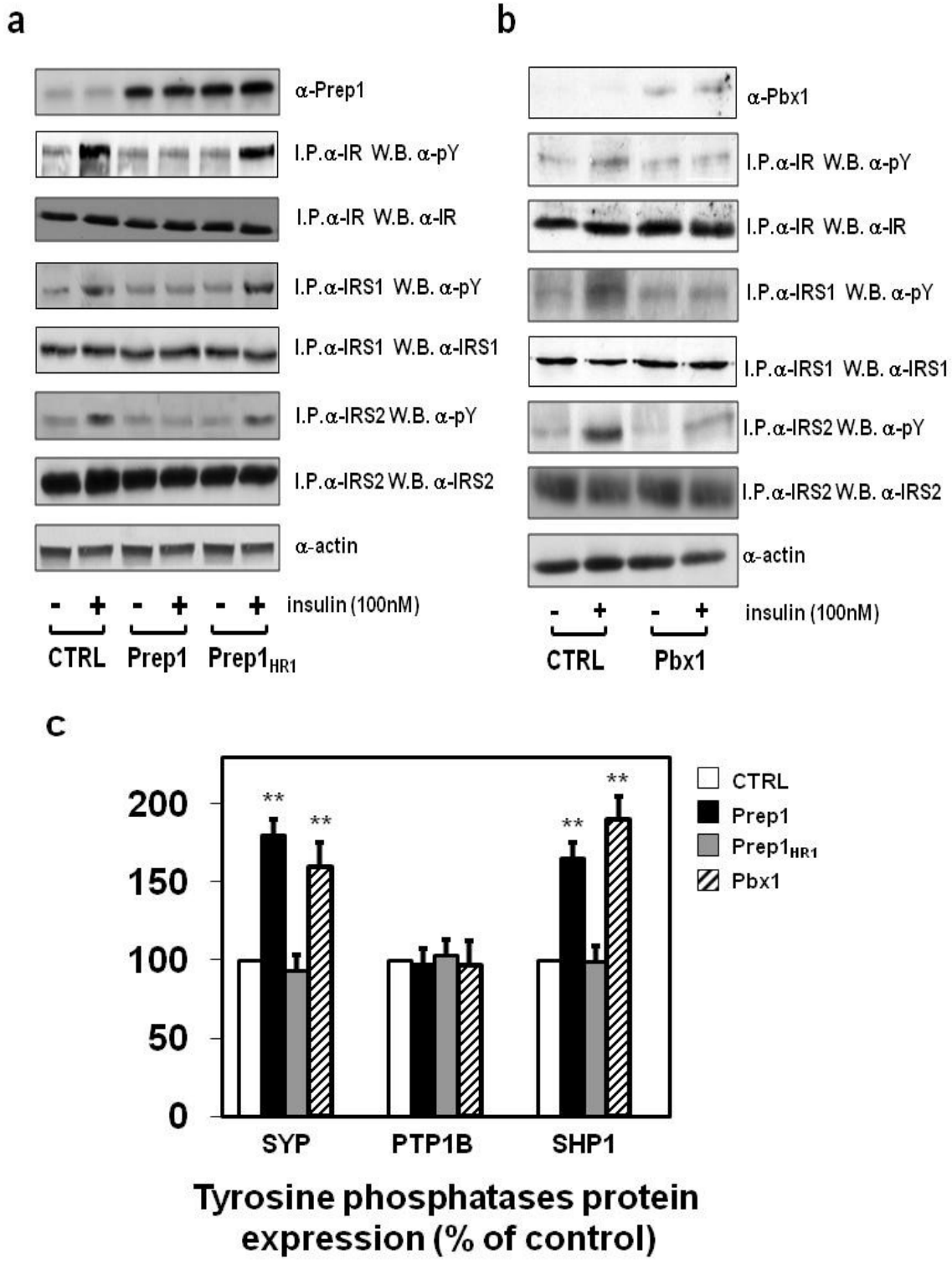
a
α-Prep1
I.P.α-IR W.B. α-pY
I.P.α-IR W.B. α-IR
I.P.α-IRS1 W.B. α-pY
I.P.α-IRS1 W.B. α-IRS1
I.P.α-IRS2 W.B. α-pY
I.P.α-IRS2 W.B. α-IRS2
α-actin
- + - + - + insulin (100nM)
CTRL Prep1 Prep1HR1
b
α-Pbx1
I.P.α-IR W.B. α-pY
I.P.α-IR W.B. α-IR
I.P.α-IRS1 W.B. α-pY
I.P.α-IRS1 W.B. α-IRS1
I.P.α-IRS2 W.B. α-pY
I.P.α-IRS2 W.B. α-IRS2
α-actin
- + - + insulin (100nM)
CTRL Pbx1
c
200
150
100
50
0
**
SYP
PTP1B
SHP1
CTRL
Prep1
Prep1HR1
Pbx1
Tyrosine phosphatases protein expression (% of control)

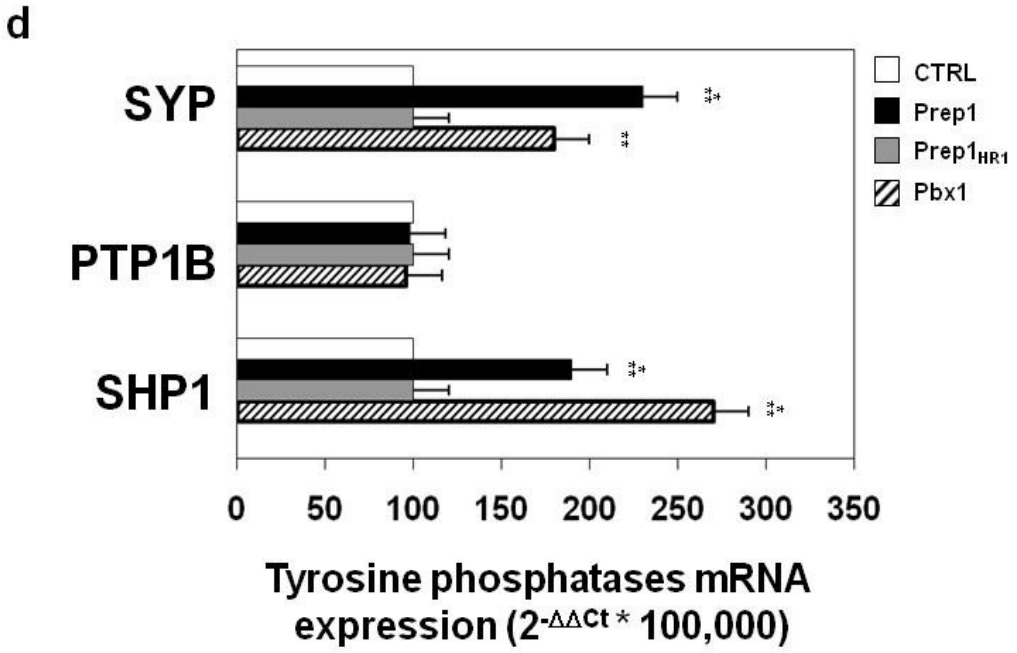

Figure 12. Effect of Prep1, Pbx1 and Prep1HR1 cDNAs transfection on insulin signaling and tyrosine phosphatases expression. HepG2 cells were transiently transfected with the Prep1, Pbx1 and Prep1HR1 mutant cDNAs and exposed to 100 nM insulin for 5 minutes. Afterwards, cells were solubilized and the lysates were immunoprecipitated with anti IR, IRS1 or IRS2 antibodies followed by blotting with pY, IR, IRS1 or IRS2 antibodies. The total lysates were blotted with anti Prep1, Pbx1 or actin antibodies. Bands were revealed by ECL and autoradiography. The autoradiograph shown is representative of four independent experiments (a,b). Lysates from HepG2 cells transiently overexpressing were subjected to western blot analysis blotted with anti SYP, PTP-1B and SHP1 antibodies. Each bar represents the mean ± SD of duplicate determinations in four independent experiments. (c). The levels of mRNAs encoding SYP, PTP-1B and SHP1 was quantified by real-time RT-PCR analysis, using beta-actin as internal standard. Bars represent the mean ± SD of four independent experiments (d). Asterisks denote statistically significant differences (**, $p < 0.01$; ***, $p < 0.001$) (c, d).

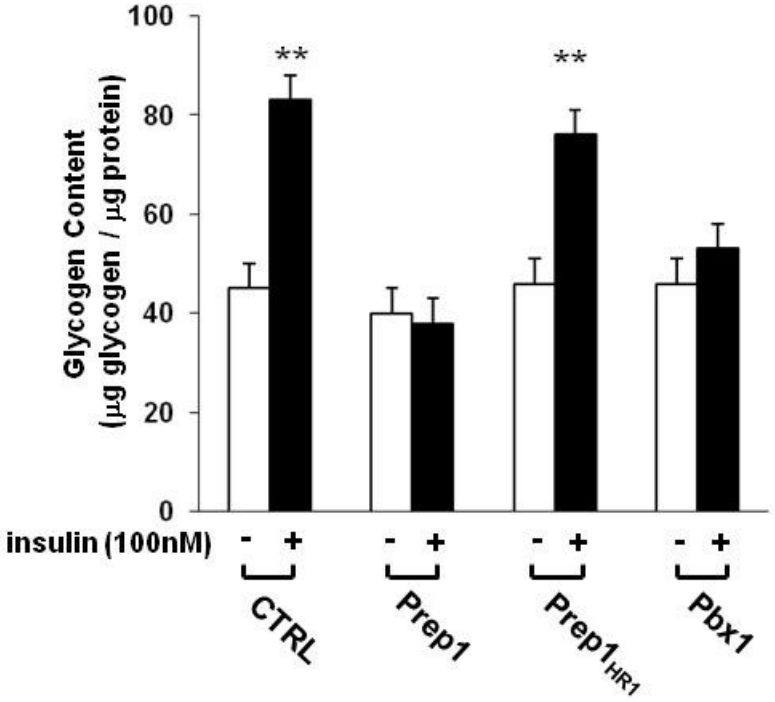

Figure 13. Insulin-induced glycogen storage in HepG2 transfected with Prep1, Pbx1 and Prep1HR1 cDNAs. HepG2 cells were transiently transfected with the Prep1, Pbx1, Prep1HR1 cDNAs and to 100 nM insulin 14-16 hours, glycogen content was assayed as described under "materials and methods" . Bars represent mean values ± SD of determinations in four independent experiments, each in duplicate. Asterisks denote statistically significant differences (**, $p < 0.01$)

These results led me to postulate an important role of Pbx1 in enabling Prep1 control of insulin action in liver cells as well as in the regulation of SYP and SHP1 expression.

Next, I studied the single contribution of SYP and SHP1 in Prep1/Pbx1-regulation of insulin signaling in liver by stably transfecting a Prep1 full-lenght cDNA in the HepG2 cells. Several clones were obtained and three of those, expressing increasing levels of Prep1 were selected and further characterized (figure 14a). The $HepG2_{Prep1c}$ clone overexpressed Prep1 by 5-fold compared to wild type HepG2 cells and featured a 4- and 3-fold increased expression of SYP and SHP1, respectively (figure 14b). Increased SYP and SHP1 levels were also measured in the $HepG2_{Prep1a}$ and $HepG2_{Prep1b}$ cells and directly paralleled the level of Prep1 overexpression achieved in each clone (data not shown). Transient transfection of the $HepG2_{Prep1c}$ cells with phosphorothioate antisense oligonucleotides specific for SYP (SYP-AS) caused a > 65% reduction in SYP levels but elicited almost no change in insulin-stimulated phosphorylation of the insulin receptor, suggesting no

change in insulin action in these cells (figure 14c). At variance, treatment with SHP1 antisense oligonucleotides (SHP1-AS) silenced SHP1 expression by only 50% but increased insulin receptor tyrosine phosphorylation by almost 3-fold (figure 14d). Indeed, the impaired insulin-dependent accumulation of glycogen observed in liver cells overexpressing Prep1 was unaffected by SYP silencing but was rescued by the SHP1 AS (figure 15). Thus, regulation of the SHP1 gene function appeared to represent a mechanism relevant to Prep1 control on insulin signaling and action in the hepatocyte. However, I cannot exclude the fact that there could be a major role for SYP in regulating insulin signaling in a different tissue or in different environmental conditions.

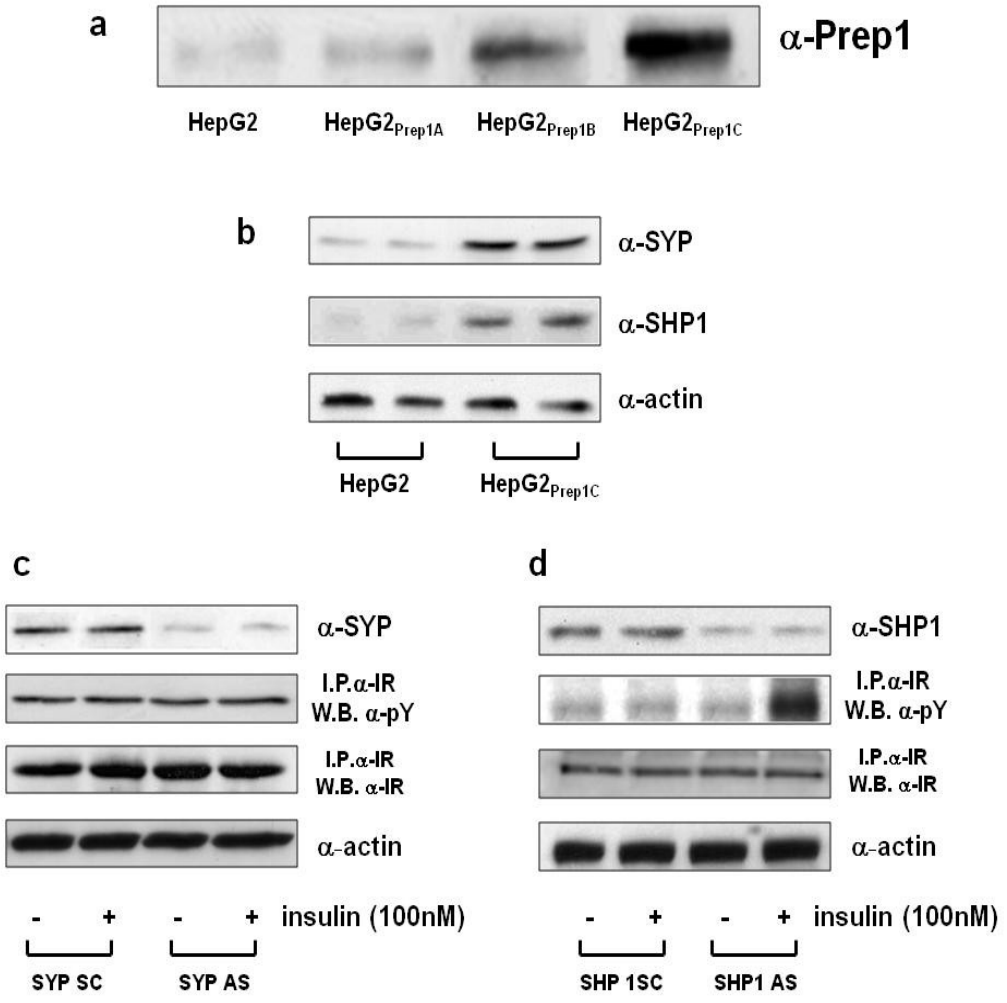

Figure 14. Effect of SYP and SHP1 silencing in HePG2 cells stably transfected with Prep1 cDNA. HepG2 cells were stably transfected with the Prep1 cDNA. Clones HepG2Prep1A,

HepG2Prep1B, HepG2Prep1C were subjected to western blot analysis, blotted with Prep1 antibodies, and compared with control cells (HepG2) (a). Cell lysates from HepG2 or HepG2Prep1c cells were blotted with anti SYP, SHP1 and actin antibodies. HepG2 and HepG2Prep1c cells were transfected with SYP (SYP-AS) (c) or SHP1 (SHP1-AS) (d) specific phosphorothioate antisense oligonucleotides, then stimulated with 100nM insulin for 5 minutes and the insulin receptor was immunoprecipitated with specific antibodies and followed by blotting with either pY and IR antibodies. For control, total lysates were blotted with anti SYP (c) or SHP1 (d) and actin antibodies. The autoradiographs shown are representative of three independent experiments.

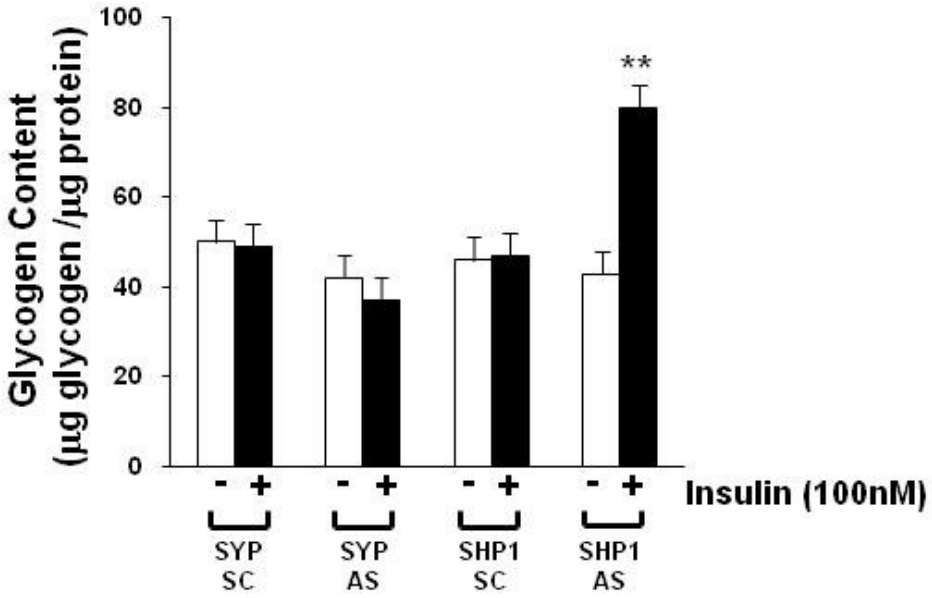

Figure 15. Insulin-induced glycogen accumulation in HepG2 cells stably overexpressing Prep1 interfered with SYP and SHP1 antisense oligonucleotides. Cells were stimulated with 100nM insulin for 14-16 hours, afterwards, glycogen content was assayed as described under "Materials and Methods". Bars represent mean values ± SD of determinations in four independent experiments, each in duplicate. Asterisks denote statistically significant differences (**, $p < 0.01$).

Understanding how Prep1-Pbx1 might regulate the expression of *SHP1* gene is a critical point to better define the action of this transcription complex in modulating insulin action in liver cells. I therefore examined the further possibility that the transcription complex Prep1-Pbx1 might directly regulates *SHP1* gene transcription. To address this hypothesis, I performed a bioinformatic analysis of 4000 base pairs region upstream the ATG codon of *SHP1* gene searching potential binding sites for the Prep1 and Pbx1 complex. This analysis revealed the presence of at least 7 potential binding sites resumed in the table 2. Interestingly, these sequences were arranged in 3 clusters, indicated as SHP1 n.1, n.2, n.3 mapping from -2489 to -2139bp, -2113 to -1778bp, -1680 to -1350bp respectively from the ATG codon (figure 16). As negative control, I also analyzed the sequence

upstream *PTP-1B* gene whose expression was not modified by Prep1 and, interestingly, this sequence showed only 2 binding sites from -3895 to 3879bp and -1004 to 988bp indicated as PTP-1B n.1 and n.2.

Prep1/Pbx1 consensus sequences

	Prep1/Pbx1
SHP1	7
PTP-1B	2

Table 2. Bioinformatic analysis of 4000 bp upstream the ATG codon of *SHP1* and *PTP-1B* genes. Mouse sequences of 4000 bp uspstream the ATG codon of *SHP1* and *PTP-1B* genes were analyzed through *Matinspector* bioinformatic software. The table indicates the potential binding sites for Prep1-Pbx1 complex which showed a score of 1 (range 0-1).

To validate the regions putatively bound by Prep1 and Pbx1 complex I performed chromatin immunoprecipitation (ChIP) and re-chromatin immunoprecipitation (re-ChIP) experiments in NmuLi mouse liver cell line. ChIP experiments confirmed that sites from -2489 to -2139bp and -2113 to -1778bp (SHP1 n.1 and n.2) were consistently bound by Prep1, importantly, re-ChIP assays revealed that Pbx1 was simultaneously present only at position -2113 to -1778bp (SHP1 n.2) (figure 16). Consistent with the lack of Prep1 regulation, no Prep1/Pbx1 complex was detected at any of the potential binding sites identified in the PTP-1B regulatory region by sequence analysis (figure 16). The results obtained with ChIP and re-ChIP procedures confirmed the binding of the Prep1-Pbx1 complex on the region -2113 to -1778bp upstream the ATG codon of *SHP1* gene.

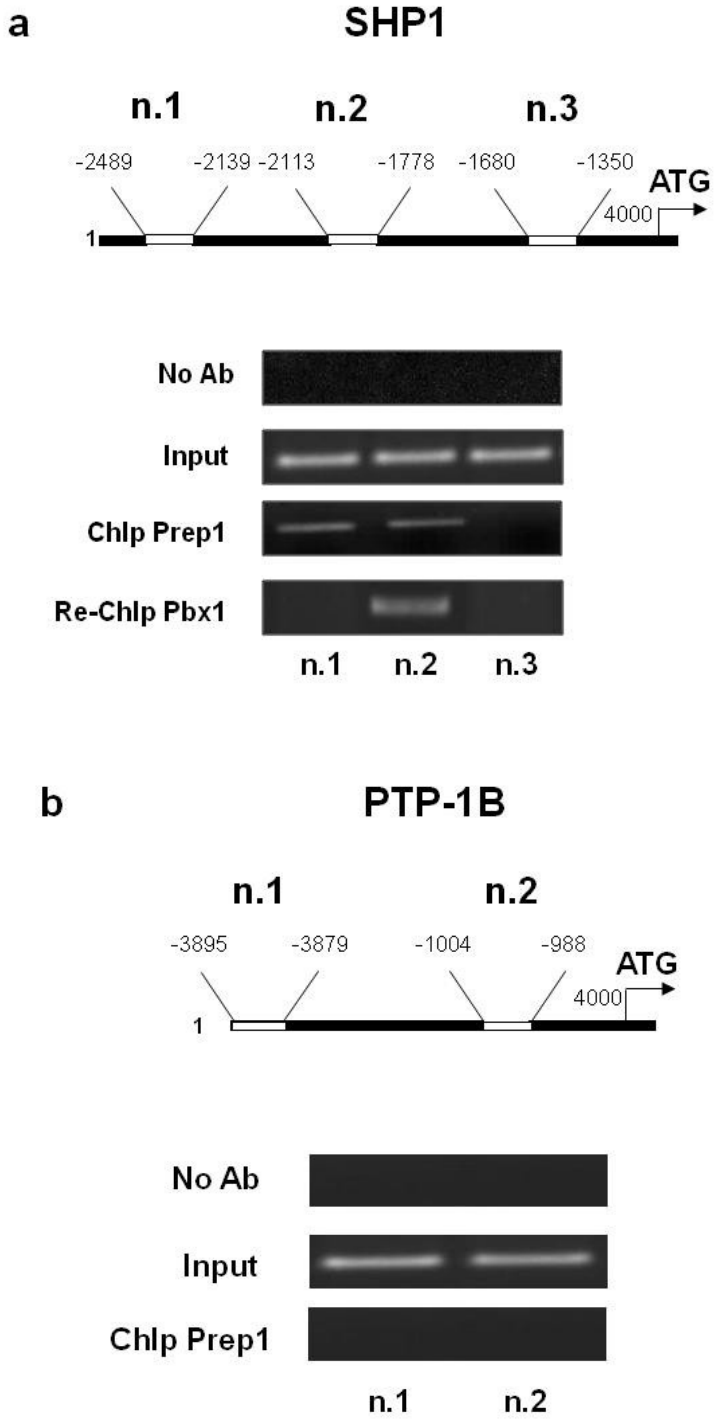

Figure 16. ChIP and re-ChIP on the sequences upstream ATG codon of *SHP1* and *PTP-1B* genes. Soluble chromatin was prepared from NMuLi mouse liver cells and immunoprecipitated with Prep1 antibodies. Total (input) and immunoprecipitated DNAs were amplified by PCR

analysis using primer pairs covering *SHP1* sequences n.1, n.2, n.3 (a) and *PTP-1B* sequences n.1, n.2 (b). Re-ChIP assay (a) with Pbx1 antibodies was performed as described in "Material and Methods".

To investigate whether this region (SHP1 n.2) might have a functional activity luciferase assays were performed. In particular, the region SHP1 n.2 was cloned into *PGL3promoter vector* plasmid upstream the *luciferase* reporter gene and SV40 promoter sequence. The construct was then co-transfected in HeLa cells together with the Prep1, Pbx1 or both plasmid cDNAs and luciferase activity was measured (figure). Prep1 and Pbx1 increased the SHP1 reporter gene activity, respectively, by 7.1 and 6-fold. Furthermore, simultneous co-transfection of the two plasmids caused an almost 30-fold induction, indicating SHP1 transcriptional regulation by the Prep1-Pbx1 complex (figure 17).

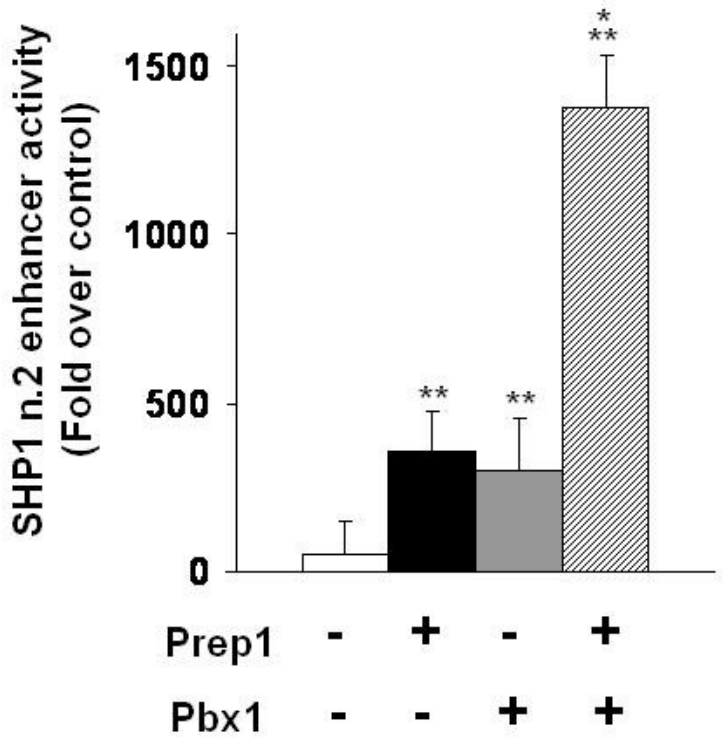

Figure 17. Luciferase activity of SHP1 -2113 to -1778bp region. HeLa cells were transfected with 2μg of the SHP1 enhancer-luciferase construct alone or in combination with Prep1 (2μg), Pbx1 (2μg) or both the cDNA plasmids. Luciferase activity was assayed and normalized as described in Material and Methods. Bars represent mean values ± SD of determinations in four independent experiments. Asterisks denote statistically significant differences (**, $p < 0.01$; ***, $p < 0.001$).

These results indicated that the transcription complex Prep1-Pbx1 may directly bind consensus sequences upstream the ATG codon of *SHP1* gene and directly up-regulate its promoter activity. In particular, since the plasmid which I have used to perform the luciferase assays already have a promoter sequence (SV40), the results indicated that the sequence SHP1 n.2 which I have cloned upstream this promoter has an enhancer activity in response to Prep1-Pbx1 complex. However, if the region SHP1 n.2 also has a promoter activity is currently under investigation, but the relatively large distance from the ATG codon (-2113 base pairs) makes unfavourable this hypothesis.

Additional data in my possess collected by ChIP procedures and luciferase assays indicated that SYP tyrosine phosphatases may also be directly regulated by Prep1-Pbx1 complex but the results obtained after the silencing of the single phosphatases (figure 15) induced me to focus my attention on SHP1 and its transcriptional regulation. How and, above all, in which tissue SYP may contribute in Prep1-dependent insulin action is actually another field of my research activity.

The quest of tyrosine phosphatases and their action is always been controversial and debated. In this work I have identified a novel transcription complex which may directly be involved in the regulation of at least 2 tyrosine phosphatases in liver cells and in mouse liver which may modulate insulin action.

CONCLUSIONS

Insulin-dependent liver glucoregulatory function plays a central role in glucose metabolism and it is known to be modulated by a number of different mechanisms. In the present work I have focused my attention on Prep1 action on hepatic glucose metabolism. I have described that Prep1 deficiency in animal models improves insulin signaling in liver increasing glycogen storage and reducing glucose output. These effects are paralleled by a significant reduction of expression of SYP and SHP1 tyrosine phosphatases. In particular, expression of SHP1 in animal and cellular models negatively correlates with insulin signaling. This evidence led me to focus the research activity on the transcriptional regulation of SHP1 by the Prep1-Pbx1 complex. In this context, I have shown that Prep1-Pbx1 may enhance *SHP1* gene transcription by acting on regulatory sequences upstream the ATG codon.

In conclusion, these findings have contributed to underline the link between the TALE proteins and insulin-resistance and/or diabetes and to clarify the role of tyrosine phosphatases on hepatic insulin-resistance.

ACKNOWLEDGEMENTS

I'd like to say thanks to:

Prof. Francesco Beguinot, for giving me the opportunity to work in his lab, believing in me and demonstrating to me everyday, by example, what devotion to work means.

Prof. Pietro Formisano, for all the time he has spent helping me, for his ability to be a guidance and for the pleasant atmosphere he is able to create even during the worst moments of this work.

Dr. Francesco Oriente, for the time spent discussing data, helping me with constructive suggestions and for passion for reaserch he transmitted me.

Dr. Serena Cabaro whose day by day help was essential to this work and to me.

Dr. Giuseppe Perruolo, Iolanda Esposito, Vittoria D'Esposito, Francesca Fiory and everyone in the lab, everyone of you, one way or another, has given me something special.

Dr. Anand Selvaraj (Anando), Ruth Gutierrez-Aguilar (Ruthita), Paulo Martins (Brazilian guy), Stefano Fumagalli (Smoked Chikens), Massimiliano Olivieri (Uè Uè Massimino), even if you are in a different Country, I will never forget the funny moments spent togheter.

Gaetano Cecere, Carmela Passaro, Domenico Del Prete, Ivana Ferriol, quando penso ad un vero amico mi spuntate in mente voi! La dimostrazione pratica del significato di amicizia… Nei momenti più difficili della mia vita mi siete stati vicini come dei fratelli! Vi voglio bene.

Ancora una volta… la mia famiglia… Mamma, Papà e Giuseppe, quello che sono e che diventerò è stato e sarà soltanto merito vostro! Farete sempre parte dei miei successi.

Last but not the least, Dr. Ginevra Botta, in questi anni ne abbiamo passate tante, ci siamo persi per un istante e ci siamo ritrovati in un attimo… Mi dai la forza e l'entusiasmo per andare avanti in questo lavoro… Insieme a te diventerò una "stella"...

REFERENCES

Alessi DR, James SR, Downes CP, Holmes AB, Gaffney PR, Reese CB, Cohen P. Characterization of a 3-phosphoinositide-dependent protein kinase which phosphorylates and activates protein kinase B alpha. Curr. Biol. 1997; 7:261–269.

Arrandale, J.M., Gore-Willse, A., Rocks, S., Ren, J.M., Zhu, J., Davis, A., Livingston, J.N. & Rabin,D.U. Insulin signaling in mice expressing reduced levels of Syp. J. Biol. Chem. 1996; 271:21353-21358.

Altshuler D, Hirschhorn JN, Klannemark M, Lindgren CM, Vohl MC, Nemesh J, Lane CR, Schaffner SF, Bolk S, Brewer C, Tuomi T, Gaudet D, Hudson TJ, Daly M, Groop L, Lander ES. The common PPARγ Pro12Ala polymorphism is associated with decreased risk of type 2 diabetes. Nature Genet. 2000; 26:76–80.

Bergman R. N. & Ader, M. Free fatty acids and pathogenesis of type 2 diabetes mellitus. Trends Endocrinol. Metab. 2000; 11:351–356.

Bergman R. N. New concepts in extracellular signaling for insulin action: the single gateway hypothesis. Recent Prog. Horm. Res. 1997; 52:359–385.

Berthelsen J., Vandekerkhove J., Blasi F. Purification and characterization of UEF3, a novel factor involved in the regulation of the urokinase and other AP-1 controlled promoters. J. Biol. Chem. 1996; 271:3822-3830.

Berthelsen J., Zappavigna V., Mavillo F., Blasi F. Prep1, a novel functional partner of Pbx proteins. EMBO J. 1998; 17:1423-1433.

Berthelsen J., Kilstrup-Nielsen C., Blasi F., Mavillo F., Zappavigna V. The subcellular lacalization of PBX1 and EXD proteins depends on nuclear import ans export signals and is modulated by association with PREP1 and HTH. Gen. Dev. 1999; 13:946-953.

Boulton TG, Nye SH, Robbins DJ, Ip NY, Radziejewska E, Morgenbesser SD, DePinho RA, Panayotatos N, Cobb MH, Yancopoulos GD. ERKs: a family of protein-serine/threonine kinases that are activated and tyrosine phosphorylated in response to insulin and NGF. Cell 1991; 65:663– 675.

Bousquet C, Delesque N, Lopez F, Saint-Laurent N, Estève JP, Bedecs K, Buscail L, Vaysse N, Susini C. sst2 somatostatin receptor mediates negative regulation of

insulin receptor signaling through the tyrosine phosphatase SHP-1. J Biol. Chem. 1998; 273: 7099-7106.

Brendolan A., Ferretti E., Salsi V., Moses K., Quaggiù S., Blasi F., Cleary M.L., Selleri L. A Pbx1-dependent genetic and transcriptional network regulates spleen ontogeny. Development 2005; 132:3113-3126.

Burglin T.R. Analysis of TALE superclass homeobox genes (MEIS, PBC, KNOX, Iroquois, TGIF) reveals a novel domain conserved between plants and animals. Nucleic Acids Res. 1997; 25:4173-4180.

Cross DA, Alessi DR, Vandenheede JR, McDowell HE, Hundal HS, Cohen P. The inhibition of glycogen synthase kinase-3 by insulin or insulin-like growth factor 1 in the rat skeletal muscle cell line L6 is blocked by wortmannin, but not by rapamycin: evidence that wortmannin blocks activation of the mitogen-activated protein kinase pathway in L6 cells between Ras and Raf. Biochem. J. 1994; 303:21-27.

Diabetes Atlas 2006, 3rd ed., International Diabetes Federation, 2006.

Dubois MJ, Bergeron S, Kim HJ, Dombrowski L, Perreault M, Fournès B, Faure R, Olivier M, Beauchemin N, Shulman GI, Siminovitch KA, Kim JK, Marette A. The SHP-1 protein tyrosine phosphatase negatively modulates glucose homeostasis. Nat. Med. 2006; 12:549-556.

Elchebly, M., Payette, P., Michaliszyn, E., Cromlish, W., Collins, S., Loy, A.L., Normandin, D., Cheng, A., Himms-Hagen, J., Chan, C.C., Ramachandran, C., Gresser, M.J., Tremblay, M.L. & Kennedy, B.P. Increased insulin sensitivity and obesity resistance in mice lacking the protein tyrosine phosphatase-1B gene. Science 1999; 283:1544-1548.

Featherstone M.. Hox proteins and their co-factors in transcriptional regulation. Adv. Dev. Biol. Biochem. 2003; 13:1569-1799.

Feng, G.S. Shp-2 tyrosine phosphatase: signaling one cell or many. Exp. Cell Res. 1999; 253:47-54.

Ferretti E, Villaescusa JC, Di Rosa P, Fernandez-Diaz LC, Longobardi E, Mazzieri R, Miccio A, Micali N, Selleri L, Ferrari G, Blasi F. Hypomorphic mutation of the TALE gene Prep1 (pKnox1) causes a major reduction of Pbx and Meis proteins and a pleiotropic embryonic phenotype. Mol. Cell. Biol. 2006; 26:5650-5662.

Frangioni, J.V., Beahm, P.H., Shifrin, V., Jost, C.A. & Neel, B.G. The nontransmembrane tyrosine phosphatase PTP-1B localizes to the endoplasmic reticulum via its 35 amino acid C-terminal sequence. Cell 1992; 68:545-560.

Goldstein, B.J., Bittner-Kowalczyk, A., White, M.F. & Harbeck,M. Tyrosine dephosphorylation and deactivation of insulin receptor substrate-1 by protein-tyrosine phosphatase 1B. Possible facilitation by the formation of a ternary complex with the Grb2 adaptor protein. J. Biol. Chem. 2000; 275:4283-4289.

Goudet G., Delhalle S., Biemar F., Martial J.A., Peers B. Functional and cooperative interactions between the homeodomain PDX1, Pbx, and Prep1 factors on the somatostatin promoter. J. Biol. Chem. 1999; 274:4067-4073.

Gudmundsson J, Sulem P, Steinthorsdottir V, Bergthorsson JT, Thorleifsson G, Manolescu A, Rafnar T, Gudbjartsson D, Agnarsson BA, Baker A, Sigurdsson A, Benediktsdottir KR, Jakobsdottir M, Blondal T, Stacey SN, Helgason A, Gunnarsdottir S, Olafsdottir A, Kristinsson KT, Birgisdottir B, Ghosh S, Thorlacius S, Magnusdottir D, Stefansdottir G, Kristjansson K, Bagger Y, Wilensky RL, Reilly MP, Morris AD, Kimber CH, Adeyemo A, Chen Y, Zhou J, So WY, Tong PC, Ng MC, Hansen T, Andersen G, Borch-Johnsen K, Jorgensen T, Tres A, Fuertes F, Ruiz-Echarri M, Asin L, Saez B, van Boven E, Klaver S, Swinkels DW, Aben KK, Graif T, Cashy J, Suarez BK, van Vierssen Trip O, Frigge ML, Ober C, Hofker MH, Wijmenga C, Christiansen C, Rader DJ, Palmer CN, Rotimi C, Chan JC, Pedersen O, Sigurdsson G, Benediktsson R, Jonsson E, Einarsson GV, Mayordomo JI, Catalona WJ, Kiemeney LA, Barkardottir RB, Gulcher JR, Thorsteinsdottir U, Kong A, Stefansson K. Two variants on chromosome 17 confer prostate cancer risk, and the one in TCF2 protects against type 2 diabetes. Nature Genet. 2007; 39:977–983.

Herzig S., Fuzesi L., Knepel W. Heterodimeric Pbx-Prep1 homeodomain protein binding to the glucagon gene restricting transcription in a cell type dependent manner. J. Biol. Chem. 2000; 275:27989-27999.

Kahn CR. Insulin action, diabetogenes, and the cause of type II diabetes. Diabetes 1994; 43:1066-1084.

Kim S.K., Selleri L., Lee J.S., Zhang A.Y., Gu X., Jacobs Y., Cleary M.L. Pbx1 inactivation disrupts pancreas development and in Ipf1 deficient mice promotes diabetes mellitus. Nat. Genet. 2002; 30: 430-435.

Klaman, L.D., Boss, O., Peroni, O.D., Kim, J.K., Martino, J.L., Zabolotny, J.M., Moghal, N., Lubkin, M., Kim, Y.B., Sharpe, A.H., Stricker-Krongrad, A., Shulman, G.I., Neel, B.G. & Kahn, B.B. Increased energy expenditure, decreased adiposity, and tissue-specific insulin sensitivity in protein-tyrosine phospha- tase 1B-deficient mice. Mol. Cell. Biol. 2000; 20:5479-5489.

Kuhne, M.R., Zhao, Z., Rowles, J., Lavan, B.E., Shen, S.H., Fischer, E.H. & Lienhard, G.E. Dephosphorylation of insulin receptor substrate 1 by the tyrosine phosphatase PTP2C. J. Biol. Chem. 1994; 269:15833-15837.

Lietzke SE, Bose S, Cronin T, Klarlund J, Chawla A, Czech MP, Lambright DG. Structural basis of 3-phosphoinositide recognition by pleckstrin homology domains. Mol. Cell. 2000; 6:385–394.

Maegawa H, Hasegawa M, Sugai S, Obata T, Ugi S, Morino K, Egawa K, Fujita T, Sakamoto T, Nishio Y, Kojima H, Haneda M, Yasuda H, Kikkawa R, Kashiwagi A. Expression of a dominant negative SHP-2 in transgenic mice induces insulin resistance. J. Biol. Chem. 1999; 274:30236–30243.

Michael MD, Kulkarni RN, Postic C, Previs SF, Shulman GI, Magnuson MA, Kahn CR. Loss of insulin signaling in hepatocytes leads to severe insulin resistance and progressive hepatic dysfunction. Mol. Cell. 2000; 6:87-97.

Moens CB, Selleri L. Hox cofactors in vertebrate development. Dev. Biol. 2006; 291:193-206.

Myers MG Jr, Backer JM, Sun XJ, Shoelson S, Hu P, Schlessinger J, Yoakim M, Schaffhausen B, White MF. IRS-1 activates phosphatidylinositol 38-kinase by associating with src homology 2 domains of p85. Proc Natl Acad Sci USA 1992; 89:10350–10354.

Nakae J., Park, B.C. & Accili, D. Insulin stimulates phosphorylation of the forkhead transcription factor FKHR on serine 253 through a Wortmannin-sensitive pathway. J. Biol. Chem. 1999; 274:15982–15985.

Newgard, C. B., Brady, M. J., O'Doherty, R. M. & Saltiel, A. R. Organizing glucose disposal: emerging roles of the glycogen targeting subunits of protein phosphatase-1. Diabetes 2000; 49: 1967–1977.

Nielsen EM, Hansen L, Carstensen B, Echwald SM, Drivsholm T, Glumer C, Thorsteinsson B, Borch-Johnsen K, Hansen T, Pedersen O. The E23K variant of

Kir6.2 associates with impaired post-OGTT serum insulin response and increased risk of type 2 diabetes. Diabetes 2003; 52:573-577.

Nourse J., Mellentin J.D., Galili N., Wilkinson J., Stambridge E., Smith S.D., Cleary M.L. Chromosomal traslocation t(1;19) results in synthesis of a homeobox fusion mRNA that codes for a potential chimeric transcription factor. Cell 1990; 60:535-545.

Owen KR, McCarthy MI. Genetics of type 2 diabetes. Curr. Op. Gen. Dev. 2007; 17:239–244.

Oriente F, Fernandez Diaz LC, Miele C, Iovino S, Mori S, Diaz VM, Troncone G, Cassese A, Formisano P, Blasi F, Beguinot F. Prep1 deficiency induces protection from diabetes and increased insulin sensitivity through a p160-mediated mechanism. Mol. Cell. Biol. 2008; 28:5634-5645.

Patti ME, Kahn CR. The insulin receptor-a critical link in glucose homeostasis and insulin action. J. Basic Clin. Physiol. Pharmacol. 1998; 9:89–109.

Pessin JE, Saltiel AR. Signaling pathways in insulin action: molecular targets of insulin resistance. J. Cli. Invest. 2000; 106:165–169.

Pickup JC, Williams G, editors.Textbook of Diabetes: selected chapters. 3rd ed. Oxford: Blackwell Publishing, 2005.

Pilkis, S. J. & Granner, D. K. Molecular physiology of the regulation of hepatic gluconeogenesis and glycolysis. Annu. Rev. Physiol. 1992; 54:885–909.

Piper D.E., Batchelor A.H., Chang C. P., Cleary M. L., Wolberg C. Structure of HoxB1-Pbx heterodimer bound to DNA: role of the exapaptide and a fourth homeodomain helix in complex formation. Cell 1999; 96:587-597.

Saltiel AR, Kahn CR. Insulin signalling and the regulation of glucose and lipidmetabolism. Nature 2001; 414:799-806.

Sandhu MS, Weedon MN, Fawcett KA, Wasson J, Debenham SL, Daly A, Lango H, Frayling TM, Neumann RJ, Sherva R, Blech I, Pharoah PD, Palmer CN, Kimber C, Tavendale R, Morris AD, McCarthy MI, Walker M, Hitman G, Glaser B, Permutt MA, Hattersley AT, Wareham NJ, Barroso I. Common variants in WFS1 confer risk of type 2 diabetes. Nature Genet. 2007; 39:951–953.

Saxton, T.M., Henkemeyer, M., Gasca, S., Shen, R., Rossi, D.J., Shalaby, F., Feng,G.S.&Pawson, T. Abnormalmesoderm patterning in mouse embryos mutant for the SH2 tyrosine phosphatase Shp-2. EMBO J. 1997; 16:2352-2364.

Selleri L., Depew M.J., Jacobs Y., Chanda S.K., Tsang K.Y., Cheah K.S., Rubenstein J.L., O'Gorman S., Cleary M. Requirement for Pbx1 in skeletal patterning and programming chondrocyte proliferation and differentiation. Development 2001; 128:3543-3557.

Shepherd PR, Nave BT, Siddle K. Insulin stimulation of glycogen synthesisand glycogen synthase activity is blocked by wortmannin and rapamycin in 3T3-L1 adipocytes: evidence for the involvement of phosphoinositide 3-kinase and p70 ribosomal protein-S6 kinase. Biochem. J. 1995; 305:25–28.

Standaert ML, Galloway L, Karnam P, Bandyopadhyay G, Moscat J, Farese RV. Protein kinase C-ζ as a downstream effector of phosphatidylinositol 3- kinase during insulin stimulation in rat adipocytes. Potential role in glucose transport. J. Biol. Chem. 1997; 272:30075–30082.

Sutherland, C., O'Brien, R. M. & Granner, D. K. New connections in the regulation of PEPCK gene expression by insulin. Phil. Trans. R. Soc. Lond. 1996; 351:191–199.

Uchida T, Matozaki T, Noguchi T, Yamao T, Horita K, Suzuki T, Fujioka Y, Sakamoto C, Kasuga M. Insulin stimulates the phosphorylation of Tyr538 and the catalytic activity of PTP1C, a protein tyrosine phosphatase with Src homology-2 domains. J. Biol. Chem. 1994; 269:12220-12228.

White MF. The IRS-signalling system: a network of docking proteins that mediate insulin action. Mol Cell Biochem 1998; 182:3–11.

Yoon JC, Puigserver P, Chen G, Donovan J, Wu Z, Rhee J, Adelmant G, Stafford J, Kahn CR, Granner DK, Newgard CB, Spiegelman BM. Control of hepatic gluconeogenesis through the transcriptional coactivator PGC-1. Nature 2001; 413:131-8.

THE JOURNAL OF BIOLOGICAL CHEMISTRY VOL. 282, NO. 12, pp. 8648–8657, March 23, 2007

Phorbol Esters Induce Intracellular Accumulation of the Anti-apoptotic Protein PED/PEA-15 by Preventing Ubiquitinylation and Proteasomal Degradation*

Received for publication, August 31, 2006, and in revised form, December 21, 2006 Published, JBC Papers in Press, January 16, 2007, DOI 10.1074/jbc.M608359200

Anna Perfetti, Francesco Oriente, Salvatore Iovino, A. Teresa Alberobello, Alessia P. M. Barbagallo, Iolanda Esposito, Francesca Fiory, Raffaele Teperino, Paola Ungaro, Claudia Miele, Pietro Formisano[1], and Francesco Beguinot

From the Dipartimento di Biologia e Patologia cellulare e Molecolare (DBPCM) and Istituto di Endocrinologia ed Oncologia Sperimentale del Consiglio Nazionale delle Ricerche, Federico II University of Naples, Via Pansini 5, 80131 Naples, Italy

Phosphoprotein enriched in diabetes/phosphoprotein enriched in astrocytes (PED/PEA)-15 is an anti-apoptotic protein whose expression is increased in several cancer cells and following experimental skin carcinogenesis. Exposure of untransfected C5N keratinocytes and transfected HEK293 cells to phorbol esters (12-*O*-tetradecanoylphorbol-13-acetate (TPA)) increased PED/PEA-15 cellular content and enhanced its phosphorylation at serine 116 in a time-dependent fashion. Ser-116 → Gly (PED_{S116G}) but not Ser-104 → Gly (PED_{S104G}) substitution almost completely abolished TPA regulation of PED/PEA-15 expression. TPA effect was also prevented by antisense inhibition of protein kinase C (PKC)-ζ and by the expression of a dominant-negative PKC-ζ mutant cDNA in HEK293 cells. Similar to long term TPA treatment, overexpression of wild-type PKC-ζ increased cellular content and phosphorylation of WT-PED/PEA-15 and PED_{S104G} but not of PED_{S116G}. These events were accompanied by the activation of Ca^{2+}-calmodulin kinase (CaMK) II and prevented by the CaMK blocker, KN-93. At variance, the proteasome inhibitor lactacystin mimicked TPA action on PED/PEA-15 intracellular accumulation and reverted the effects of PKC-ζ and CaMK inhibition. Moreover, we show that PED/PEA-15 bound ubiquitin in intact cells. PED/PEA-15 ubiquitinylation was reduced by TPA and PKC-ζ overexpression and increased by KN-93 and PKC-ζ block. Furthermore, in HEK293 cells expressing PED_{S116G}, TPA failed to prevent ubiquitin-dependent degradation of the protein. Accordingly, in the same cells, TPA-mediated protection from apoptosis was blunted. Taken together, our results indicate that TPA increases PED/PEA-15 expression at the post-translational level by inducing phosphorylation at serine 116 and preventing ubiquitinylation and proteosomal degradation.

Cancer cells feature both excessive proliferation and abandonment of the ability to die (1, 2). Thus, alterations of genes involved in the control of apoptosis have been implicated in a number of human malignancies. In certain lymphomas, for example, cell death is blocked by excessive production of the anti-apoptotic factor Bcl-2 (2). Similarly, some tumors prevent apoptosis by up-regulating the expression of anti-apoptotic death effector domain (DED)[2]-containing proteins, which, in turn, inhibit Fas from conveying signals to the death machinery (3).

Phosphoprotein enriched in diabetes/phosphoprotein enriched in astrocytes (PED/PEA)-15 is a DED-containing protein originally identified in astrocytes as a protein kinase C (PKC) substrate (4–6) and found overexpressed in insulin target tissues of patients with type 2 diabetes (7). Raised PED/PEA-15 levels have also been detected in several human tumor cell lines (7–9). A growing body of evidence indicates that increased PED/PEA-15 expression may provide a mechanism to escape cell death upon a number of pro-apoptotic stimuli (10–14). Moreover, in transgenic mice, overexpression of PED/PEA-15 enhances the susceptibility to develop experimentally induced skin tumors (15). The molecular mechanism of PED/PEA-15 anti-apoptotic action has been extensively investigated. In several cell types, PED/PEA-15 blocks Fas- and tumor necrosis factor-α-induced apoptosis by competing with its DED with the interaction between FADD and caspase 8 (10). In addition, in several cell lines of human glioma, PED/PEA-15 inhibits tumor necrosis factor-related apoptosis-inducing ligand (TRAIL)-induced apoptosis, thereby generating resistance to this anti-neoplastic agent (9). At variance with other anti-apoptotic proteins inhibiting caspase 8 activation via FADD trapping (3), PED/PEA-15 overexpression also prevents apoptosis induced by growth factors deprivation, UV exposure, and osmotic stimuli (11, 13).

Besides the anti-apoptotic function, a role for PED/PEA-15 in restraining cell proliferation has been proposed (16–20). It

* This work was supported by Grant LSHM-CT-2004-512013 from the European Community FP6 EUGENE2, grants from the Associazione Italiana per la Ricerca sul Cancro (AIRC) (to F. B. and P. F.) and the Ministero dell'Università e della Ricerca Scientifica Grant PRIN (to F. B. and P. F.) and Grant FIRB RBNE0155LB (to F. B.), and by a grant from Telethon – Italy. The costs of publication of this article were defrayed in part by the payment of page charges. This article must therefore be hereby marked "*advertisement*" in accordance with 18 U.S.C. Section 1734 solely to indicate this fact.

[1] To whom correspondence should be addressed. Dipartimento di Biologia e Patologia Cellulare e Molecolare, Università di Napoli "Federico II," Via S. Pansini 5, 80131 Naples, Italy. Tel.: 39-081-7463608; Fax: 39-081-7463235; E-mail: fpietro@unina.it.

[2] The abbreviations used are: DED, death effector domain; PED/PEA, phosphoprotein enriched in diabetes/phosphoprotein enriched in astrocytes; TPA, 12-*O*-tetradecanoylphorbol-13-acetate; PKB, protein kinase B; PKC, protein kinase C; CaMK, calmodulin kinase; FADD, Fas-associated death domain; HA, hemagglutinin; DMEM, Dulbecco's modified Eagle's medium; RT, reverse transcription; PBS, phosphate-buffered saline; Ab, antibody; ASO, antisense oligonucleotides; DN, dominant-negative; WT, wild type; SO, scrambled.

has been described that PED/PEA-15 directly binds extracellular signal-regulated kinase 2 (ERK2) and RSK2 and prevents their nuclear translocation and transduction of biological effects (16–19). Together with the anti-apoptotic effect, this action may expand cellular senescence (20).

PED/PEA-15 is a phosphorylated protein (4, 5). It has recently been shown that PED/PEA-15 phosphorylation at specific sites controls the ability of the protein to form complexes with specific intracellular interactors (21). PED/PEA-15 serine phosphorylation has also been shown to enhance protein stability (22). Several kinases were evidenced to phosphorylate PED/PEA-15 at specific serines. Ser-104 represents the main target for PKC phosphorylation (4, 5, 23), whereas Ser-116 has been shown to be a target site for both Ca^{2+}-calmodulin kinase (CaMK) II (23) and protein kinase B (PKB)/Akt (22). However, the precise function of these phosphorylation sites in controlling PED/PEA-15 expression is currently unknown. Recent evidence indicates that abnormal accumulation of PED/PEA-15 may lead to derangement of cell growth and metabolism (15, 24, 25).

In this study, we have shown that phorbol esters, which are tumor promoters and inhibitors of insulin action, up-regulate PED/PEA-15 expression by inhibiting its ubiquitinylation and proteasomal targeting. This effect involves activation of CaMKII and subsequent phosphorylation of PED/PEA-15 at Ser-116. PKC-ζ activity is required for phorbol ester-induced activation of CaMKII and for the regulation of PED/PEA-15 degradation.

EXPERIMENTAL PROCEDURES

Materials—Media, sera, and antibiotics for cell culture and the Lipofectamine reagent were purchased from Invitrogen (Paisley, UK). Rabbit polyclonal PKC-α, PKC-β, PKC-δ, PKC-ζ, and phospho-PKC antibodies were from Santa Cruz Biotechnology (Santa Cruz, CA). PED/PEA-15, p-Ser-104PED, and p-Ser-116PED and antibodies have been previously reported (7, 22). Mouse monoclonal polyubiquitinylated protein antibodies (FK1) were from Biomol International. Mouse monoclonal HA antibody were from Roche Applied Science. Phosphorothioate PKC-α, PKC-β, PKC-δ, PKC-ζ antisense and scrambled control oligonucleotides have been previously described (26–28) and were synthesized by PRIMM (Milan, Italy). PKC-ζ wild-type and dominant-negative constructs were kindly provided by Dr. M. S. Marber (St. Thomas Hospital, London, UK) and Dr. S.Gutkind (NCI, National Institutes of Health, Bethesda, MD), respectively. SDS-PAGE reagents were purchased from Bio-Rad. Western blotting and ECL reagents and radiochemicals were from Amersham Biosciences. All other reagents were from Sigma.

Plasmid Preparation, Cell Culture, and Transfection—The PED_{S104G} and PED_{S116G} mutant cDNAs were prepared by using pcDNAIIIPEDY1 cDNA (pcDNAIII containing His_6-Myc-tagged PED/PEA-15) as template with the site-directed mutagenesis kit by Promega according to the manufacturer's instructions. Stable expression of the mutants and wild-type PEDY1 cDNAs in HEK293 cells (293_{PEDY1}) was achieved as reported in Condorelli *et al.* (11). The cells were cultured in Dulbecco's modified Eagle's medium (DMEM) supplemented with 10% fetal calf serum, 100 IU of penicillin/ml, 100 IU of streptomycin/ml, and 2% L-glutamine in a humidified CO_2 incubator. Transient transfection of phosphorothioate oligonucleotides and plasmid DNA in HEK293 cells was accomplished by using the Lipofectamine method according to the manufacturer's instructions. Briefly, the cells were cultured in 60-mm-diameter dishes and incubated for 24 h in serum-free DMEM supplemented with 3 μg of cDNA and 15 μl of Lipofectamine reagent. An equal volume of DMEM supplemented with 20% fetal calf serum was then added for 5 h followed by replacement with DMEM supplemented with 10% serum for 24 h before the assays.

Western Blot Analysis—For Western blotting, cells were solubilized in lysis buffer (50 mM HEPES (pH 7.5), 150 mM NaCl, 4 mM EDTA, 10 mM Na_4PO_7, 2 mM Na_3VO_4, 100 mM NaF, 10% glycerol, 1% Triton X-100, 1 mM phenylmethylsulfonyl fluoride, 100 mg of aprotinin/ml, 1 mM leupeptin) for 60 min at 4 °C. Cell lysates were clarified at 5,000 × *g* for 15 min. Solubilized proteins were then separated by SDS-PAGE and transferred onto 0.45-μm-pore size Immobilon-P membranes (Millipore, Bedford, MA). Upon incubation with the primary (PED, etc.) antibody and secondary antibodies, immunoreactive bands were detected by ECL according to the manufacturer's instructions.

Real-time RT-PCR Analysis—Total cellular RNA was isolated from C5N cells by the use of RNeasy kit (Qiagen) according to the manufacturer's instructions. For real-time RT-PCR analysis, 1 μg of cell RNA was reverse-transcribed using SuperScript II reverse transcriptase (Invitrogen). PCR reaction mixes were analyzed using SYBR Green mix (Invitrogen). Reactions were performed using Platinum SYBR Green quantitative PCR Super-UDG using an iCycler IQ multicolor real-time PCR detection system (Bio-Rad). All reactions were performed in triplicate, and β-actin was used as an internal standard. Primer sequences used were as follows: PED/PEA-15, forward, 5′-TTCCCGCTGTTCCCTTAGG-3′, and PED/PEA-15, reverse 5′-TCTGGCTCATCCGCATCC-3′.

Immunoprecipitation of PED/PEA-15—Cells grown in 100-mm Petri dishes were treated as indicated and washed once with ice-cold PBS and solubilized in lysis buffer for 2 h at 4 °C. Then, lysates were clarified by centrifugation at 5,000 × *g* for 20 min. 500 μg of protein lysates was immunoprecipitated with Myc or PED antibodies for 16 h. The precipitates were incubated with protein G-Sepharose beads at 4 °C for 1 h with shaking. Beads were precipitated by centrifugation at 1,000 × *g* for 5 min at 4 °C and washed five times with ice-cold washing buffer. After the final wash, the pellets were resuspended in 30 μl of 1× SDS electrophoresis buffer and heated to 95 °C for 5 min prior to protein separation by 15% SDS-PAGE. Western blot analysis was performed as described above.

Purification of Ubiquitin-PED/PEA-15 Conjugates—Cellular ubiquitinylation assay was performed as described by Musti *et al.* (29). Briefly, 24 h after transfection, cells expressing His-tagged-PED/PEA-15 (PED/PEA-15Y1) and HA-ubiquitin were harvested in 2 ml of 6 M guanidium-HCl, 0.1 M Na_2HPO_4/NaH_2PO_4 (pH 8) plus 5 mM imidazole/100-mm dish and sonicated with a Branson micro-tipped sonifier for 30 s to reduce viscosity. Lysates were mixed on a rotator with 0.2 ml (settled volume) of Ni^{2+}-nitrilotriacetic acid-agarose (Qiagen) for 4 h at room temperature. The slurry was applied to a Bio-Rad Econo-Col-

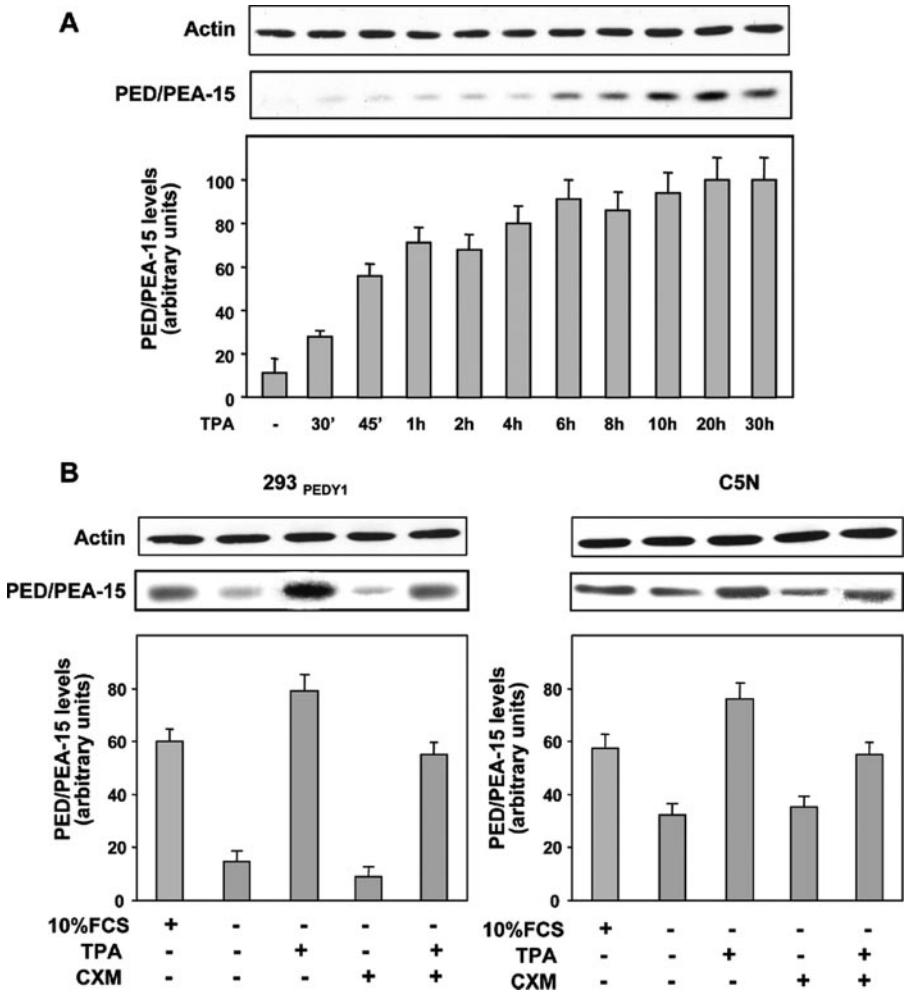

FIGURE 1. **TPA effect on PED/PEA-15 protein expression.** *A*, 293_{PEDY1} cells were serum-starved for 40 h and stimulated with 1 μM TPA for the indicated times. Cell lysates were separated on SDS-PAGE and immunoblotted with PED Ab. Filters have been analyzed by laser densitometry. The *error bars* represent the mean ± S.D. of the densitometric analyses. *B*, 293_{PEDY1} cells (*left panel*) and C5N keratinocytes (*right panel*) were serum-starved, as indicated, and treated with 1 μM TPA for 20 h in the absence or in the presence of 40 μg/ml cycloheximide (*CXM*). Cell lysates were then analyzed by PED immunoblot, and the results were quantitated by laser densitometry. The autoradiographs shown are representative of three (*A*) and four (*B*) independent experiments.

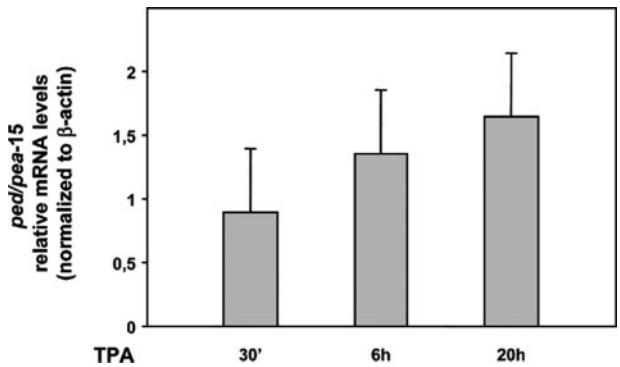

FIGURE 2. **TPA effect on PED/PEA-15 mRNA levels.** The abundance of mRNAs for PED/PEA-15 was determined by real-time RT-PCR analysis of total RNA isolated from C5N cells following treatment with TPA (1 μM) for the indicated times, using β-actin as internal standard. The mRNA levels in TPA-stimulated cells are relative to those in control cells. Each *error bar* represents the mean ± S.D. of four independent experiments in each of which reactions were performed in triplicate.

umn. The column was successively washed with the following: 1 ml of 6 M guanidium-HCl, 0.1 M Na_2 HPO_4, NaH_2 PO_4 (pH 8); 2 ml of 6 M guanidium-HCl, 0.1 M Na_2 HPO_4, NaH_2 PO_4 (pH 5.8); 1 ml of 6 M guanidium-HCl, 0.1 M Na_2 HPO_4, NaH_2 PO_4 (pH 8); 2 ml of (6 M guanidium-HCl, 0.1 M Na_2 HPO_4, NaH_2 PO_4 (pH 8), protein buffer) 1:1; 2 ml of (6 M guanidium-HCl, 0.1 M Na_2 HPO_4, NaH_2 PO_4 (pH 8), protein buffer) 1:3; 2 ml of protein buffer; 1 ml of protein buffer plus 10 mM imidazole. Elution was performed with 1 ml of protein buffer plus 200 mM imidazole. Protein buffer is 50 mM Na_2 HPO_4, NaH_2 PO_4 (pH 8), 100 mM KCl, 20% glycerol, and 0.2% Nonidet P-40. The eluate was trichloroacetic acid-precipitated for further analysis by Western blot with HA antibody.

Cell Death Analysis by Flow Cytometry—Cells were harvested and suspended in the sample buffer (PBS + 2% fetal bovine serum; PBS + 0.1% bovine serum albumin) and washed and resuspended in 0.3 ml of PBS. After adding 0.7 ml of cold absolute ethanol, cells were fixed for at least 2 h at −20 °C, washed twice, and resuspended in 0.4 ml of PBS. Samples were then incubated with 20 μl of propidium iodide (1 mg/ml stock solution) and 2 μl of RNaseA (500 mg/ml stock solution) in dark for 30 min at room temperature. Samples were stored at 4 °C until analyzed by flow cytometry.

RESULTS

Regulation of PED/PEA-15 Protein Expression by Phorbol Esters—The expression of PED/PEA-15 is up-regulated by phorbol myristate acetate (TPA) in the mouse skin upon experimental carcinogenesis as well as in different human tumors (7–9, 15). To investigate the molecular mechanisms regulating PED/PEA-15 expression, HEK-293 cells, stably transfected with PED/PEA-15 cDNA (293_{PEDY1}), were incubated with serum-free medium in the absence or in the presence of 1 μM TPA. Treatment of 293_{PEDY1} cells with TPA increased PED/PEA-15 levels in a time-dependent manner (Fig. 1*A*). Serum deprivation alone was sufficient to reduce PED/PEA-15 protein levels by >3-fold (Fig. 1*B*). This decrease was totally reverted by the simultaneous exposure to TPA. Pretreatment of the cells with the protein synthesis inhibitor cycloheximide (40 μg/ml) reduced TPA effect by only 25% (Fig. 1*B*, *left panel*). Similar results were also obtained by evaluating the levels of PED/PEA-15 in C5N keratinocytes, expressing only the endogenous compendium of the protein (Fig. 1*B*, *right panel*). Moreover, as shown in Fig. 2, PED/PEA-15 mRNA was also increased in untransfected C5N cells following 6 and 20 h of TPA treatment. Thus, TPA up-regulates PED/PEA-15 mRNA and protein

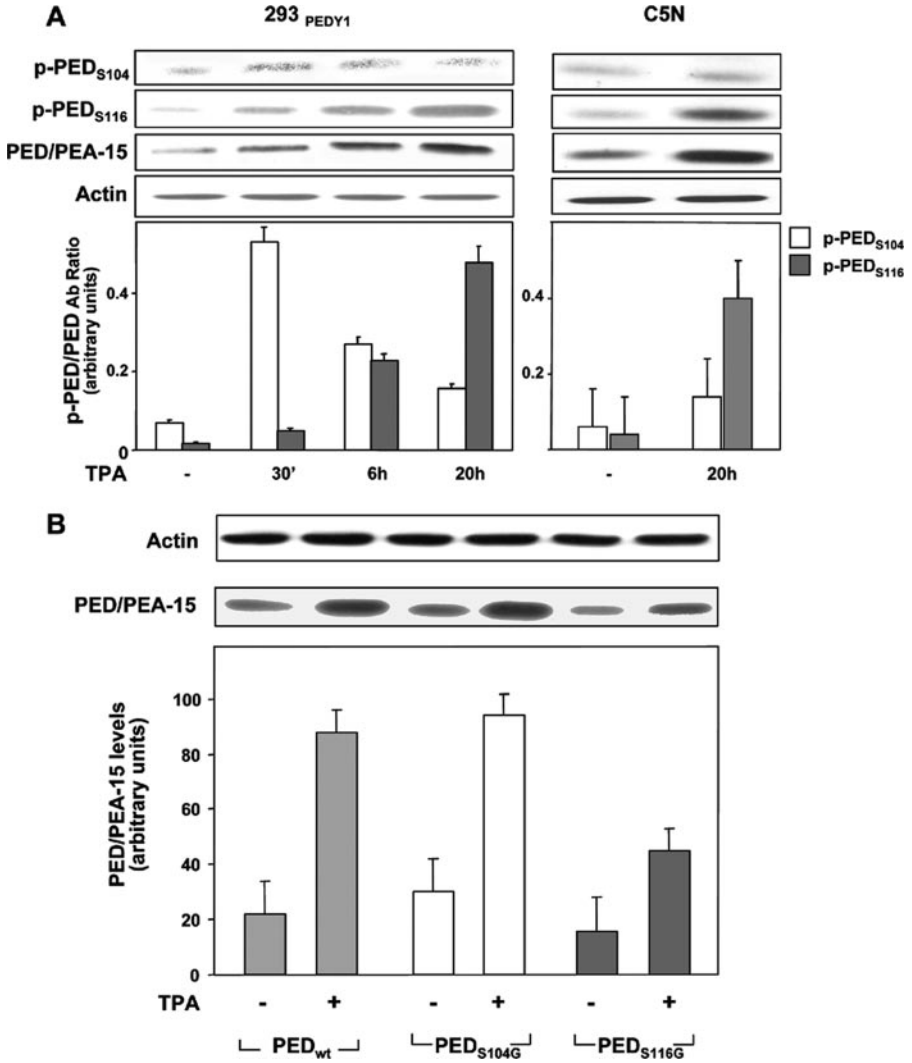

FIGURE 3. **Regulation of PED/PEA-15 phosphorylation levels by TPA.** *A*, 293_{PEDY1} and C5N cells were serum-starved and stimulated with 1 μM TPA for the indicated times. Cell lysates were separated on SDS-PAGE and immunoblotted either with p-PEDS104 Ab or with p-PEDS116 Ab. Each filter has been reprobed with PED Ab for the normalization. The results have been analyzed by laser densitometry, and the *error bars* represent the mean ± S.D. of the densitometric analyses obtained in four duplicate experiments. *B*, HEK293 cells have been transfected with PED_{WT}, PED_{S104G}, and $293PED_{S116G}$, as indicated. Next, cells were serum-starved and stimulated with 1 μM TPA for 20 h. Cell lysates were separated on SDS-PAGE and immunoblotted with PED Ab. Filters have been analyzed by laser densitometry. The autoradiograph shown is representative of five independent experiments. The *error bars* represent the mean ± S.D. of the densitometric analysis.

expression. However, TPA regulation is, at least in part, independent of protein synthesis.

Regulation of PED/PEA-15 Expression by Serine Phosphorylation—It has been shown that PED/PEA-15 expression is tightly regulated by its phosphorylation state (22). We therefore investigated whether TPA could induce PED/PEA-15 phosphorylation. To this end, protein extracts of TPA-stimulated 293_{PEDY1} and C5N cells were immunoblotted with antibodies against the phosphorylated forms of Ser-104 and Ser-116 (Fig. 3*A*). In 293_{PEDY1} cells, Ser-104 phosphorylation increased within the initial 30 min of TPA exposure, declining thereafter. At variance, Ser-116 phosphorylation was barely detectable at 30 min and progressively raised for up to 20 h after TPA exposure. Similarly, in C5N keratinocytes, 20 h of TPA treatment led to a significant increase of Ser-116 phosphorylation, with almost undetectable changes of Ser-104 phosphorylation (Fig. 3*A*).

To assess the relevance of those phosphorylation sites, PED/PEA-15 mutants bearing Ser-104 → Gly (PED_{S104G}) or Ser-116 → Gly (PED_{S116G}) substitutions were transfected in HEK293 cells. TPA treatment increased the levels of the wild-type PED/PEA-15 (PED_{WT}) and of PED_{S104G} by about 4-fold. At variance, PED_{S116G} expression was increased by only 2-fold upon TPA exposure (Fig. 3*B*), suggesting that phosphorylation of Ser-116 is required for TPA regulation of PED/PEA-15 expression.

PKC Regulation of PED/PEA-15 Expression—To identify the kinase responsible for the regulation of PED/PEA-15 expression, 293PEDY1 cells were treated with specific phosphorothioate antisense oligonucleotides (ASO) toward individual PKC isoforms (Fig. 4). Based on Western blot experiments, ASO for PKC-α, -β, and -δ did not significantly affect PED/PEA-15 expression levels when compared with scrambled (SO) oligonucleotide controls. The expression of the targeted PKC isoform was selectively reduced by >50%, however. At variance, ASO-mediated silencing of PKC-ζ expression (PKCζ-ASO) was accompanied by a significant 70% decrease of PED/PEA-15 levels (Fig. 4). A scrambled oligonucleotide (PKCζ-SO) did not induce any detectable change (Fig. 4). A reduction of PED/PEA-15 expression was also observed when 293_{PEDY1} cells were transfected with a dominant-negative (DN) PKC-ζ mutant or with PKCζ-ASO and stimulated with TPA for 20 h (Fig. 5*A*). CaMKII and Akt/PKB have been shown to directly phosphorylate PED/PEA-15 at Ser-116 (22, 23). Interestingly, a 75% decrease of PED/PEA-15 expression was also detected in 293_{PEDY1} cells treated with the CaMK inhibitor, KN-93 (Fig. 5*A*). Similarly, in C5N keratinocytes, TPA-induced up-regulation of PED/PEA-15 protein expression was reduced by about 70% by KN-93 treatment (Fig. 5*B*).

Next, we investigated whether TPA could regulate CaMKII activity in 293_{PEDY1} and in C5N cells. In this regard, CaMKII phosphorylation (Fig. 6*A*) was induced by TPA and well correlated with increased PED/PEA-15 expression levels and Ser-116 phosphorylation in 293_{PEDY1} cells (Figs. 1*A* and 3*A*). Consistently, 20 h of TPA treatment of C5N cells was accompanied by a 2.5-fold increase of CaMKII phosphorylation (Fig. 6*A*). The

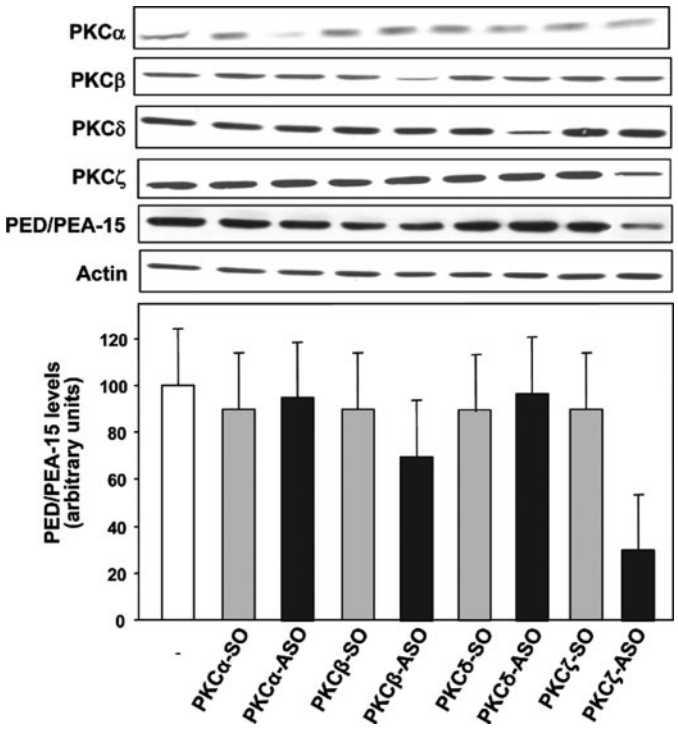

FIGURE 4. **Regulation of PED/PEA-15 expression levels by PKC isoforms.** 293_{PEDY1} cells were treated with phosphorothioate antisense (ASO) and sense (SO) oligonucleotides (3 μg/ml) directed against PKC-α, -β, -δ, and -ζ. Cell lysates were then analyzed by PED immunoblot, and the results were quantitated by laser densitometry. The autoradiograph shown is representative of five independent experiments. The *error bars* represent the mean ± S.D. of the densitometric analysis.

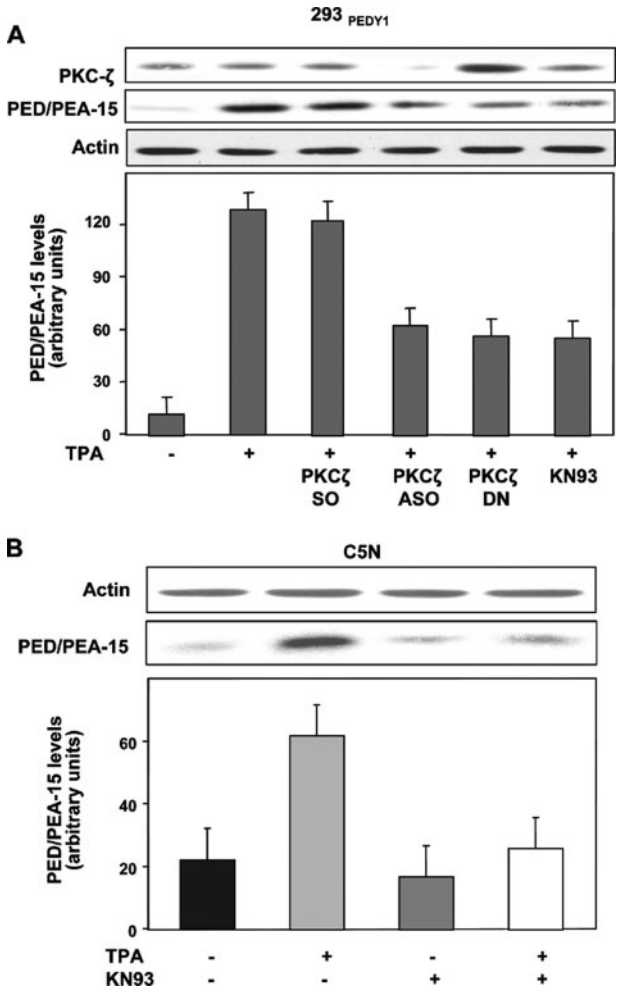

FIGURE 5. **Regulation of PED/PEA-15 expression levels by PKCζ and CaMK.** 293_{PEDY1} (*A*) and C5N (*B*) cells were serum-starved and treated with 1 μM TPA or with 10 μM KN-93 for 20 h in the absence or in the presence of PKCζ-ASO and PKCζ-SO or DN-PKCζ, as indicated. Cell lysates were then analyzed by PKC-ζ (*upper part*) or PED Ab (*lower part*) immunoblot, and the results were quantitated by laser densitometry. The autoradiographs shown are representative of four (*A*) and three (*B*) independent experiments. The *error bars* represent the mean ± S.D. of the densitometric analyses.

expression of DN-PKC-ζ and the treatment of 293PEDY1 cells with PKCζ-ASO reduced by about 65% TPA-induced CaMKII activation (Fig. 6*B*). Conversely, overexpression of the wild-type PKC-ζ led to >3-fold increase of CaMKII activity. At variance, Akt/PKB activity was not induced following 20 h of TPA treatment of both 293_{PEDY1} and C5N cells (Fig. 6*C*).

Moreover, TPA treatment and PKC-ζ overexpression increased by >5-fold the phosphorylation of PED/PEA-15 at Ser-116. Pretreatment of 293PEDY1 cells with KN-93 almost completely reverted both TPA- and PKC-ζ-induced phosphorylation of PED/PEA-15 (Fig. 7*A*). TPA-induced Ser-116 phosphorylation was also reduced by KN-93 in C5N keratinocytes. Consistent results were obtained in transiently transfected HEK293 cells by analyzing the expression of PED_{WT} and PED_{S104G} but not of PED_{S116G} (Fig. 7*B*). Indeed, PKC-ζ-mediated changes of PED_{WT} and PED_{S104G} were prevented by KN-93, which, instead, had no effect on the regulation of PED_{S116G} expression.

Regulation of PED/PEA-15 Ubiquitinylation—We hypothesized that PED/PEA-15 protein accumulation within the cell was due to decreased degradation. To investigate the mechanisms regulating PED/PEA-15 degradation, 293_{PEDY1} cells were treated with the proteasomal inhibitor lactacystin. Lactacystin (30 μM) inhibited the degradation of PED/PEA-15 induced by serum deprivation by 70% and almost completely reverted the effect of the PKCζ-ASO (Fig. 8*A*). Lactacystin treatment also prevented PED/PEA-15 degradation induced by KN-93 in the 293_{PEDY1} cells (data not shown). In addition, lactacystin, at variance with TPA, increased the expression of PED_{S116G} at a similar extent as PED_{WT} (Fig. 8*B*), suggesting that PED/PEA-15 phosphorylation at the Ser-116 was required to escape degradation. Following lactacystin treatment of the untransfected C5N cells, PED/PEA-15 protein levels were also increased by 2.5- and 3-fold, respectively, in the absence or in the presence of TPA (Fig. 8*B*). In both cases, the incubation with KN-93 did not significantly reduce lactacystin effect on PED/PEA-15 protein levels. Thus, CaMK block was overcome by proteasome inhibitors.

These data were consistent with the hypothesis that PED/PEA-15 is largely degraded within the proteasomal compartment. Proteasome-targeted proteins are usually ubiquitinylated (30). His-tagged PED/PEA-15 and HA-tagged ubiquitin have been transfected, alone or in combination, in HEK293 cells, and PED/PEA-15-bound ubiquitin was detected by Western blot with HA antibodies (Fig. 9*A*). A typical smear was observed in cells co-transfected with both constructs, indicating that PED/PEA-15 is a ubiquitinylated protein (Fig. 9*A*).

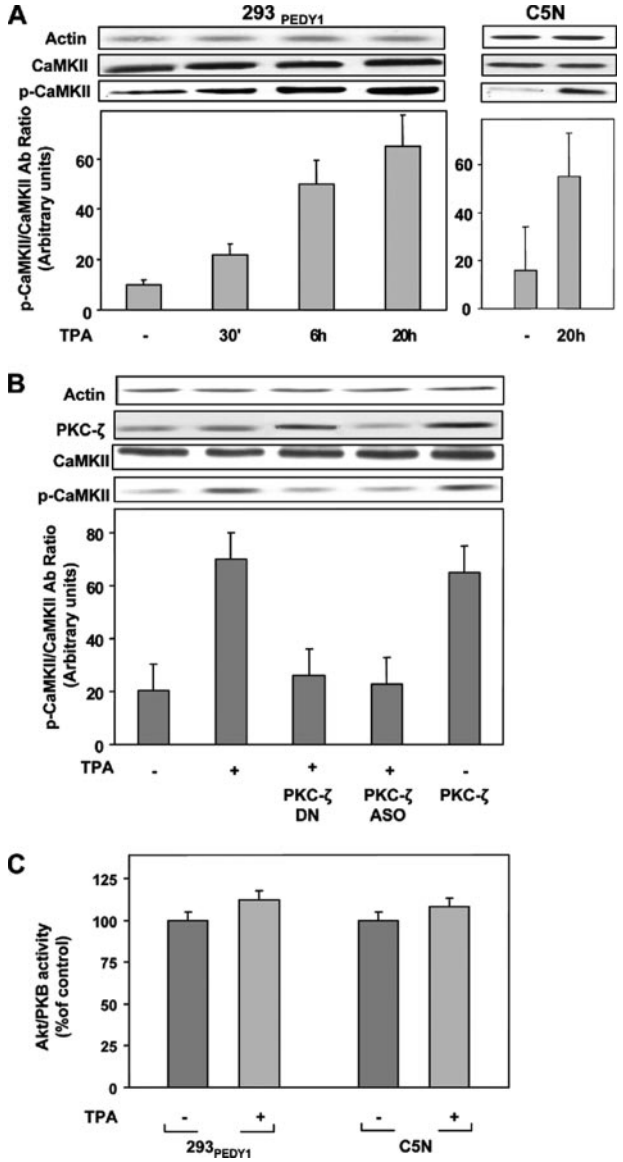

FIGURE 6. **TPA and PKC-ζ effect on CaMKII phosphorylation.** *A*, 293_{PEDY1} cells were serum-starved and treated with 1 μM TPA for the indicated times. Cell lysates were analyzed by p-CaMKII immunoblot. Filters were then reprobed with CaMKII Ab for normalization, and the results were quantitated by laser densitometry. The autoradiograph shown is representative of five (for 293_{PEDY1}) and three (for C5N) independent experiments. The *error bars* represent the mean ± S.D. of the densitometric analysis. *B*, 293_{PEDY1} cells were serum-starved and treated with 1 μM TPA for 20 h in the absence or in the presence of PKCζ-ASO or of wild-type or a dominant-negative PKC-ζ mutant. Cell lysates were then analyzed by immunoblot with p-CaMKII and CaMKII Abs, and the results were quantitated by laser densitometry. The autoradiograph shown is representative of four independent experiments. The *error bars* represent the mean ± S.D. of the densitometric analysis. *C*, 293_{PEDY1} and C5N cells were serum-starved and treated with 1 μM TPA for 20 h. Akt/PKB activity has been measured as described previously (35). The *error bars* represent the mean ± S.D. of three independent experiments in triplicate.

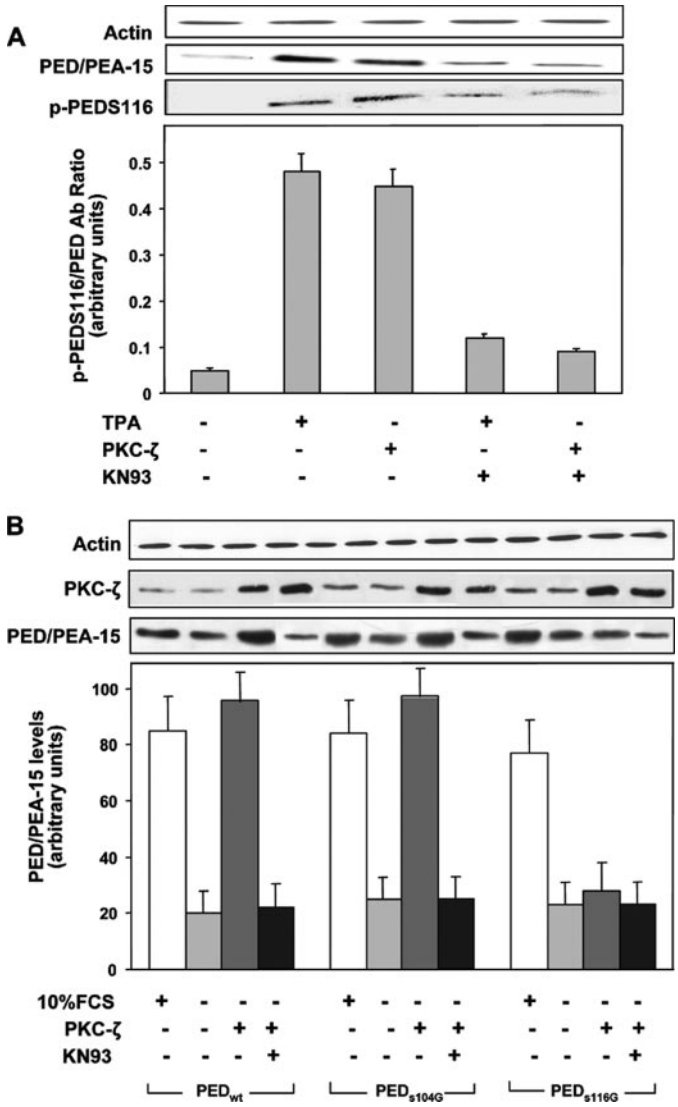

FIGURE 7. **Regulation of PED/PEA-15 phosphorylation and expression by CaMKII.** *A*, 293_{PEDY1} and C5N cells were serum-starved and treated with 1 μM TPA for 20 h or transfected with a PKC-ζ cDNA, in the absence or in the presence of 10 μM KN-93. Cell lysates were then analyzed by immunoblot with p-PEDS116 and PED Abs. The results have been analyzed by laser densitometry, and the *error bars* represent the mean ± S.D. of the densitometric analyses obtained in four duplicate experiments. *B*, HEK293 cells transfected with PED_{WT}, PED_{S104G}, and PED_{S116G} alone or in combination with PKC-ζ cDNA and further incubated in the absence or in the presence of 10 μM KN-93. Cell lysates were then analyzed by PKC-ζ and PED immunoblot, and the results were quantitated by laser densitometry. The autoradiographs shown are representative of four independent experiments. The *error bars* represent the mean ± S.D. of the densitometric analyses.

Next, 293_{PEDY1} cells were incubated in serum-free medium and treated with TPA for 20 h or transfected with wild-type PKC-ζ. PED/PEA-15 immunoprecipitates were then blotted with FK1 antibodies, which recognize polyubiquitinylated proteins. Interestingly, PED/PEA-15 ubiquitinylation was 2.5-fold increased by serum starvation. At the opposite, it was reduced by >2-fold by TPA treatment and by overexpression of PKC-ζ (Fig. 9*B*). Both TPA and PKC-ζ failed to decrease PED/PEA-15 ubiquitinylation in the presence of KN-93. Also, ubiquitinylation of the PED_{S104G} mutant was reduced in a manner comparable with that of PED_{WT}, whereas that of the PED_{S116G} mutant did not significantly change (Fig. 9*C*).

Functional Relevance of Ser-116 Phosphorylation—To further investigate the relevance of PED/PEA-15 phosphorylation on its anti-apoptotic action, 293_{PEDY1} cells have been deprived of serum for 20 h in the absence or in the presence of TPA (Fig. 10). As expected, TPA exposure largely rescued the cell death induced by serum starvation. TPA effect was also mimicked by PKC-ζ overexpression in 293PEDY1 cells (Fig. 10*A*). However, the incubation with KN-93 prevented both TPA and PKC-ζ

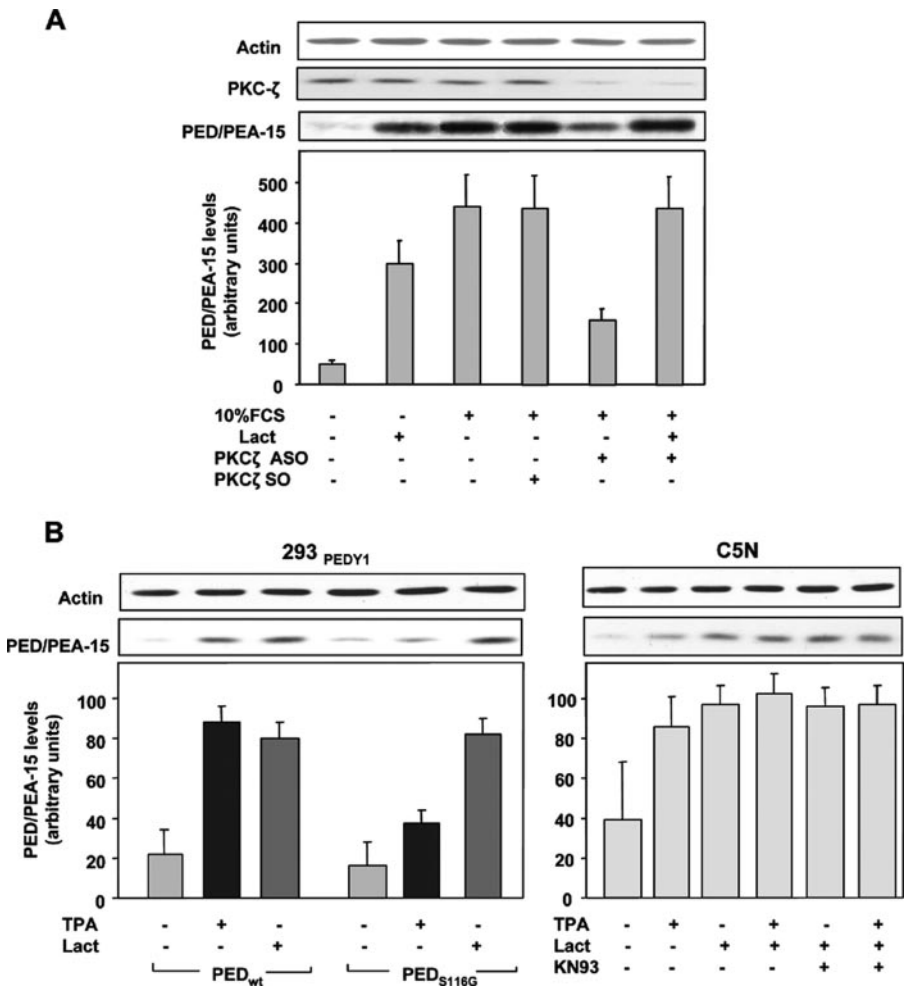

FIGURE 8. **Effect of lactacystin on PED/PEA-15 expression.** *A*, 293_{PEDY1} cells were treated with either PKCζ-ASO or PKCζ-SO and further incubated in the absence or in the presence of 30 μM lactacystin (*Lact*), as indicated. Cell lysates were then analyzed by PED immunoblot, and the results were quantitated by laser densitometry. The autoradiograph shown is representative of four independent experiments. The *error bars* represent the mean ± S.D. of the densitometric analysis. *FCS*, fetal calf serum. *B*, HEK293 cells transfected with PED_{WT} or PED_{S116G} were treated with 1 μM TPA or 30 μM lactacystin for 20 h as indicated. C5N cells were serum-starved and incubated with TPA (1 mM), KN-93 (10 mM), and lactacystin (30 mM) as indicated. Cell lysates were then analyzed by PED immunoblot, and the results were quantitated by laser densitometry. The autoradiographs shown are representative of four (for HEK293) and three (for C5N) independent experiments. The *error bars* represent the mean ± S.D. of the densitometric analyses.

tion. In this work, we have investigated the molecular mechanisms through which the tumor-promoting agent TPA affects PED/PEA-15 expression. Two lines of evidence indicate that, at least in part, PED/PEA-15 expression is regulated by TPA at the post-translational level. Firstly, similar to previous observations in mouse skin and in keratinocyte cell lines (15), phorbol esters up-regulate PED/PEA-15 protein expression in HEK293 cells ectopically expressing the PED/PEA-15 cDNA under the transcriptional control of the cytomegalovirus promoter. In addition, in these cells, as well as in untransfected keratinocytes, PED/PEA-15 regulation by TPA also occurs in the presence of the protein synthesis inhibitor cycloheximide. The evidence that TPA effect was partially reduced by cycloheximide, however, suggests that additional regulation may occur at the transcriptional level. Indeed, PED/PEA-15 mRNA levels are also significantly increased in untransfected C5N cells following TPA stimulation.

Nonetheless, PED/PEA-15 phosphorylation is a major event for the regulation of its stability (22). Here, we show that Ser-116 is the key phosphorylation site enabling TPA regulation of PED/PEA-15 expression. We have previously described that Ser-116 phosphorylation by Akt/PKB increases PED/PEA-15 half-life following insulin stimulation (22). It is unlikely that Akt/PKB is involved in TPA control of PED/PEA-15 expression since there is no sustained Akt/PKB activation upon TPA exposure of HEK293 cells and C5N keratinocytes. CaMKII is a more likely candidate. Indeed, Kubes *et al.* (23) have reported that CaMKII may also phosphorylate PED/PEA-15 at Ser-116 and, consistent with findings in other cell types (31), we found that TPA increases CaMKII activity in HEK293 and in C5N cells (Fig. 6). In addition, the timing of CaMKII activation closely parallels PED/PEA-15 phosphorylation at Ser-116 following TPA stimulation. Finally, pharmacological inhibition of CaMKII with KN-93 almost totally blocked TPA-induced Ser-116 phosphorylation. At variance, Ser-104 phosphorylation was rapidly induced by TPA and then decreased upon prolonged incubation. Ser-104 is known to be directly phosphorylated by PKC following endothelin-1 treatment of astrocytic cells (23). The same occurs with TPA since the down-regulation of conventional PKC isoforms after long term exposure was accompanied

rescue of cell death, suggesting that CaMKII-induced phosphorylation of PED/PEA-15 at Ser-116 was required for this effect (Fig. 10*A*). To further sustain this hypothesis, we have tested TPA protection from cell death in HEK293 cells transfected with either PED_{WT} or PED_{S116G}. Although normally inducing survival of serum-starved cells transfected with PED_{WT}, TPA effect was >2-fold reduced in cells overexpressing PED_{S116G} (Fig. 10*B*).

DISCUSSION

Elevated expression of the anti-apoptotic protein PED/PEA-15 has been found in transformed cell lines and confers resistance to apoptotic stimuli (7–11, 15, 22). An increase of PED/PEA-15 levels is also detected in the papillomatous skin of dimethylbenzanthracene/TPA-treated mice upon experimental carcinogenesis protocols (15), further indicating that raised PED/PEA-15 expression may play a role in cellular transforma-

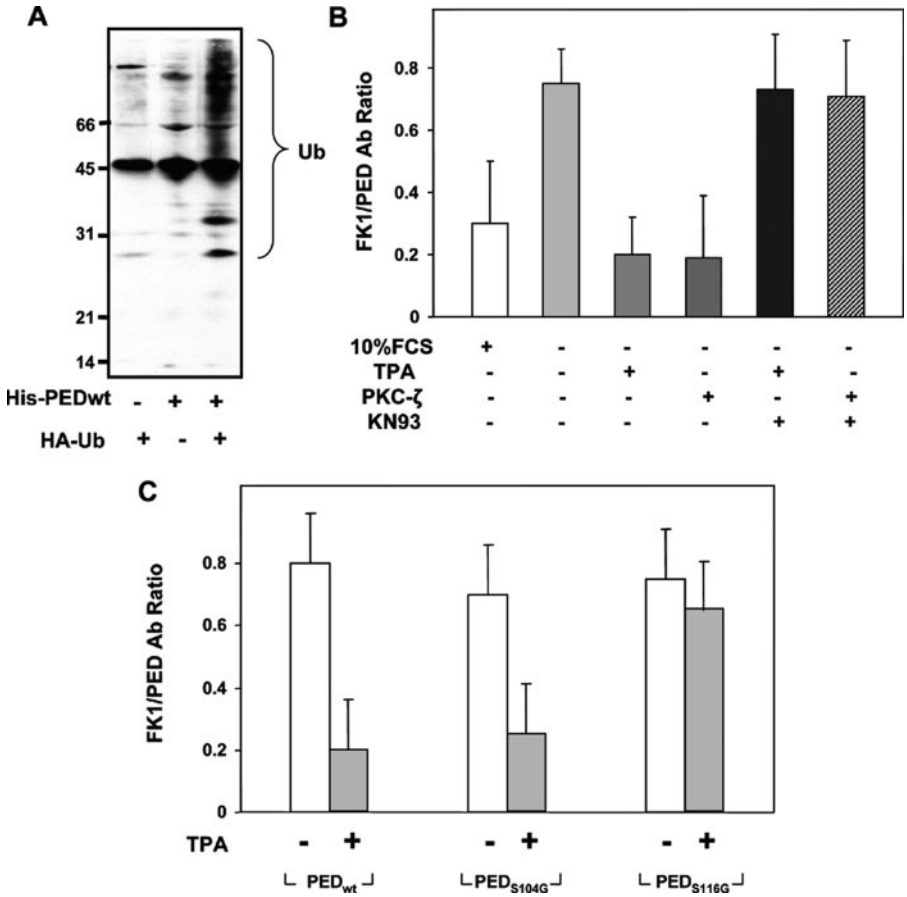

FIGURE 9. **Regulation of PED/PEA-15 ubiquitinylation.** *A*, HEK293 cells were transfected with His-Myc-PED/PEA-15 and HA-ubiquitin (*HA-Ub*) alone or in combination. Upon purification of His-Myc-PED/PEA-15 and separation on SDS-PAGE, filters were probed with HA Ab. The autoradiograph shown is representative of five independent experiments. *B*, 293$_{PEDY1}$ cells were serum-starved and treated with 1 μM TPA for 20 h or transfected with PKC-ζ cDNA in the absence or in the presence of 10 μM KN-93. Cell lysates were separated on SDS-PAGE and immunoblotted with FK1 and PED Abs. The results have been analyzed by laser densitometry, and the *error bars* represent the mean ± S.D. of the densitometric analyses obtained in four duplicate experiments. *FCS*, fetal calf serum. *C*, HEK293 cells transfected with PED$_{WT}$, PED$_{S104G}$, and PED$_{S116G}$ were serum-starved and treated with 1 μM TPA for 20 h. Cell lysates were separated on SDS-PAGE and immunoblotted with FK1 and PED Abs. The results have been analyzed by laser densitometry, and the *error bars* represent the mean ± S.D. of the densitometric analyses obtained in four duplicate experiments.

by a decline of Ser-104 phosphorylation. However, genetic silencing of conventional and novel PKC isoforms, which are canonical intracellular targets of TPA, further argued against the involvement of Ser-104 phosphorylation by PKC in direct regulation of PED/PEA-15 expression. Consistent with this, the Ser-104 → Gly mutant, but not the Ser-116 → Gly mutant, was equally sensitive to TPA action as the wild-type PED/PEA-15. Altogether, these observations indicate that insulin and phorbol esters use different pathways to regulate PED/PEA-15 protein expression, both converging at the level of Ser-116 phosphorylation. For instance, whereas Akt/PKB is the major candidate kinase for the insulin action (22), CaMKII may mediate PED/PEA-15 phosphorylation at the Ser-116 in response to TPA. The finding that LY294002 inhibition of phosphatidylinositol 3-kinase activity also reduces TPA effect on PED/PEA-15 expression (data not shown) may be due to decreased activity of other downstream molecules different from Akt/PKB.

Indeed, a pivotal role has emerged for PKC-ζ in TPA regulation of PED/PEA-15 expression. Both the antisense reduction of PKC-ζ and the expression of a dominant-negative PKC-ζ mutant led to a decrease of TPA-regulated PED/PEA-15 phosphorylation at Ser-116, accompanied by a reduction of PED/PEA-15 protein levels. This led us to hypothesize that PKC-ζ could either directly phosphorylate Ser-116 or directly affect CaMKII activity. No PED/PEA-15 phosphorylation at Ser-116 was induced *in vitro* by active recombinant PKC-ζ (data not shown). At variance, inhibition of PKC-ζ expression and/or function in HEK293 cells almost completely abolished CaMKII induction by TPA, supporting the hypothesis that PKC-ζ could affect PED/PEA-15 expression by acting upstream of CaMKII. Accordingly, PKC-ζ-increased CaMKII activity was paralleled by raised Ser-116 phosphorylation and PED/PEA-15 expression levels. Whether PKC-ζ is directly activated by phorbol esters is still debated (32–34). Alternatively, however, prolonged exposure of the cell to TPA, which is known to down-regulate conventional PKC isoforms, may up-regulate PKC-ζ activity by removing the tonic inhibitory constraint exerted by the firsts on the latter. This is consistent with our previous observation, indicating that PKC-α hyperactivation causes a downstream inhibition on PKC-ζ (24, 35).

Regulation of PED/PEA-15 phosphorylation may be a common event, which contributes to protection from apoptosis, driven by either PKC-ζ (36–38) or CaMKII (39–41). Intriguingly, we have previously described that PED/PEA-15 overexpression inhibits insulin induction of PKC-ζ, thereby impairing glucose uptake (24, 35). It is now emerging that PKC-ζ activation instead up-regulates PED/PEA-15 protein levels, which in turn, may negatively affect PKC-ζ function. This is also in agreement with recent evidence showing that forced expression of PKC-ζ may inhibit insulin and growth factor signaling (42–44).

Recently, Renganathan *et al.* (21) have proposed that PED/PEA-15 phosphorylation at specific residues is important in enabling its interaction with selected intracellular proteins. In particular, phosphorylation at Ser-116 promotes its binding to FADD and plays an important role in protecting cells from apoptosis (9, 10, 21). Here, we show that Ser-116 phosphorylation is also involved in preventing PED/PEA-15 degradation in the 26 S proteasome. Indeed, lactacystin treatment mimicked the effect of TPA and prevented PED/PEA-15 protein loss follow-

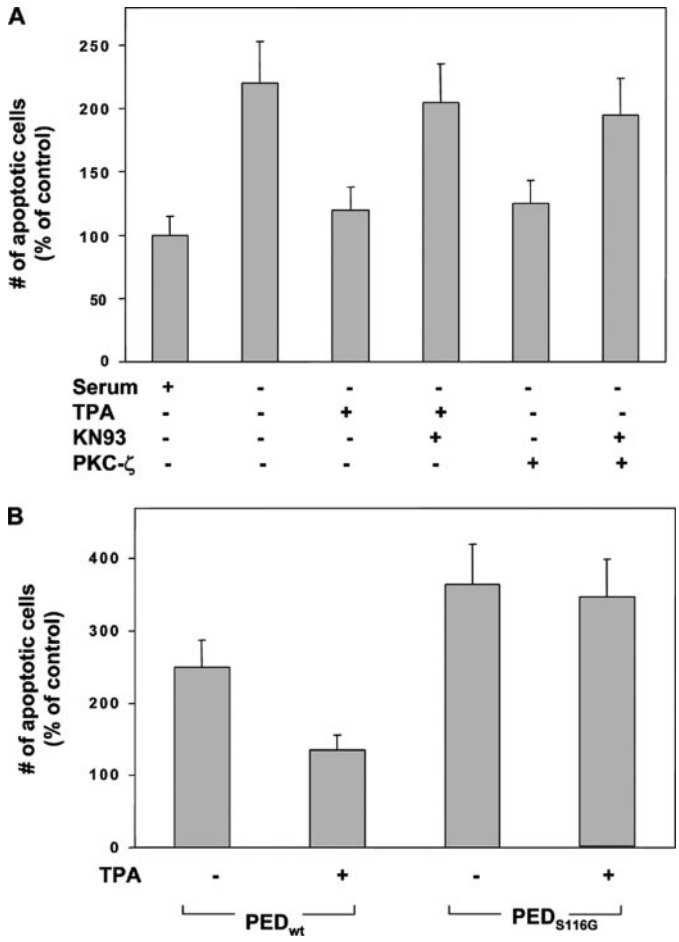

FIGURE 10. **TPA-mediated regulation of cell death by PED/PEA-15 phosphorylation.** *A*, 293$_{PEDY1}$ cells were serum-starved and treated with 1 μM TPA for 20 h or transfected with PKC-ζ, in the absence or in the presence of 10 μM KN-93, as indicated. Cell suspensions were stained with propidium iodide and analyzed by flow cytometry. Data are presented as the percentage of value obtained with cells kept in serum only. Values represent the mean ± S.D. of the results obtained in four triplicate experiments. *B*, HEK293 cells transfected with PED$_{WT}$ or PED$_{S116G}$ were serum-starved and treated with 1 μM TPA for 20 h, as indicated. Cell suspensions were stained with propidium iodide and analyzed by flow cytometry. Data are presented as the percentage of value obtained with cells kept in serum only. Values represent the mean ± S.D. of the results obtained in three triplicate experiments.

ing growth factor deprivation or PKC-ζ silencing. Different from TPA, however, lactacystin also rescued the expression levels of the non-phosphorylatable Ser-116 → Gly mutant, indicating that phosphorylation at this site may confer the ability to escape proteasomal degradation. Proteasomal targeting and degradation are typical features of ubiquitinylated proteins (30). Sur and Ramos (45) have recently shown that vanishin, a death effector domain protein with a high degree of homology with PED/PEA-15, is ubiquitinylated. We now present evidence that PED/PEA-15 directly binds ubiquitin. Treatment with TPA as well as PKC-ζ overexpression reduced the ubiquitinylation of wild-type PED/PEA-15 but had no effect on the Ser-116 phosphorylation-deficient mutant. Preserved ubiquitinylation was also observed in the presence of KN-93, indicating that CaMKII phosphorylation plays an important role in the regulation of PED/PEA-15 expression by controlling its ubiquitinylation state. Finally, both KN-93 and Ser-116 → Gly substitution reduced TPA anti-apoptotic action, suggesting that CaMKII activation and PED/PEA-15 phosphorylation at Ser-116 are relevant for this effect.

Thus, we have shown that phorbol esters up-regulate PED/PEA-15 expression by controlling its proteasomal degradation. PKC-ζ and CaMKII activities are necessary to enable TPA-dependent phosphorylation of PED/PEA-15 at Ser-116. This phosphorylation prevents ubiquinylation and proteasomal targeting and induce PED/PEA-15 intracellular accumulation, thereby enhancing its anti-apoptotic action.

Acknowledgments—We thank Prof. A. M. Musti (University of Cosenza) and Prof. G. Portella (DBPCM, "Federico II," University of Naples) for providing important reagents, very helpful discussion, and critical reading of the manuscript and Dr. R. De Mattia and Dr. S. Libertini (DBPCM, "Federico II," University of Naples) for technical help.

REFERENCES

1. Duke, R. C., Ojcius, D. M., and Young, J. D. (1996) *Sci. Am.* **275,** 80–87
2. Thompson, C. B. (1995) *Science* **267,** 1456–1462
3. Barnhart, B. C., Lee, J. C., Alappat, E. C., and Peter, M. E. (2003) *Oncogene* **22,** 8634–8644
4. Araujo, H., Danziger, N., Cordier, J., Glowinski, J., and Chneiweiss, H. (1993) *J. Biol. Chem.* **268,** 5911–5920
5. Danziger, N., Yokoyama, M., Jay, T., Cordier, J., Glowinski, J., and Chneiweiss, H. (1995) *J. Neurochem.* **64,** 1016–1025
6. Estelles, A., Yokoyama, M., Nothias, F., Vincent, J. D., Glowinski, J., Vernier, P., and Chneiweiss, H. (1996) *J. Biol. Chem.***271,** 14800–14806
7. Condorelli, G., Vigliotta, G., Iavarone, C., Caruso, M., Tocchetti, C. G., Andreozzi, F., Cafieri, A., Tecce, M. F., Formisano, P., Beguinot, L., and Beguinot, F. (1998) *EMBO J.* **17,** 3858–3866
8. Dong, G., Loukinova, E., Chen, Z., Gangi, L., Chanturita, T. I., Liu, E. T., and Van Waes, C. (2001) *Cancer Res.* **61,** 4797–4808
9. Hao, C., Beguinot, F., Condorelli, G., Trencia, A., Van Meir, E. G., Yong, V. W., Parney, I. F., Roa, W. H., and Petruk, K. C. (2001) *Cancer Res.* **61,** 1162–1170
10. Condorelli, G., Vigliotta, G., Cafieri, A., Trencia, A., Andalo, P., Oriente, F., Miele, C., Caruso, M., Formisano, P., and Beguinot, F. (1999) *Oncogene* **18,** 4409–4415
11. Condorelli, G., Trencia, A., Vigliotta, G., Perfetti, A., Goglia, U., Cassese, A., Musti, A. M., Miele, C., Santopietro, S., Formisano, P., and Beguinot, F. (2002) *J. Biol. Chem.* **277,** 11013–11018
12. Sharif, A., Canton, B., Junier, M. P., and Chneiweiss, H. (2003) *Ann. N. Y. Acad. Sci.* **1010,** 43–50
13. Trencia, A., Fiory, F., Maitan, M. A., Vito, P., Barbagallo, A. P., Perfetti, A., Miele, C., Ungaro, P., Oriente, F., Cilenti, L., Zervos, A. S., Formisano, P., and Beguinot, F. (2004) *J. Biol. Chem.* **279,** 46566–46572
14. Stassi, G., Garofano, M., Zerilli, M., Ricci-Vitiani, L., Zanca, C., Todaro, M., Aragona, F., Limite, G., Petrella, G., and Condorelli, G. (2005) *Cancer Res.* **65,** 6668–6675
15. Formisano, P., Perruolo, G., Libertini, S., Santopietro, S., Troncone, G., Raciti, G. A., Oriente, F., Portella, G., Miele, C., and Beguinot, F. (2005) *Oncogene* **24,** 7012–7021
16. Formstecher, E., Ramos, J. W., Fauquet, M., Calderwood, D. A., Hsieh, J. C., Canton, B., Nguyen, X. T., Barnier, J. V., Camonis, J., Ginsberg, M. H., and Chneiweiss, H. (2001) *Dev. Cell* **1,** 239–250
17. Hill, J. M., Vaidyanathan, H., Ramos, J. W., Ginsberg, M. H., and Werner, M. H. (2002) *EMBO J.* **21,** 6494–6504
18. Vaidyanathan, H., and Ramos, J. W. (2003) *J. Biol. Chem.* **278,** 32367–32372
19. Whitehurst, A. W., Robinson, F. L., Moore, M. S., and Cobb, M. H. (2004) *J. Biol. Chem.* **279,** 12840–12847
20. Gaumont-Leclerc, M. F., Mukhopadhyay, U. K., Goumard, S., and Ferbeyre, G. (2004) *J. Biol. Chem.* **279,** 46802–46809

21. Renganathan, H., Vaidyanathan, H., Knapinska, A., and Ramos, J. W. (2005) *Biochem. J.* **390,** 729–735
22. Trencia, A., Perfetti, A., Cassese, A., Vigliotta, G., Miele, C., Oriente, F., Santopietro, S., Giacco, F., Condorelli, G., Formisano, P., and Beguinot, F. (2003) *Mol. Cell Biol.* **23,** 4511–4521
23. Kubes, M., Cordier, J., Glowinski, J., Girault, J. A., and Chneiweiss, H. (1998) *J. Neurochem.* **71,** 1307–1314
24. Vigliotta, G., Miele, C., Santopietro, S., Portella, G., Perfetti, A., Maitan, M. A., Cassese, A., Oriente, F., Trencia, A., Fiory, F., Romano, C., Tiveron, C., Tatangelo, L., Troncone, G., Formisano, P., and Beguinot, F. (2004) *Mol. Cell Biol.* **24,** 5005–5015
25. Sharif, A., Renault, F., Beuvon, F., Castellanos, R., Canton, B., Barbeito, L., Junier, M. P., and Chneiweiss, H. (2004) *Neuroscience* **126,** 263–275
26. Formisano, P., Oriente, F., Fiory, F., Caruso, M., Miele, C., Maitan, M. A., Andreozzi, F., Vigliotta, G., Condorelli, G., and Beguinot, F. (2000) *Mol. Cell Biol.* **20,** 6323–6333
27. Caruso, M., Maitan, M. A., Bifulco, G., Miele, C., Vigliotta, G., Oriente, F., Formisano, P., and Beguinot, F. (2001) *J. Biol. Chem.* **276,** 45088–45097
28. Oriente, F., Formisano, P., Miele, C., Fiory, F., Maitan, M. A., Vigliotta, G., Trencia, A., Santopietro, S., Caruso, M., Van Obberghen, E., and Beguinot, F. (2001) *J. Biol. Chem.* **276,** 37109–37119
29. Musti, A. M., Treier, M., and Bohmann, D. (1997) *Science* **275,** 400–402
30. Ciechanover, A. (2005) *Mol. Cell Biol.* **6,** 79–87
31. Hughes, K., Edin, S., Antonsson, A., and Grundstrom, T. (2001) *J. Biol. Chem.* **276,** 36008–36013
32. Ways, D. K., Cook, P. P., Webster, C., and Parker, P. J. (1992) *J. Biol. Chem.* **267,** 4799–4805
33. Kim, S. J., Chang, Y. Y., Kang, S. S., and Chun, J. S. (1997) *Biochem. Biophys. Res. Commun.* **237,** 336–339
34. Hirai, T., and Chida, K. (2003) *J Biochem.* (*Tokyo*) **133,** 1–7; Correction *J. Biochem.* (*Tokyo*) **133,** 395
35. Condorelli, G., Vigliotta, G., Trencia, A., Maitan, M. A., Caruso, M., Miele, C., Oriente, F., Santopietro, S., Formisano, P., and Beguinot, F. (2001) *Diabetes* **50,** 1244–1252
36. Spitaler, M., Wiesenhofer, B., Biedermann, V., Seppi, T., Zimmermann, J., Grunicke, H., and Hofmann, J. (1999) *Anticancer Res.* **19,** 3969–3976
37. de Thonel, A., Bettaieb, A., Jean, C., Laurent, G., and Quillet-Mary, A. (2001) *Blood* **98,** 3770–3777
38. Leroy, I., de Thonel, A., Laurent, G., and Quillet-Mary, A. (2005) *Cell Signal.* **17,** 1149–1157
39. Tombes, R. M., Grant, S., Westin, E. H., and Krystal, G. (1995) *Cell Growth Differ.* **6,** 1063–1070
40. Yang, B. F., Xiao, C., Roa, W. H., Krammer, P. H., and Hao, C. (2003) *J. Biol. Chem.* **278,** 7043–7050
41. Xiao, C., Yang, B. F., Song, J. H., Schulman, H., Li, L., and Hao, C. (2005) *Exp. Cell Res.* **304,** 244–255
42. Liu, Y. F., Paz, K., Herschkovitz, A., Alt, A., Tennenbaum, T., Sampson, S. R., Ohba, M., Kuroki, T., LeRoith, D., and Zick, Y. (2001) *J. Biol. Chem.* **276,** 14459–14465
43. Liu, Y. F., Herschkovitz, A., Boura-Halfon, S., Ronen, D., Paz, K., Leroith, D., and Zick, Y. (2004) *Mol. Cell Biol.* **24,** 9668–9681
44. Zick, Y. (2005) *Sci. STKE. 2005* **25,** 268
45. Sur, R., and Ramos, J. W. (2005) *Biochem. J.* **387,** 315–324

MOLECULAR AND CELLULAR BIOLOGY, Sept. 2008, p. 5634–5645 Vol. 28, No. 18
0270-7306/08/$08.00+0 doi:10.1128/MCB.00117-08

Prep1 Deficiency Induces Protection from Diabetes and Increased Insulin Sensitivity through a p160-Mediated Mechanism▽

Francesco Oriente,[1] Luis Cesar Fernandez Diaz,[3] Claudia Miele,[1] Salvatore Iovino,[1] Silvia Mori,[3] Victor Manuel Diaz,[4] Giancarlo Troncone,[2] Angela Cassese,[1] Pietro Formisano,[1] Francesco Blasi,[3,4] and Francesco Beguinot[1]*

Dipartimento di Biologia e Patologia Cellulare e Molecolare & Istituto di Endocrinologia ed Oncologia Sperimentale del CNR, Università degli Studi di Napoli Federico II, Naples, Italy[1]; Dipartimento di Scienze Biomorfologiche e Funzionali, Università degli Studi di Napoli Federico II, Naples, Italy[2]; IFOM (FIRC Institute of Molecular Oncology), via Adamello 16, 20134 Milan, Italy[3]; and Università Vita Salute San Raffaele, via Olgettina 60, 20132 Milan, Italy[4]

Received 22 January 2008/Returned for modification 8 March 2008/Accepted 4 July 2008

We have examined glucose homeostasis in mice hypomorphic for the homeotic transcription factor gene *Prep1*. *Prep1*-hypomorphic (*Prep1*$^{i/i}$) mice exhibit an absolute reduction in circulating insulin levels but normal glucose tolerance. In addition, these mice exhibit protection from streptozotocin-induced diabetes and enhanced insulin sensitivity with improved glucose uptake and insulin-dependent glucose disposal by skeletal muscle. This muscle phenotype does not depend on reduced expression of the known *Prep1* transcription partner, *Pbx1*. Instead, in *Prep1*$^{i/i}$ muscle, we find normal Pbx1 but reduced levels of the recently identified novel Prep1 interactor p160. Consistent with this reduction, we find a muscle-selective increase in mRNA and protein levels of PGC-1α, accompanied by enhanced expression of the GLUT4 transporter, responsible for insulin-stimulated glucose uptake in muscle. Indeed, using L6 skeletal muscle cells, we induced the opposite effects by overexpressing Prep1 or p160, but not Pbx1. In vivo skeletal muscle delivery of p160 cDNA in *Prep1*$^{i/i}$ mice also reverses the molecular phenotype. Finally, we show that Prep1 controls the stability of the p160 protein. We conclude that Prep1 controls insulin sensitivity through the p160-GLUT4 pathway.

Prep1 is an homeodomain transcription factor belonging to the MEINOX subfamily of the TALE (three amino acid loop extension) proteins (32). Prep1 forms DNA-independent dimeric complexes with all isoforms of the Pbx homeodomain transcription factor, enhancing target specificity and regulatory function (4, 6, 24, 36, 39).

Prep1 is an important gene in development: its downregulation in zebrafish and its deletion in mice induces embryonic lethality (9; L. C. Fernandez-Diaz and F. Blasi, unpublished data). Hypomorphic mice expressing about 2% of *Prep1* mRNA (*Prep1*$^{i/i}$) have a leaky embryo-lethal phenotype with major anomalies in hematopoiesis, oculogenesis, and angiogenesis (15). About 25% of the homozygous *Prep1*$^{i/i}$ embryos survive, and the mice are born and live a normal-length life. However, they show defects in T-cell development (38).

In all these systems, the reduction or the absence of Prep1 is accompanied by a reduction of its Pbx partners (9, 15, 38). The reduction in the mouse appears to be cell type and isoform specific (15). Direct studies have shown that the reduction of Pbx expression is due largely to a posttranscriptional mechanism (15, 38), in particular to a decrease in the protein half-life. In fact, dimerization with Prep1 protects Pbx from proteasomal degradation (26).

Previous studies also demonstrated that the generation of Pbx-Prep heterodimers is necessary to enable nuclear localization of Prep1 and to prevent nuclear export of Pbx (5, 20). Indeed, the balance of Prep and Pbx has been shown to be functionally important both during embryogenesis and in adult life (9, 15, 26, 46).

We recently discovered that p160 Myb-binding protein (p160) (44) is a new direct Prep1-interacting protein that competes with Pbx1 for Prep1 binding (11). Thus, Prep1 functions may depend on not only its interaction with Pbx but also that with p160. The role of the Prep1-p160 interaction, however, is still unknown. Interestingly, p160 is a repressor of the regulator of glucose and energy metabolism, PPAR-gamma coactivator-1α (PGC-1α) (13).

The importance of Pbx and Hox protein interaction in glucose homeostasis, pancreatic cell proliferation, and pancreas development has been studied. Transgenic mice expressing *Pbx* interaction-defective *Pdx1* genes were used to investigate the requirements for Pdx1-Pbx complexes in pancreatic morphogenesis, islet cell differentiation, and glucose homeostasis (12). In these studies, Pdx1-Pbx complexes were dispensable for glucose homeostasis and differentiation of stem cells into ductal, endocrine, and acinar lineages; however, they were essential for expansion of these cell populations during development. Further studies of transheterozygous *Pbx1*$^{+/-}$ *Pdx1*$^{+/-}$ mice revealed in vivo genetic interactions between Pbx1 and Pdx1 that are essential for postnatal pancreatic function (22). Indeed, these mice developed age-dependent overt diabetes mellitus, while *Pbx1*$^{+/-}$ and *Pdx1*$^{+/-}$ mice showed only reduced glucose tolerance. Mutations of Pdx1 protein cause diabetes in both mice and humans (1, 18, 27, 43), suggesting that *Pbx1* perturbation may also determine susceptibility to diabe-

* Corresponding author. Mailing address: Dipartimento di Biologia e Patologia Cellulare e Molecolare, Università di Napoli Federico II, Via Sergio Pansini, 5, Naples 80131, Italy. Phone: 39 081 746 3248. Fax: 39 081 746 3235. E-mail: beguino@unina.it.

▽ Published ahead of print on 21 July 2008.

tes. Whether the perturbation of other MEINOX transcription factors, like Prep1, affects the development and function of the endocrine pancreas and glucose tolerance is presently unknown.

It is not known whether Prep1 has any role in glucose and energy metabolism. Because of the ability of Prep1 to interact with both Pbx1 and p160, we have studied glucose homeostasis in *Prep1*$^{i/i}$ mice. We show that adult *Prep1*$^{i/i}$ animals exhibit enhanced sensitivity to insulin action and are protected from developing streptozotocin-induced diabetes. The increased sensitivity to insulin in these mice is due, at least in part, to a novel Pbx1-independent and p160-dependent mechanism. We demonstrate, for the first time, a role for Prep1 in glucose homeostasis mediated by the newly identified interactor p160.

MATERIALS AND METHODS

Materials. Media, sera, antibiotics for cell culture, and the Lipofectamine reagent were from Invitrogen (Grand Island, NY). The anti-Prep1 polyclonal antibody and pBOS-Prep1 vector were described previously (3). pSG5-Pbx1, PSG5-Prep1$_{HR1}$, and pRUFneo-p160 vectors were described previously (11). PGC-1α and GLUT4 antibodies were from Santa Cruz Biotechnology, Inc. (Santa Cruz, CA). The p160 antibody was from Zymed Laboratories (San Francisco, CA). Protein electrophoresis reagents were purchased from Bio-Rad (Richmond, VA), and Western blotting and enhanced chemiluminescence (ECL) reagents were from Amersham Biosciences (Arlington Heights, IL). All other chemicals were from Sigma (St. Louis, MO).

Generation and characterization of *Prep1*-hypomorphic mice. *Prep1* targeted mice were generated by gene trapping by Lexikon Genetics, Inc. (The Woodlands, TX) and have been described (15, 38). In the experiments reported in this paper, heterozygous mice were backcrossed with wild-type C57BL/6 mice for four generations. All animal handling conformed to regulations of the Ethics Committee on Animal Use of H. S. Raffaele (IACUC permission number 207). Southern blot analysis of EcoRI-digested total DNA from tail biopsy specimens or yolk sacs was accomplished through a 132-bp double-stranded *Prep1* cDNA probe prepared from full-length *Prep-1* cDNA with the forward primer 5′-ATG ATGGCGACACAGACGCTAAGTATA-3′ and the reverse primer 5′-GGGG TCTGAGACTCGATGGGAGGAGGACTC-3′. The PCR genotyping strategy employed the oligonucleotides Prep-R1 and LTR2 (sequences provided below), which amplify a 230-bp fragment in the disrupted allele, while the Prep-F1–Prep-R1 pair amplifies a 300-bp fragment of the wild-type allele. Sequences of oligonucleotides are as follows: Prep-F1, 5′-CCAAGGGCAGTAAGAGAAGC TCTGGAG-3′; Prep-R1 5′GGAGTGCCAACCATGTTAAGAAGAAGTCC C-3′; LTR2, 5′CAAAATGGCGTTACTTAAGCTAGCTTGCC-3′.

Pancreatic islet sections were stained with hematoxylin and eosin. For morphometry, pancreases were obtained from 3-month-old control and hypomorphic littermate mice, and immunohistochemical detection of insulin and glucagon was performed in three sections (2 to 3 μm) separated by 200 μm, as described in reference 10.

Tissue samples (tibialis muscles and pancreases) were collected rapidly after mice were sacrificed by pentobarbitone overdose. Tissues were snap-frozen in liquid nitrogen and stored at −80°C for subsequent Western blotting.

Mouse phenotyping. Blood glucose levels were measured with a glucometer (A. Menarini Diagnostics); insulin and glucagon were measured by radioimmunological assay (RIA) with a rat insulin standard (insulin rat RIA kit; Linco Research, St. Charles, MO) and glucagon standard (glucagon RIA kit; Linco Research).

For glucose and insulin tolerance tests, mice fasted overnight and then were injected with glucose (2 g · kg of body weight^{-1}) intraperitoneally. Venous blood was drawn by tail clipping at 0, 15, 30, 45, 60, 90, and 120 min without reclipping of the tails. For insulin tolerance, random-fed mice were injected intraperitoneally with insulin (0.75 mU · g of body weight^{-1}) (Eli Lilly, Indianapolis, IN). Venous blood was subsequently drawn by tail clipping at 0, 15, 30, 45, 60, 90, and 120 min after insulin injection to determine blood glucose levels. To assess ex vivo insulin secretion, islets were isolated from 6-month-old mice by collagenase digestion and subsequent centrifugation on a Histopaque (Sigma-Aldrich) gradient (23) A total of 20 islets were manually selected and preincubated in Dulbecco's modified Eagle's medium (Life Technologies) at 37°C in a 5% CO_2 atmosphere for 24 h. Islets were further incubated in Krebs-Ringer buffer (120 mmol/liter NaCl, 1.2 mmol/liter $MgSO_4$, 5 mmol/liter KCl, 10 mmol/liter $NaHCO_3$, 1.3 mmol/liter $CaCl_2$, and 1.2 mmol/liter KH_2PO_4) for 30 min and then stimulated at 37°C with various concentrations of glucose for 1 h. Islets were subsequently collected by centrifugation, and supernatants were assayed for insulin content by RIA.

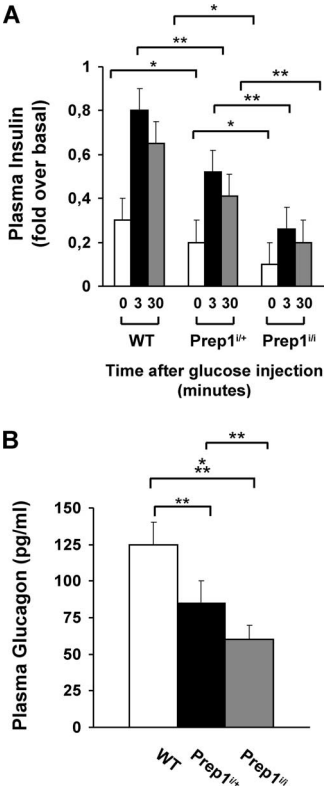

FIG. 1. Insulin and glucagon levels in *Prep1*-hypomorphic mice. For determination of circulating insulin (A) and glucagon (B) levels, control and hypomorphic mice fasted overnight and were then injected with glucose (3 g/kg body wt) intraperitoneally. Plasma insulin concentrations were quantitated at the indicated times by radioimmunoassay. Glucagon levels were assessed in the fasting state. Data are means plus standard deviations for 12 mice/group. Asterisks indicate statistically significant differences (*, $P < 0.05$; **, $P < 0.01$).

For low-dose streptozotocin treatment, mice fasted for 6 h prior to intraperitoneal (i.p.) injection with streptozotocin (40 mg/kg body weight) dissolved in sterile citrate buffer or with the vehicle, citrate buffer (0.05 M sodium citrate, pH 4.5). Streptozotocin was administered for five consecutive days, and glycemia and body weight were measured during the next 4 weeks. Some mice were sacrificed during the streptozotocin treatment to evaluate the morphological alteration of the pancreas.

In vivo glucose utilization. An intravenous flash injection of 1 μCi of the nonmetabolizable glucose analog 2-[1-^{3}H]deoxy-D-glucose (2-DG) (Amersham Pharmacia Biotech) and an i.p. injection of insulin (0,75 mU · g of body weight^{-1}) were administered to random-fed mice. The specific blood 2-DG clearance was determined with 25-μl blood samples (tail vein) obtained 1, 10, 20, and 30 min after injection using the Somogyi procedure (42). Tibialis skeletal muscle tissue samples were removed 30 min after injection. The glucose utilization index was determined by measuring the accumulation of radiolabeled compounds (14). The amount of 2-DG–6 phosphate per milligram of protein was divided by the integral of the concentration ratio of 2-DG to unlabeled glucose measured. Glucose utilization is expressed as picomoles per milligram of protein per minute.

p160 gene delivery in skeletal muscle of *Prep1*-hypomorphic mice. We adopted an established technique (19, 40) to inject mouse tibialis muscles with 100 μg of pRUFneo-p160 naked DNA (encoding a Flag-tagged p160 cDNA), using 1-ml syringes and 27-gauge needles. After 48 h, mice were sacrificed and muscles were processed for RNA and/or protein extraction as described in the appropriate section.

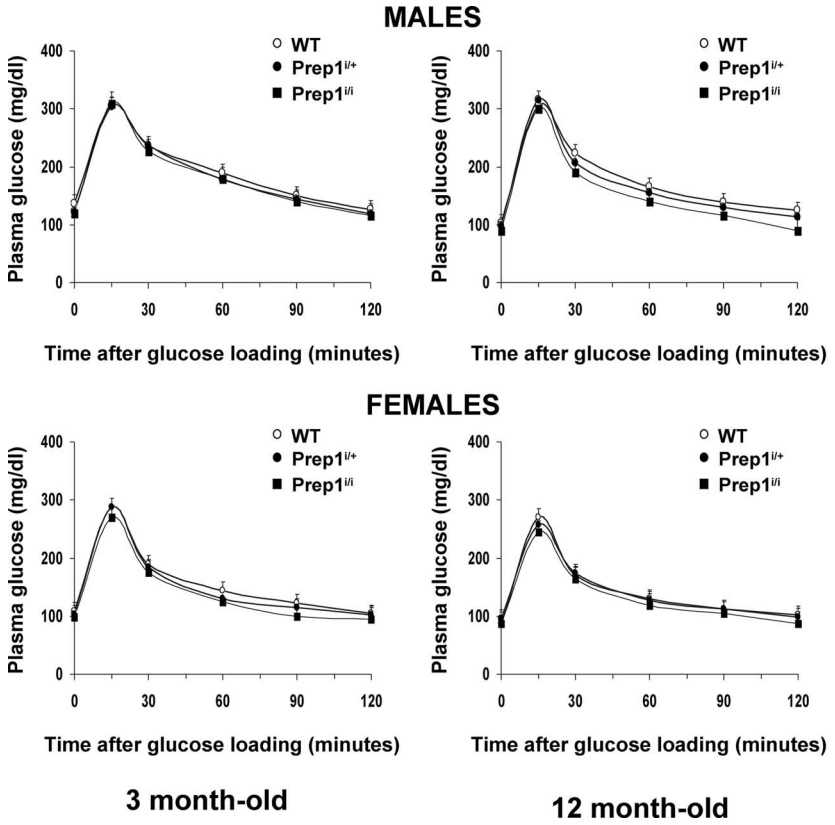

FIG. 2. Glucose tolerance tests in *Prep1*-hypomorphic mice. Six groups (22/group) of male and female *Prep1*-hypomorphic and control mice were analyzed at 3 and 12 months of age. Following determinations of basal glycemias, mice were injected intraperitoneally with glucose (2 mg · kg^{-1}), followed by further blood glucose level determinations at the indicated times as described in Materials and Methods. Data are means ± standard deviations for each group of animals. Areas under the curves showed no significant difference between groups.

Cell culture procedures and transfection. L6 skeletal muscle cells were cultured at 37°C in Dulbecco's modified Eagle's medium (DMEM) supplemented with 10% fetal calf serum, 2% L-glutamine, 10,000 U/ml penicillin, and 10,000 μg/ml streptomycin. Transient transfection of Prep1, $Prep1_{HR}$, p160, and Pbx1 plasmids or small interfering RNA oligonucleotides was performed by the Lipofectamine method according to the manufacturer's instructions. For these studies, 60 to 80% confluent cells were washed twice with Optimem (Invitrogen) and incubated for 8 h with 5 μg of plasmid construct or with 12 μg of oligonucleotides and 45 to 60 μl of Lipofectamine reagent. The medium was then replaced with DMEM with 10% fetal calf serum, and cells were further incubated for 15 h before being assayed.

2-DG uptake by the L6 cells was measured as previously reported (7). Briefly, confluent cells were incubated in DMEM supplemented with 0.25% albumin for 18 h at 37°C. The medium was aspirated, and cells were further incubated for 30 min in glucose-free HEPES buffer (5 mmol/liter KCl, 120 mmol/liter NaCl, 1.2 mmol/liter $MgSO_4$, 10 mmol/liter $NaHCO_3$, 1.2 mmol/liter $KHPO_4$, and 20 mmol/liter HEPES [pH 7.8]; 2% albumin). The cells were incubated with 100 nmol/liter insulin for 30 min, supplemented during the final 10 min with 0.2 mmol/liter [^{14}C]2-DG. Cells were then solubilized, and 2-DG uptake was quantitated by liquid scintillation counting.

Western blot analysis and immunoprecipitation procedures. Tissue samples were homogenized in a Polytron (Brinkman Instruments) in 20 ml T-PER reagent per gram of tissue according to manufacture (Pierce). After centrifugation at 10,000 rpm for 5 min, supernatant was collected. Cells were solubilized in lysis buffer (50 mmol/liter HEPES [pH 7.5], 150 mmol/liter NaCl, 10 mmol/liter EDTA, 10 mmol/liter $Na_4P_2O_7$, 2 mmol/liter Na_3VO_4, 100 mmol/liter NaF, 10% glycerol, 1% Triton X-100, 1 mmol/liter phenylmethylsulfonyl fluoride, 10 mg/ml aprotinin) for 1 h at 4°C, and lysates were centrifuged at 5,000 × *g* for 20 min. Total or immunoprecipitated homogenates were separated by sodium dodecyl sulfate-polyacrylamide gel electrophoresis (SDS-PAGE) and transferred to 0.45-μm Immobilon-P membranes. Upon incubation with primary and secondary antibodies, immunoreactive bands were detected by ECL according to the manufacturer's instructions (30).

Real-time reverse transcription (RT)-PCR analysis. Total cellular RNA was isolated from tibialis muscle and L6 cells by using an RNeasy kit (Qiagen Sciences), according to manufacturer's instructions. One microgram of tissue or cell RNA was reverse transcribed using Superscript II reverse transcriptase (Invitrogen). PCR products were analyzed using Sybr green mix (Invitrogen). Reactions were performed using Platinum Sybr green qPCR Super-UDG using an iCycler IQ multicolor real-time PCR detection system (Bio-Rad). All reactions were performed in triplicate, and β-actin was used as an internal standard. Primer sequences used were as follows: GLUT4 R, 5′-AATGATGCCAATGAGAAAGG-3′; GLUT4 F, 5′-CAGAAGGTGATTGAACAGAG-3′; Prep1-R, 5′-GGAGTGCCAACCATGTTAAGAAGAAGTCCC-3′; Prep1-F, 5′-GACACCGTGTGCTTCTCGCTCAAG-3′; P160 R, 5′-AGACAAGCAATGTACCGACTACAG-3′; P160 F, 5′-GGCTCTGGTGGACATCCTCTC-3′; PGC-1α R, 5′-AGGGTCATCGTTTGTGGTCAG-3′; PGC-1α F, 5′CAGCGGTCTTAGCACTCAG-3′; Pbx1 R, 5′-TCATGATCCTGCGCTCCCGGTTCCTGGAT-3′; Pbx1 S, 5′-GATGCCCTGCGGACTGTACATCTGACTG-3′; β-actin F, 5′-GCGTGACATCAAAGAGAAG-3′; and β-actin R, 5′-ACTGTGTTGGCATAGAGG-3′.

Statistical procedures. Data were analyzed with Statview software (Abacus Concepts) by one-factor analysis of variance. *P* values of less than 0.05 were considered statistically significant. The total area under the curve for glucose response during the insulin tolerance test was calculated by the trapezoidal method (45).

RESULTS

***Prep1*-hypomorphic mice are protected from streptozotocin-induced hyperglycemia.** To address the role of *Prep1* in glucose metabolism, we compared wild-type, $Prep1^{i/+}$, and $Prep1^{i/i}$ lit-

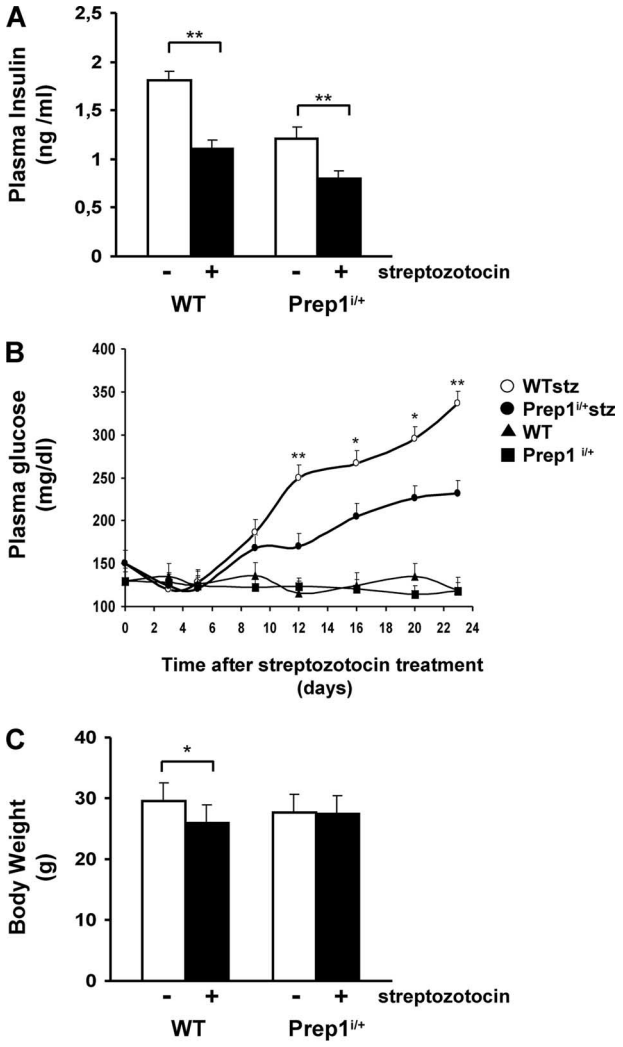

FIG. 3. Effect of streptozotocin in *Prep1*-hypomorphic mice. Heterozygous hypomorphic and control mice (12 mice/group) were subjected to daily i.p. administrations of either streptozotocin (40 mg/kg) or citrate buffer for five consecutive days as described in Materials and Methods. Fasting plasma insulin levels (A) and body weight (C) were assessed both before and 12 days after the end of the treatment. Blood glucose levels (B) were measured before and at the indicated times after streptozotocin administration. Data are means ± standard deviations of values obtained from each group of animals. Asterisks denote statistically significant differences (*, $P < 0.05$; **, $P < 0.01$).

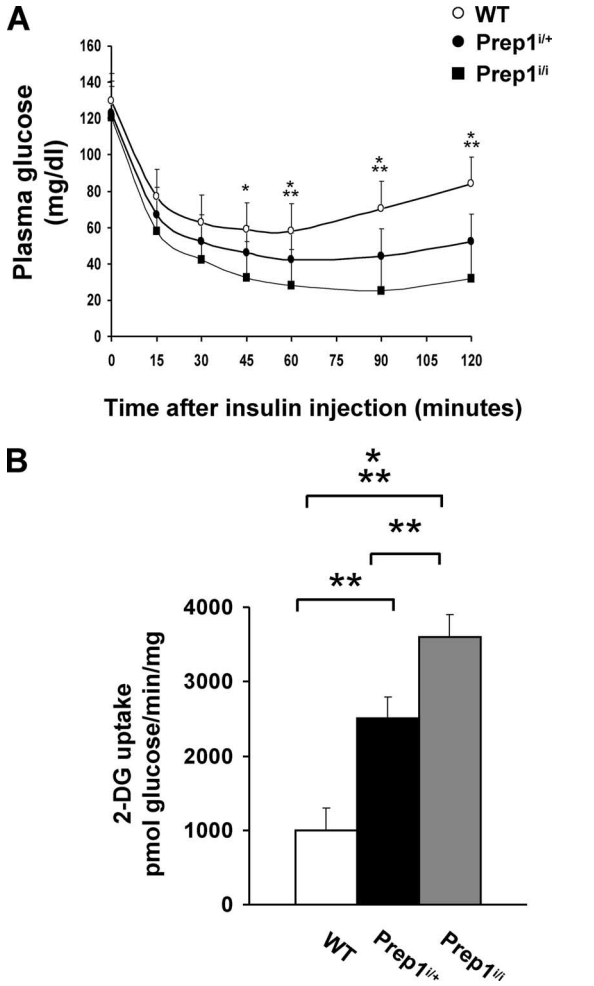

FIG. 4. Insulin action on glucose disposal in *Prep1*-hypomorphic mice. (A) Six-month-old *Prep1*-hypomorphic and control mice (23/group) were i.p. injected with insulin (0.75 mU/g body weight) followed by determinations of blood glucose levels at the indicated times. Data are means ± SD for each group of mice. (B) $Prep1^{i/+}$ and control mice were subjected to intravenous flash injection of 1 μCi of 2-DG and to i.p. injection of insulin (0.75 mU/g of body weight). Tibialis muscles were removed after 30 min and snap-frozen in liquid nitrogen. 2-DG accumulated in muscle tissue was quantitated as described in Materials and Methods (B). Data are means plus standard deviations for 10 mice/group. Asterisks denote statistically significant differences (*, $P < 0.05$; ***, $P < 0.001$).

termate mice. We observed a gene dosage-dependent reduction in plasma insulin levels both under fasting conditions and upon glucose loading (Fig. 1A). As with insulin, circulating glucagon levels were also depressed in the *Prep1*-hypomorphic mice (Fig. 1B).

In spite of the absolute reduction in the insulin levels, i.p. glucose loading indicated preserved glucose tolerance in both the $Prep1^{i/+}$ and $Prep1^{i/i}$ mice, with no gender-related difference (Fig. 2). In addition, glucose tolerance remained normal in 12-month-old hypomorphic mice, suggesting protection of these animals from developing glucose tolerance abnormalities. To analyze this hypothesis further, we targeted β-cell function in the *Prep1*-hypomorphic mice with low-dosage (40 mg/kg) streptozotocin administration. As shown in Fig. 3A, this treatment reduced fasting plasma insulin levels by almost 40% in both $Prep1^{i/+}$ and wild-type littermates. By day 12 of streptozotocin treatment, the wild-type mice developed overt hyperglycemia, accompanied by a 12% reduction in body weight ($P < 0.05$; Fig. 3B and C). In contrast, the $Prep1^{i/+}$ mice showed twofold-smaller changes in plasma glucose levels with no significant weight loss. These data show that, despite their absolute hypoinsulinemia, $Prep1^{i/+}$ mice are protected from streptozotocin-induced diabetes. Similar experiments could not be performed on homozygous $Prep1^{i/i}$ mice because of their frailness.

***Prep1* gene hypomorphism causes enhanced insulin sensitivity in glucose disposal.** TUNEL (terminal deoxynucleotidyl-

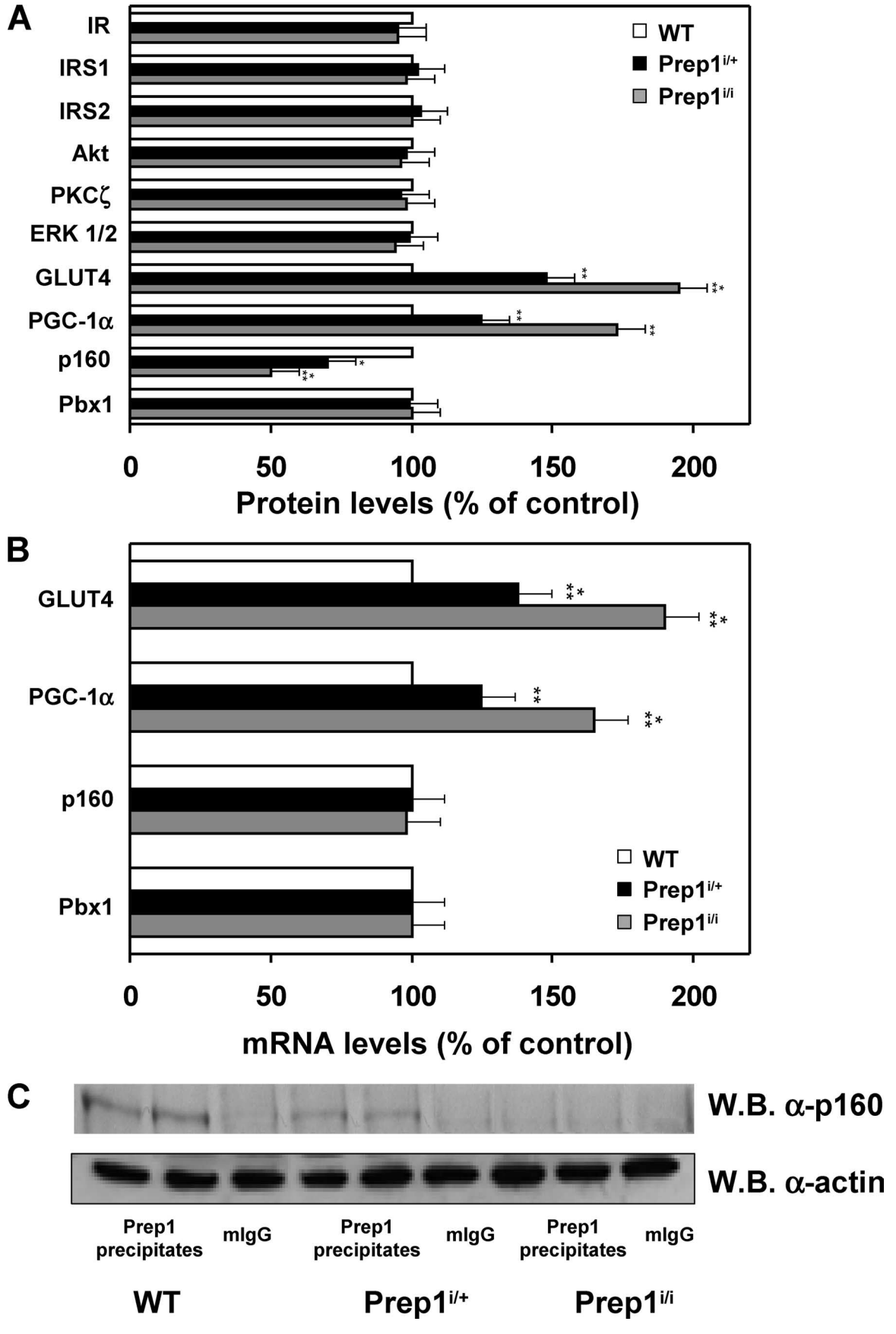

transferase-mediated dUTP-biotin nick end labeling) assays revealed no difference in streptozotocin-induced β-cell apoptosis in hypomorphic and control mice (data not shown). We hypothesized therefore that the protection from development of hyperglycemia observed in the *Prep1*-hypomorphic mice could result from improved insulin sensitivity of glucose disposal. Indeed, upon i.p. insulin injection, the $Prep1^{i/+}$ heterozygous and $Prep1^{i/i}$ homozygous mice developed more sustained and prolonged hypoglycemia than control mice (glucose area-under-the-curve difference between hypomorphic and control mice was significant at the $P < 0.001$ level), with a *Prep1* gene dosage effect (Fig. 4A). Importantly, in vivo insulin-mediated 2-DG uptake by the skeletal muscle was almost 2.5- and 3.5-fold improved, respectively, in the $Prep1^{i/+}$ and in the $Prep1^{i/i}$ mice (Fig. 4B). These results suggested a molecular mechanism operating in skeletal muscle and compensating for the absolute hypoinsulinemia caused by *Prep1* deficiency.

Skeletal muscle from *Prep1*-hypomorphic mice shows altered expression of GLUT4, PGC-1α, and p160. To address the mechanisms responsible for increased insulin-mediated glucose disposal in *Prep1*-hypomorphic mice, we investigated the expression of several proteins playing an important role in insulin sensitivity and glucose disposal. Protein levels measured by immunoblotting of insulin receptor (IR), IR substrate 1 (IRS-1), IRS-2, Akt/PKB, PKC-ζ, ERK1/2, and Pbx1 were not significantly different in $Prep1^{i/i}$, $Prep1^{i/+}$, and control mice (Fig. 5A). Interestingly, however, GLUT4 expression was increased by 75 and 25%, respectively, in skeletal muscle of $Prep1^{i/i}$ and $Prep1^{i/+}$ mice, at both the protein and the mRNA levels (Fig. 5A and B). Similar to GLUT4, the mRNA and protein expression of PGC-1α (29) was also upregulated in the muscle of *Prep1*-hypomorphic mice. The protein (though not the mRNA) levels of the PGC-1α repressor and Prep1-binding Pbx competitor p160 were reduced by 30 and 50%, respectively, in the $Prep1^{i/+}$ and the $Prep1^{i/i}$ mice (Fig. 5A and B). At variance from muscle, liver expression of p160 as well as of PGC-1 exhibited no difference in *Prep1*-hypomorphic and in control mice, indicating tissue selectivity in Prep1 action (data not shown).

P160 has been shown to directly interact with Prep1 in various cell lines (11). We also obtained evidence of Prep1-p160 interaction in tibialis muscle extracts of wild-type mice by immunoprecipitating with anti-Prep1 and blotting with p160 antibodies (Fig. 5C). Indeed, reduced coimmunoprecipitation was noted in the $Prep1^{i/+}$ extracts, with no interaction in the $Prep1^{i/i}$ extracts. These findings raised the possibility that, in the skeletal muscle, Prep1 downregulation results in activation of the glucose transport machinery by decreasing p160 levels.

p160 mediates Prep1-dependent GLUT4 downregulation in L6 skeletal muscle cells. We analyzed this hypothesis further by transiently transfecting *Prep1* cDNA in differentiating L6 skeletal muscle cells, leading to a ninefold overexpression of Prep1 in these cells (Fig. 6A). Consistent with the findings in muscles of hypomorphic mice, overexpression of the wild-type *Prep1* cDNA determined a >70% inhibition of insulin-stimulated 2-DG uptake by these cells (Fig. 6B) and a similar decline in the expression of GLUT4 protein and mRNA (Fig. 6A and C). These effects were accompanied by a threefold decline in PGC-1α protein and mRNA levels (Fig. 6A and D) and opposite changes in the levels of p160 protein (though p160 mRNA remained unchanged) (Fig. 6A and E).

To test for the specificity of the Prep1 effect, we transfected the $Prep1_{HR1}$ mutant, in which two leucines of the HR1 region of Prep1 are mutated to alanine, which prevents binding to both Pbx1 and p160 (11). Transfection with the $Prep1_{HR1}$ mutant had no effect either on GLUT4, PGC-1α, p160, and Pbx1 protein levels (Fig. 6A) or on 2-DG uptake (Fig. 6B). However, transfection of *p160* cDNA blocked GLUT4 and PGC-1α expression to an extent comparable to that caused by *Prep1* (Fig. 6A) and decreased 2-DG uptake (Fig. 6B). Pbx1 levels were low in the L6 cells and did not change upon transfection with *Prep1* cDNA but were further decreased by *p160* (Fig. 6A). Overexpression of *Pbx1*, on the other hand, caused a twofold increase in PGC-1α and GLUT4 levels (Fig. 6A), a similar decrease of p160 (Fig. 6A), and an increase in 2-DG uptake (Fig. 6B).

Delivery of p160 in skeletal muscle reverts the $Prep1^{i/i}$ phenotype. Next, we injected 100 μg of p160 cDNA into the tibialis muscles of wild-type, heterozygous, and homozygous littermate mice. Consistent with the above findings, ectopic expression of p160 in tibialis muscles of $Prep1^{i/i}$ and $Prep1^{i/+}$ mice by naked DNA delivery markedly reduced PGC-1α and GLUT4 levels, thereby rescuing the molecular phenotype (Fig. 7). The introduction of p160 cDNA into the muscles of wild-type mice also led to a reduction of PGC-1α and GLUT4. The data are therefore consistent with the view that Prep1 downregulates PGC-1α and GLUT4, and thereby the insulin-dependent glucose transport machinery, through p160 and not Pbx1.

Prep1 regulates proteasomal degradation of p160. Prep1 controls the half-life of Pbx at the protein stability level (15, 26). To test whether Prep1 can likewise regulate the stability of p160, we exposed L6 myotubes to the protein synthesis inhibitor cycloheximide and found that this treatment reduced p160 cellular levels in a time-dependent manner (Fig. 8A). Interestingly, the degradation of p160 in the presence of cycloheximide was abolished in the Prep1-overexpressing cells, implying that,

FIG. 5. Expression profile of skeletal muscle from *Prep1*-hypomorphic mice. (A) Tibialis muscles from *Prep1*-hypomorphic and control mice were dissected, solubilized, and subjected to Western blotting with IR, IRS1, IRS2, Akt, PKCζ, ERK-1/2, GLUT4, PGC-1α, p160, and Pbx1 antibodies. Blots were revealed by ECL and autoradiography, and bands were quantitated by laser densitometry and normalized for actin. Data are means plus standard deviations of duplicate determinations for 12 mice/group. (B) The abundance of RNAs for the indicated proteins was determined by real-time RT-PCR analysis of total RNA isolated from tibialis muscles of the hypomorphic and control mice, using beta-actin as an internal standard. Data are means plus standard deviations for four independent experiments in each of which reactions were performed in triplicate using the pooled total RNAs obtained from six mice/genotype. (C) Protein lysates (250 μg) from tibialis muscles of wild-type and *Prep1*-hypomorphic mice were precipitated with Prep1 antibody or with nonimmune mouse immunoglobulin G (mIgG) followed by blotting with p160 antibody, ECL, and autoradiography. The same lysates were directly blotted with antiactin antibodies for normalization. The autoradiograph shown is representative of four independent experiments.

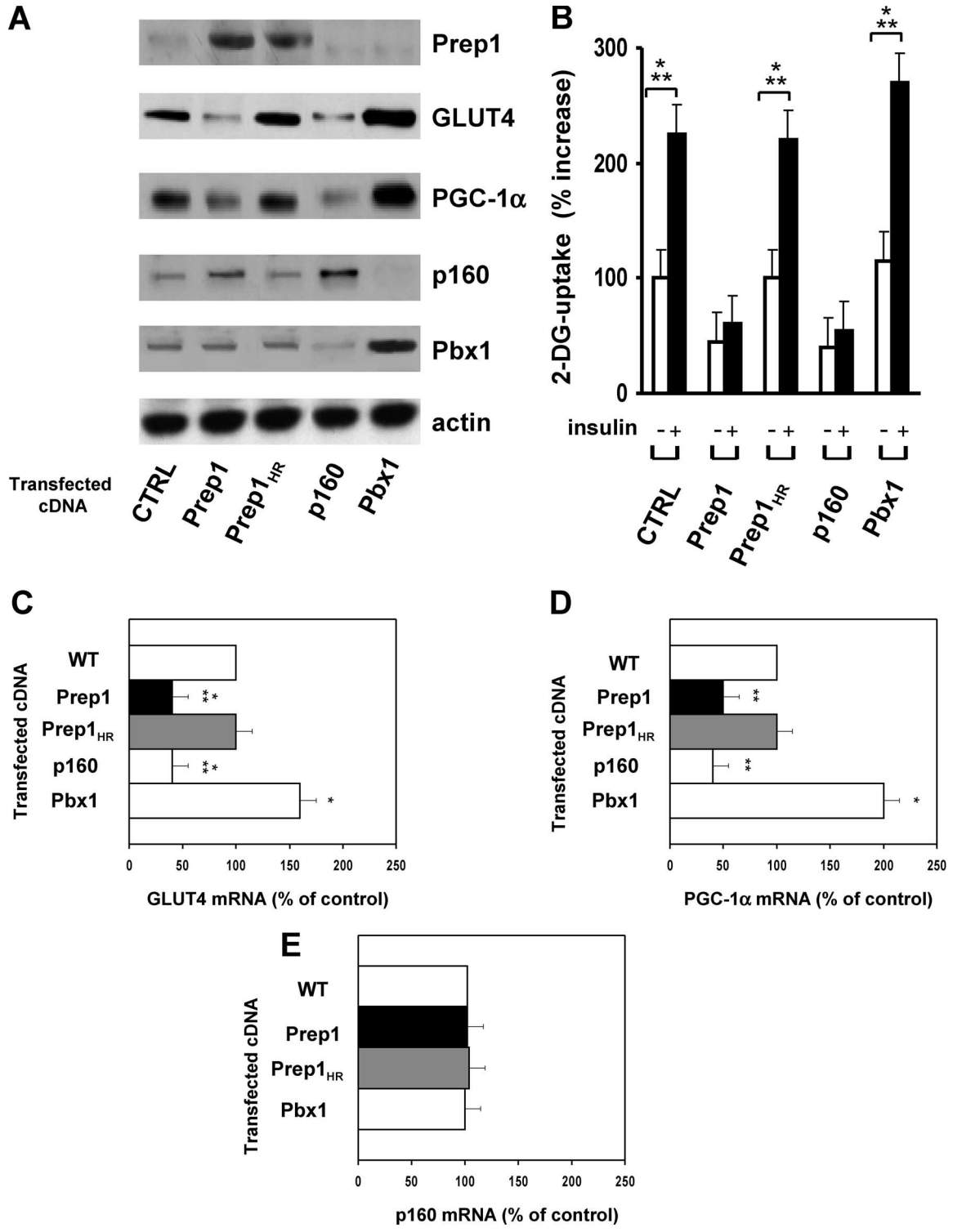

FIG. 6. Effect of *Prep1* overexpression in L6 skeletal muscle cells. (A) L6 myotubes were transiently transfected with the *Prep1*, $Prep1_{HR1}$ mutant, *p160*, and *Pbx1* cDNAs or with the empty vector (CTRL). Cells were solubilized, and lysates were analyzed by SDS-PAGE and subjected to Western blotting with GLUT4, PGC-1, p160, and Pbx1 antibodies. As a control, filters were reblotted with actin antibodies. Bands were revealed by ECL and autoradiography. The autoradiograph shown is representative of five independent experiments. (B) L6 myotubes transfected with the *Prep1*, $Prep1_{HR1}$ mutant, *p160*, and *Pbx1* cDNAs or with the empty vector (CTRL) were exposed to 100 nM insulin, and 2-DG uptake was assayed as described in Materials and Methods. Data are means plus standard deviations from four independent experiments, each in duplicate. (C, D, and E) Levels of mRNAs encoding GLUT4, PGC-1α, and p160 in cells transfected with the *Prep1*, $Prep1_{HR1}$ mutant, *p160*, and *Pbx1* cDNAs were quantitated by real-time RT-PCR analysis, using beta-actin as an internal standard. Data are means plus standard deviations from four independent experiments.

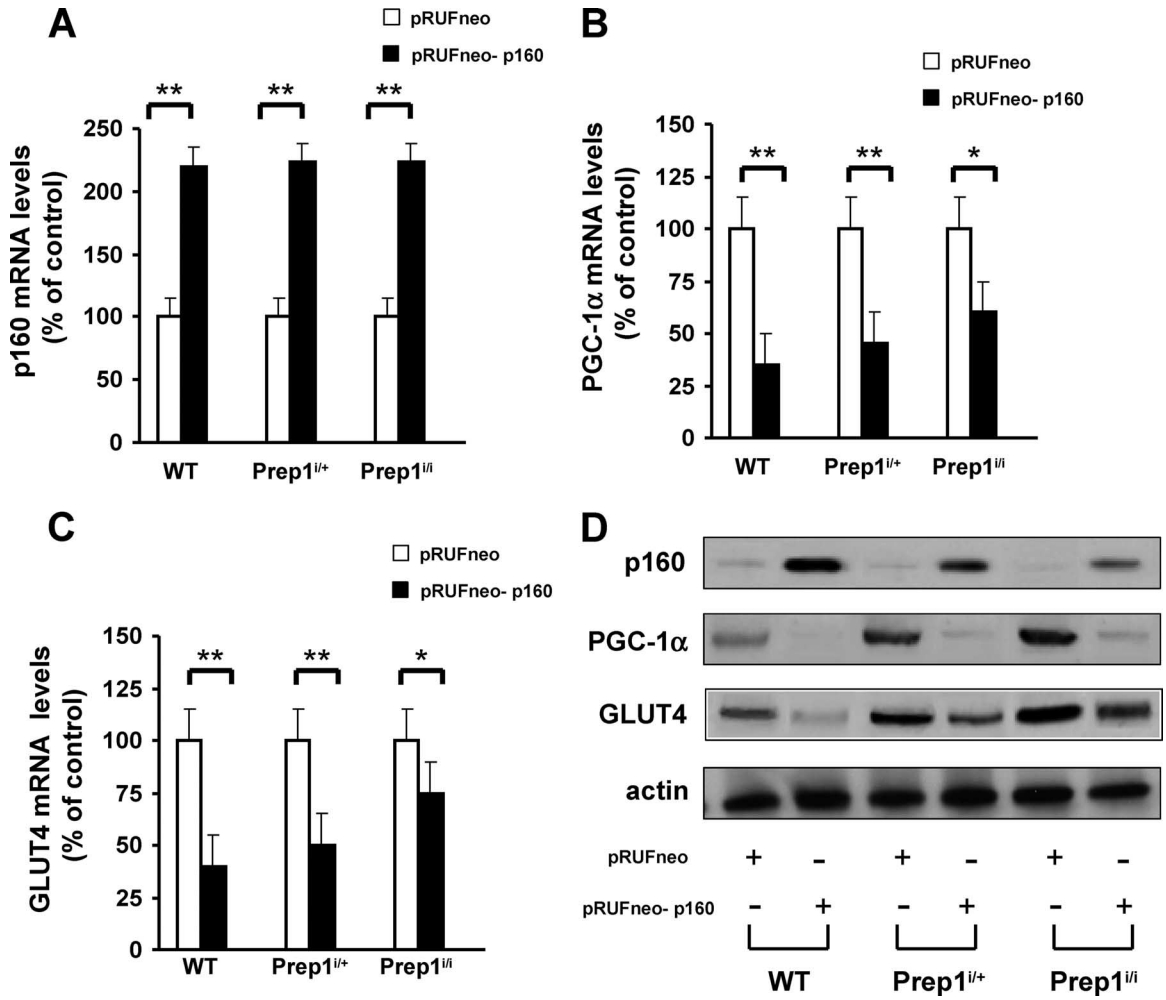

FIG. 7. p160, PGC-1α, and GLUT4 levels in *Prep1*-hypomorphic mice injected with pRUFneo-p160 vector. Mouse tibialis muscles were injected with 100 μg of pRUFneo-p160 vector. RNA was extracted 48 h later to measure p160 (A), PGC-1α (B), and GLUT4 (C) levels. The abundance of the indicated mRNA was determined by real-time RT-PCR analysis of total RNA isolated from tibialis muscles of the wild-type, $Prep1^{i/+}$, and $Prep1^{i/i}$ and control mice, using beta-actin as an internal standard. Data are means plus standard deviations for three independent experiments in each of which reactions were performed in triplicate using pooled total RNAs from three mice/genotype. (D) Proteins were also extracted as described in Materials and Methods and analyzed by immunoblotting with specific antibodies.

at least in part, upregulation of p160 by Prep1 (Fig. 6) involves posttranslational mechanisms. To better define these events, we also incubated L6 cells with the proteasome inhibitor MG132. As shown in Fig. 8B, exposure to this agent for 6 h increased p160 intracellular levels by 10-fold. In the Prep1 overexpressing cells, the proteasome inhibitor induced a further 2.5-fold accumulation of the protein. Also, in these same cells, p160-Prep1 coprecipitation was 3-fold more effective than in cells expressing only their physiological complement of *Prep1* (Fig. 8C). These data indicate that Prep1 interaction enhances p160 protein stability and explain the mechanism of p160 decrease in $Prep1^{i/i}$ muscle. Thus, we conclude that the *Prep1* function on glucose disposal depends on its interaction with p160. This represents the first identified Pbx1-independent function of *Prep1*.

Effect of Prep1 deficiency on islet development and islet function. As the Prep1 partner Pbx1 is required for pancreas development and adult function (22), and in view of the lower insulin and glucagon plasma level of $Prep1^{i/i}$ mice, we also tested whether Prep1 deficiency has an effect on endocrine pancreas function. We first compared islet morphology in adult (3-month-old) $Prep1^{i/+}$, $Prep1^{i/i}$, and wild-type littermates. In these animals, pancreas weight correlated with the genotype, being lowest in the homozygous $Prep1^{i/i}$ mice (Table 1). However, the percentage of the area occupied by islets, including both α and β cells, was normal. Also, whole-islet and β-cell masses were decreased in the $Prep1^{i/i}$ mice. The heterozygous $Prep1^{i/+}$ mice displayed an intermediate phenotype (Table 1). This phenotype could be assessed by histological and immunohistochemical examination of pancreatic sections (Fig. 9) showing smaller islets, with normal spatial distribution of α and β cells. The smaller size of the islets is consistent with the reduced plasma levels of insulin and glucagon (see Fig. 1).

Since Prep1 stabilizes Pbx1 (15) and since Pbx1 is important in pancreas development and glucose tolerance (22), we measured

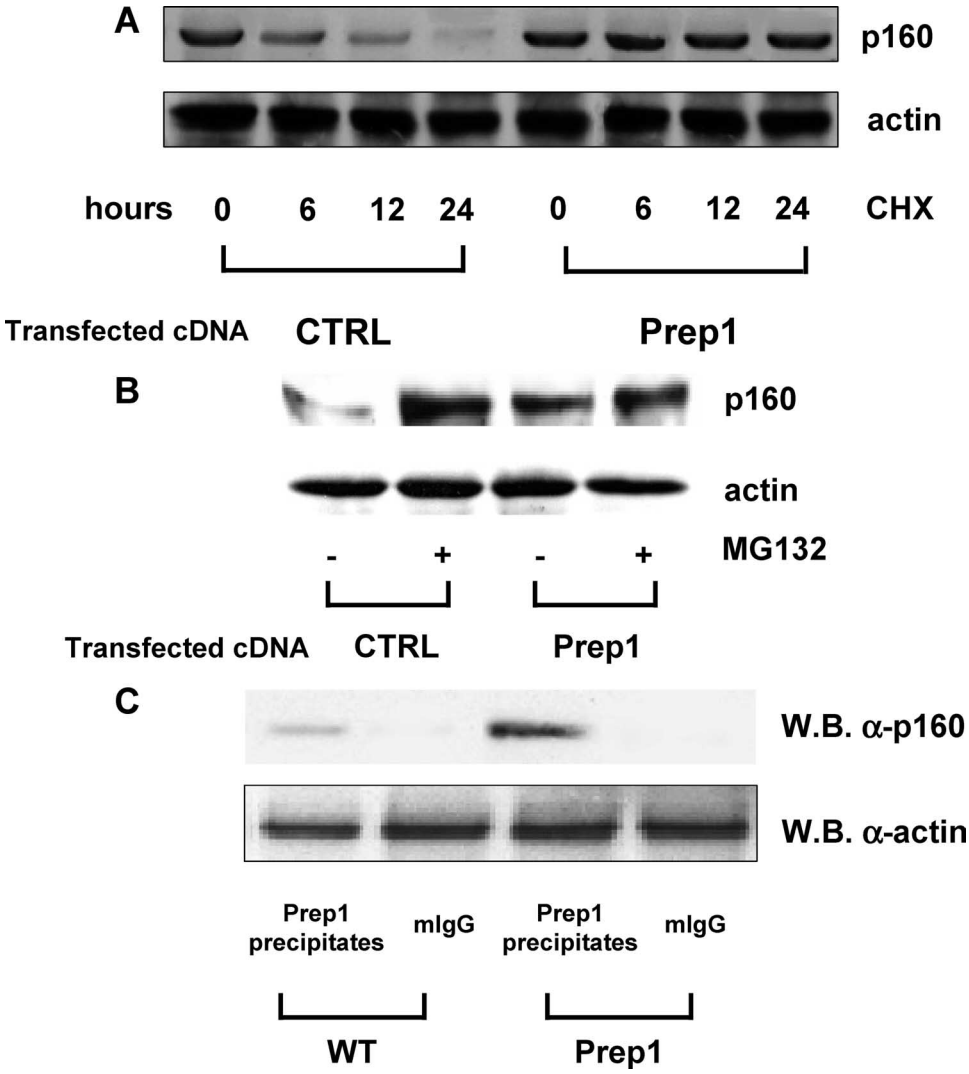

FIG. 8. Effect of cycloheximide and MG132 on p160 levels. L6 skeletal muscle cells overexpressing Prep1 or transfected with the empty vector (CTRL) were incubated with 40 μg/ml cycloheximide (CHX) for the indicated times (A) or 10 μM MG132 for 3 h (B). Cell lysates were separated by SDS-PAGE and analyzed by Western blotting with p160 and actin antibodies. Blots were revealed by ECL and autoradiography. The autoradiographs shown are representative of four (A) and five (B) independent experiments. (C) L6 cells were transiently transfected with either a cDNA encoding *Prep1* or a control vector. Aliquots of the cell lysates were precipitated with Prep1 or with nonimmune mouse IgG (mIgG) antibodies followed by blotting with p160 antibodies. Blots were revealed by ECL and autoradiography. The same lysates were directly blotted with antiactin antibodies for normalization. The autoradiographs shown are representative of four independent experiments.

Pbx-1 levels in pancreatic tissue by immunoblotting. As shown in Fig. 10A, Pbx1 levels were severely reduced in extracts of *Prep1*-hypomorphic pancreas. Again, the extent of this reduction correlated with the genotype. Other Pbx isoforms as well as p160 show a reduction similar to that of Pbx1 (data not shown). Importantly, however, islets isolated from the *Prep1*-hypomorphic and control littermates mice exhibited comparable insulin secretion responses when exposed to 16.7 mM glucose-containing culture medium

TABLE 1. Morphometric analysis of Prep1 hypomorphic pancreas[a]

Mouse group	Islet area/pancreatic area	% in islet			Wt or mass (mg)		
		Beta cells	Alpha cells	Other cells	Pancreas	Islet cells	Beta cells
Control	0.54 ± 0.07	77.21 ± 4.52	17.15 ± 2.10	5.64 ± 1.06	179 ± 15	0.97 ± 0.10	0.75 ± 0.06
Prep1$^{i/+}$	0.50 ± 0.04	76.54 ± 3.11	15.75 ± 2.25	7.71 ± 1.44	144 ± 11*	0.72 ± 0.08*	0.57 ± 0.03*
Prep1$^{i/i}$	0.48 ± 0.04*	77.32 ± 2.12	16.33 ± 3.24	6.35 ± 0.82	127 ± 9*	0.61 ± 0.04**	0.47 ± 0.02**

[a] Mice were analyzed as described in Materials and Methods. Data are means ± standard deviations for eight *Prep1*$^{i/+}$ and an equal number of *Prep1*$^{i/i}$ and wild-type (control) mice. Asterisks indicate statistically significant differences (*, $P < 0.05$; **, $P < 0.01$).

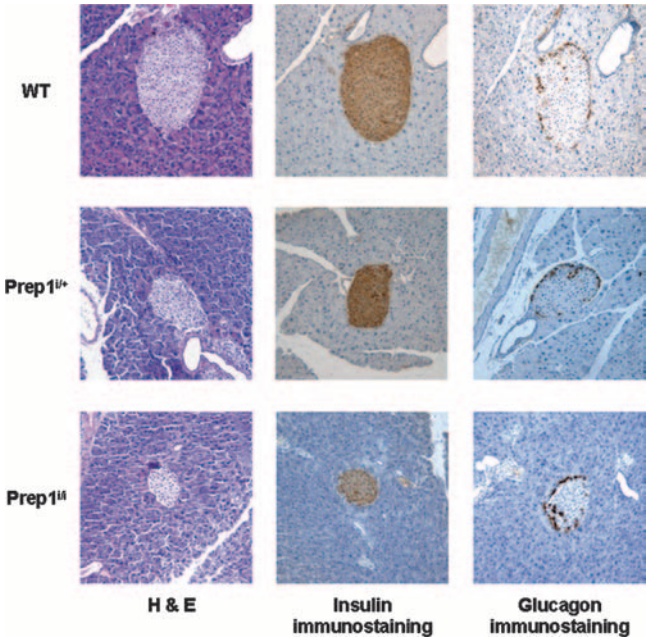

FIG. 9. Immunohistochemical analysis of islets from *Prep1*-hypomorphic mice. Formalin-fixed and paraffin-embedded pancreas sections from 3-month-old $Prep1^{i/+}$, $Prep1^{i/i}$, and wild-type (WT) mice were stained with hematoxylin-eosin (H & E) or immunostained with insulin or glucagon antibodies. Microphotographs are representative of findings obtained from 12 heterozygous, 7 homozygous, and 8 wild-type mice. Magnification, ×100.

(Fig. 10B), suggesting that Prep1 deficiency has no effect on the insulin secretion machinery.

DISCUSSION

We have shown that *Prep1*-hypomorphic mice have a complex phenotype with at least two metabolically relevant features. One is increased insulin sensitivity in skeletal muscle accompanied by protection from streptozotocin-induced diabetes. The second is pancreatic islet hypoplasia accompanied by absolute hypoinsulinemia.

So far, the Pbx proteins have been considered the unique partners of Prep1 (8, 4, 21, 33, 34, 35). However, it was recently shown that p160 can compete with Pbx1 for binding to Prep1 (11), although the functional in vivo relevance of this interaction is unknown. *Pbx1* has a major role in pancreas development, as $Pbx1^{-/-}$ embryos feature pancreatic hypoplasia as well as defective endocrine and exocrine cell differentiation prior to death at embryonic day 15 to 16 (22, 41). An important role of Pbx1 in pancreatic adult function is also shown by the reduced glucose tolerance phenotype of heterozygous $Pbx1^{+/-}$ mice and by the overt diabetic phenotype of the compound $Pbx1^{+/-}$ $Pdx1^{+/-}$ mice (22). In the present paper, however, we show that the increased insulin sensitivity occurring in the skeletal muscle of $Prep1^{i/+}$ and $Prep1^{i/i}$ mice does not depend on *Pbx1*. First, Pbx1 mRNA and protein levels were unchanged in skeletal muscle (unlike other organs) (Fig. 5A and B and Fig. 10). Second, studies with L6 cells show that overexpression of Prep1 and Pbx1 have opposite effects. *Prep1* reduces the level of PGC-1α and GLUT4 in these cells (Fig. 6). Overexpression of Pbx1, on the other hand, boosts the levels of PGC-1α and GLUT4. Thus, *Pbx1* and *Prep1* have opposite effects on insulin-dependent glucose disposal by muscle.

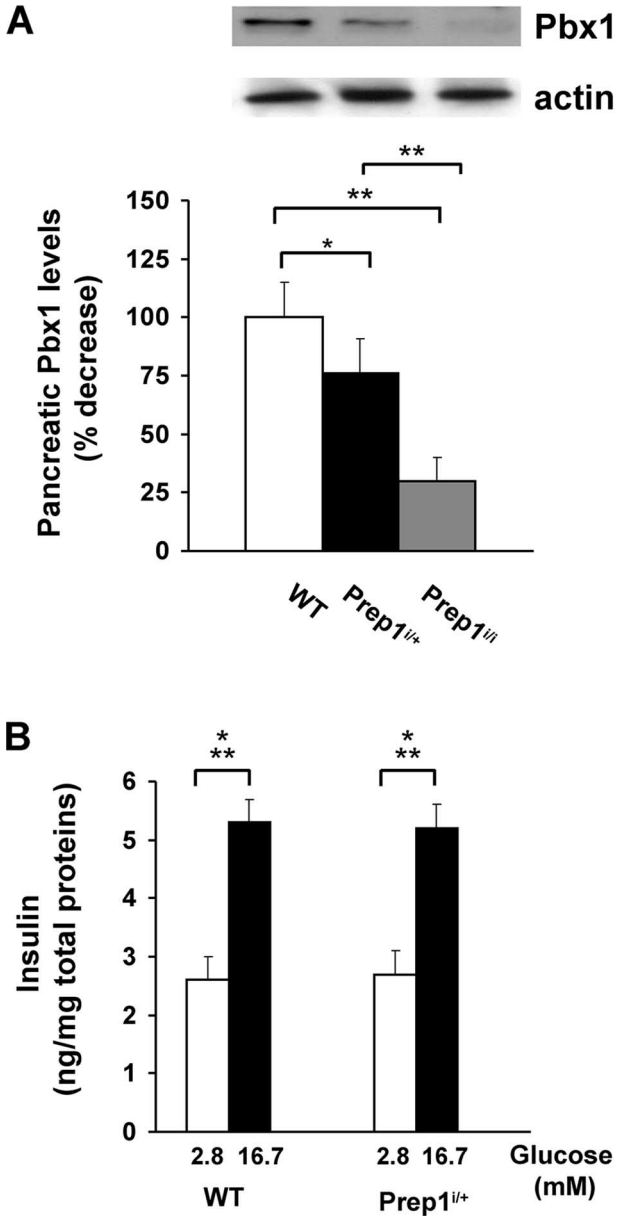

FIG. 10. Pbx1 expression and islet function in *Prep1*-hypomorphic mice. (A) Upon sacrifice, pancreases from hypomorphic and control mice were rapidly removed as described in Materials and Methods, solubilized, and subjected to Western blotting with Pbx1 antibodies. Specific bands were revealed by ECL and autoradiography, followed by densitometric quantitation. Data are means plus standard deviations for 15 mice/group. (B) Islets from 6-month-old control and *Prep1*-hypomorphic mice were dissected and cultured as described in Materials and Methods. Islets were exposed to the indicated concentrations of glucose, and insulin release was assessed in the culture media by radioimmunoassay. Data are means plus standard deviations from 10 independent experiments done in duplicate.

At variance with Pbx1, p160 is key to Prep1 action on glucose disposal, consistent with the known function of p160 in regulating PGC-1α and energy metabolism in skeletal muscles

(13). Indeed, we show that Prep1 increases the levels of p160 in muscle cells (Fig. 6). Overexpression of p160 in the L6 cells and direct delivery of a p160 cDNA in the muscle of *Prep1*$^{i/+}$ and *Prep1*$^{i/i}$ mice mimic the effect of Prep1, decreasing PGC-1α and GLUT4 expression. No change of PGC-1α mRNA or protein was detected in the liver of the *Prep1*-hypomorphic mice (data not shown), suggesting that the interplays between these molecules are cell type selective. Together, these data are in agreement with several published papers reporting a positive correlation between PGC-1α and GLUT4 in rodent (29) and human (2) muscle cells and in humans in vivo (37) and may account for the enhanced insulin sensitivity in muscles of *Prep1*-hypomorphic mice (Fig. 6). Previous work by Miura et al. demonstrated GLUT4 downregulation in transgenic mice overexpressing PGC-1α (31). However, as suggested by those authors, a reduction in the lower-molecular-weight PGC-1α form might have caused the negative correlation between PGC-1α and GLUT4 levels in this model.

Cycloheximide experiments demonstrated that the regulation of the p160 expression by Prep1 was, at least in part, posttranslational. Furthermore, the stabilizing effect of MG132 shows that p160 degradation involves the proteasome. In the presence of excess Prep1, the proteasome inhibitor had a much smaller effect (Fig. 8), indicating that Prep1 interaction stabilizes p160 and induces p160 escape from proteasomal degradation.

The present results highlight a novel regulatory mechanism of insulin sensitivity occurring in the skeletal muscle upstream of the p160/PGC-1α complex and operated by the balance of p160 and Pbx1. When p160 exceeds Pbx1, it binds Prep1, is stabilized, and represses *GLUT4* and insulin sensitivity. When Pbx1 is present in excess, the reverse occurs. These regulatory mechanisms must be more complex, however, since one would otherwise expect that a decrease in Pbx1 would directly lead to decreased insulin sensitivity, which is not the case. Indeed, *Pbx1*$^{+/-}$ mice display a slightly improved insulin sensitivity accompanied by early impairment of glucose tolerance (22). These mice differ from both the *Prep1*$^{i/i}$ and the *Prep1*$^{i/+}$ mice, which show a significant enhancement in insulin sensitivity and exhibit no tendency to develop abnormal glucose tolerance. Furthermore, *Prep1*-hypomorphic mice are protected from streptozotocin-induced diabetes in spite of their decreased β-cell mass and circulating insulin levels. Based on TUNEL assays, this protection was independent of differences in streptozotocin-induced β-cell apoptosis between the hypomorphic and control mice (data not shown). The increase in the sensitivity to insulin action on glucose disposal and on glucose uptake by the skeletal muscle, together with the reduced glucagon levels, may contribute to the stability of glucose tolerance in the *Prep1*-hypomorphic mice.

Another important aspect of our work is that Prep1 and Pbx1 have distinct roles in pancreas function in the adult. Indeed, Prep1 binds and stabilizes Pbx proteins in a cell-specific manner (15, 26, 38, 46). Consistently, we show that the level of Pbx1 in *Prep1*$^{i/i}$ hypomorphic mice is decreased in the adult pancreas (Fig. 10A), though not in the skeletal muscle (Fig. 6). Therefore, the *Prep1*$^{i/i}$ animals were expected to display a pancreatic phenotype similar to that of *Pbx1*$^{+/-}$ mice, i.e., disrupted architecture of the pancreatic islets and hypoinsulinemia (22). Surprisingly, *Prep1*-hypomorphic mice were found to have normal islet architecture. However, they did show islet hypoplasia, accompanied by significantly reduced absolute insulin levels (both basal and postloading). Why the pancreatic phenotype of the *Prep1*$^{i/i}$ mice, which includes a strong reduction of *Pbx1* pancreas expression (Fig. 10A), is different from that of the *Pbx1*$^{+/-}$ heterozygous mice (22) is not completely clear. The deficiency of *Prep1* might have been complemented by the overexpression of other family members. This is unlikely, however, as no increase of Prep2 or Meis proteins is observed in *Prep1*$^{i/i}$ embryos (15). More simply, the reduction of Pbx1 in *Prep1*-hypomorphic mice may not be enough to generate the phenotype of the *Pbx*$^{+/-}$ mouse. It is also possible that other TALE family members (e.g., one of the *Meis* genes) cooperate with *Pbx1* in pancreas development and in functions where *Prep1* is not involved. Finally, it is possible that the islet phenotype of the *Prep1*-hypomorphic mice is established as an adaptive response to their enhanced insulin sensitivity. Indeed, islets isolated from *Prep1*$^{i/+}$ mice exhibit a normal secretory response to glucose in culture (Fig. 10B). A decreased β-cell mass in conditions of chronically improved insulin sensitivity has been previously observed in mice. For instance, pancreatic β-cell area is decreased in protein tyrosine phosphatase 1b-deficient mice owing to increased peripheral insulin sensitivity and reduced insulin requirement (25).

The present results may have clinical relevance. In individuals with normal glucose tolerance, insulin sensitivity and secretion span a wide range and are determined by a number of different genes (16, 28). Variability in some of these genes is known to provide an important contribution to major human disorders, including type 2 diabetes (16, 17). For example, Pdx1 point mutations cause impaired insulin secretion and a rare form of non-insulin-dependent diabetes formerly termed MODY4 (43). On the basis of the results of this study, *Prep1* might also be involved in the pathogenesis of these diseases. Whether genetic variability at the *Prep1* locus affects insulin sensitivity in humans is an important issue presently under investigation in the laboratory.

ACKNOWLEDGMENTS

This work was supported, in part, by the European Community's FP6 EUGENE2 (contract LSHM-CT-2004-512013) and FP7 PREPROBEDIA (grant 201681), by an EFSD/Lilly grant, by the Associazione Italiana per la Ricerca sul Cancro (AIRC), and by the Ministero dell'Università e della Ricerca Scientifica (PRIN and FIRB RBNE0155LB). The financial support of Telethon—Italy is gratefully acknowledged. V. M. Diaz was a recipient of a Marie Curie Fellowship from the EU.

We are grateful to A. Zabatta for helping with the morphometric analysis. The technical help of Salvatore Sequino is also acknowledged.

REFERENCES

1. **Ahlgren, U., J. Jonsson, L. Jonsson, K. Simu, and H. Edlund.** 1998. Beta-cell-specific inactivation of the mouse Ipf1/Pdx1 gene results in loss of the beta-cell phenotype and maturity onset diabetes. Genes Dev. **12:**1763–1768.
2. **Al-Khalili, L., M. Forsgren, K. Kannisto, J. R. Zierath, F. Lönnqvist, and A. Krook.** 2005. Enhanced insulin-stimulated glycogen synthesis in response to insulin, metformin or rosiglitazone is associated with increased mRNA expression of GLUT4 and peroxisomal proliferator activator receptor gamma co-activator 1. Diabetologia **48:**1173–1179.
3. **Berthelsen, J., V. Zappavigna, F. Mavilio, and F. Blasi.** 1998a. Prep1, a novel functional partner of Pbx proteins. EMBO J. **17:**1423–1433.
4. **Berthelsen, J., V. Zappavigna, E. Ferretti, F. Mavilio, and F. Blasi.** 1998b. The novel homeoprotein Prep1 modulates Pbx-Hox protein cooperativity. EMBO J. **17:**1434–1445.

5. **Berthelsen, J., C. Kilstrup-Nielsen, F. Blasi, F. Mavilio, and V. Zappavigna.** 1999. The subcellular localization of PBX1 and EXD proteins depends on nuclear import and export signals and is modulated by association with PREP1 and HTH. Genes Dev. **13:**946–953.
6. **Calvo, K. R., P. Knoepfler, S. McGrath, and M. P. Kamps.** 1999. An inhibitory switch derepressed by pbx, hox, and Meis/Prep1 partners regulates DNA-binding by pbx1 and E2a-pbx1 and is dispensable for myeloid immortalization by E2a-pbx1. Oncogene **18:**8033–8043.
7. **Caruso, M., C. Miele, F. Oriente, A. Maitan, G. Bifulco, F. Andreozzi, G. Condorelli, P. Formisano, and F. Beguinot.** 1999. In L6 skeletal muscle cells, glucose induces cytosolic translocation of protein kinase C-alpha and transactivates the insulin receptor kinase. J. Biol. Chem. **274:**28637–28644.
8. **Chen, H., C. Dossier, Y. Nakamura, A. Lynn, A. Chakravarti, and S. E. Antonarakis.** 1997. Cloning of a novel homeobox-containing gene, PKNOX1, and mapping to human chromosome 21q22.3. Genomics **41:**193–200.
9. **Deflorian, G., N. Tiso, E. Ferretti, D. Meyer, F. Blasi, M. Bortolussi, and F. Argenton.** 2004. Prep1.1 has essential genetic functions in hindbrain development and cranial neural crest cell differentiation. Development **131:**613–627.
10. **Devedjian, J. C., M. George, A. Casellas, A. Pujol, J. Visa, M. Pelegrin, L. Gros, and F. Bosch.** 2000. Transgenic mice overexpressing insulin-like growth factor-II in beta cells develop type 2 diabetes. J. Clin. Investig. **105:**731–740.
11. **Diaz, V. M., S. Mori, E. Longobardi, G. Menendez, C. Ferrai, R. A. Keough, A. Bachi, and F. Blasi.** 2007. p160 myb-binding-protein interacts with Prep1 and inhibits its transcriptional activity. Mol. Cell. Biol. **27:**7981–7990.
12. **Dutta, S., M. Gannon, B. Peers, C. Wright, S. Bonner-Weir, and M. Montminy.** 2001. PDX:PBX complexes are required for normal proliferation of pancreatic cells during development. Proc. Natl. Acad. Sci. USA **98:**1065–1070.
13. **Fan, M., J. Rhee, J. St-Pierre, C. Handschin, P. Puigserver, J. Lin, S. Jäeger, H. Erdjument-Bromage, P. Tempst, and B. M. Spiegelman.** 2004. Suppression of mitochondrial respiration through recruitment of p160 myb binding protein to PGC-1α: modulation by p38 MAPK. Genes Dev. **18:**278–289.
14. **Ferre, P., A. Leturque, A. F. Burnol, L. Penicaud, and J. Girard.** 1985. A method to quantify glucose utilization in vivo in skeletal muscle and white adipose tissue of the anaesthetized rat. Biochem. J. **228:**103–110.
15. **Ferretti, E., J. C. Villaescusa, P. Di Rosa, L. C. Fernandez-Diaz, E. Longobardi, R. Mazzieri, A. Miccio, N. Micali, L. Selleri, G. Ferrari, and F. Blasi.** 2006. Hypomorphic mutation of the TALE gene Prep1 (pKnox1) causes a major reduction of Pbx and Meis proteins and a pleiotropic embryonic phenotype. Mol. Cell. Biol. **26:**5650–5662.
16. **Freeman, H., and R. D. Cox.** 2006. Type-2 diabetes: a cocktail of genetic discovery. Hum. Mol. Genet. **15:**R202–209.
17. **Freimer, N. B., and C. Sabatti.** 2007. Variants in common diseases. Nature **445:**828–830.
18. **Hani, E. H., J. Hager, A. Philippi, F. Demenais, P. Froguel, and N. Vionnet.** 1997. Mapping NIDDM susceptibility loci in French families: studies with markers in the region of NIDDM1 on chromosome 2q. Diabetes **46:**1225–1226.
19. **Horiki, M., E. Yamato, H. Ikegami, T. Ogihara, and J. Miyazaki.** 2004. Needleless in vivo gene transfer into muscles by jet injection in combination with electroporation. J. Gene Med. **6:**1134–1138.
20. **Jaw, T. J., L. R. You, P. S. Knoepfler, L. C. Yao, C. Y. Pai, C. Y. Tang, L. P. Chang, J. Berthelsen, F. Blasi, M. P. Kamps, and Y. H. Sun.** 2000. Direct interaction of two homeoproteins, homothorax and extradenticle, is essential for EXD nuclear localization and function. Mech. Dev. **91:**279–291.
21. **Kamps, M. P., C. Murre, X. H. Sun, and D. Baltimore.** 1990. A new homeobox gene contributes the DNA binding domain of the t(1;19) translocation protein in pre-B ALL. Cell **60:**547–555.
22. **Kim, S. K., L. Selleri, J. S. Lee, A. Y. Zhang, X. Gu, Y. Jacobs, and M. L. Cleary.** 2002. Pbx1 inactivation disrupts pancreas development and in Ipf1 deficient mice promotes diabetes mellitus. Nat. Genet. **30:**430–435.
23. **Kitamura, T., Y. Kido, S. Nef, J. Merenmies, L. F. Parada, and D. Accili.** 2001. Preserved pancreatic beta-cell development and function in mice lacking the insulin receptor-related receptor. Mol. Cell. Biol. **21:**5624–5630.
24. **Knoepfler, P. S., K. R. Calvo, H. Chen, S. E. Antonarakis, and M. P. Kamps.** 1997. Meis1 and pKnox1 bind DNA cooperatively with Pbx1 utilizing an interaction surface disrupted in oncoprotein E2a-Pbx1. Proc. Natl. Acad. Sci. USA **94:**14553–14558.
25. **Kushner, J. A., F. G. Haj, L. D. Klaman, M. A. Dow, B. B. Kahn, B. G. Neel, and M. F. White.** 2004. Islet-sparing effects of protein tyrosine phosphatase-1b deficiency delays onset of diabetes in IRS2 knockout mice. Diabetes **53:**61–66.
26. **Longobardi, E., and F. Blasi.** 2003. Overexpression of PREP-1 in F9 teratocarcinoma cells leads to a functionally relevant increase of PBX-2 by preventing its degradation. J. Biol. Chem. **278:**39235–39241.
27. **Macfarlane, W. M., T. M. Frayling, S. Ellard, J. C. Evans, L. I. Allen, M. P. Bulman, S. Ayres, M. Shepherd, P. Clark, A. Millward, A. Demaine, T. Wilkin, K. Docherty, and A. T. Hattersley.** 1999. Missense mutations in the insulin promoter factor-1 gene predispose to type 2 diabetes. J. Clin. Investig. **104:**R33–39.
28. **Marchetti, P., S. Del Prato, R. Lupi, and S. Del Guerra.** 2006. The pancreatic beta-cell in human type 2 diabetes. Nutr. Metab. Cardiovasc. Dis. **16:**S3–S6.
29. **Michael, L. F., Z. Wu, R. B. Cheatham, P. Puigserver, G. Adelmant, J. J. Lehman, D. P. Kelly, and B. M. Spiegelman.** 2001. Restoration of insulin-sensitive glucose transporter (GLUT4) gene expression in muscle cells by the transcriptional coactivator PGC-1. Proc. Natl. Acad. Sci. USA **98:**3820–3825.
30. **Miele, C., M. Caruso, V. Calleja, R. Auricchio, F. Oriente, P. Formisano, G. Condorelli, A. Cafieri, D. Sawka-Verhelle, E. Van Obberghen, and F. Beguinot.** 1999. Differential role of insulin receptor substrate (IRS)-1 and IRS-2 in L6 skeletal muscle cells expressing the Arg1152→Gln insulin receptor. J. Biol. Chem. **274:**3094–3102.
31. **Miura, S., Y. Kai, M. Ono, and O. Ezaki.** 2003. Overexpression of peroxisome proliferator-activated receptor gamma coactivator-1α down-regulates GLUT4 mRNA in skeletal muscles. J. Biol. Chem. **278:**31385–31390.
32. **Moens, C. B., and L. Selleri.** 2006. Hox cofactors in vertebrate development. Dev. Biol. **291:**193–206.
33. **Monica, K., N. Galili, J. Nourse, D. Saltman, and M. L. Cleary.** 1991. PBX2 and PBX3, new homeobox genes with extensive homology to the human proto-oncogene PBX1. Mol. Cell. Biol. **11:**6149–6157.
34. **Moskow, J. J., F. Bullrich, K. Huebner, I. O. Daar, and A. M. Buchberg.** 1995. Meis1, a PBX1-related homeobox gene involved in myeloid leukemia in BXH-2 mice. Mol. Cell. Biol. **15:**5434–5443.
35. **Nourse, J., J. D. Mellentin, N. Galili, J. Wilkinson, E. Stanbridge, S. D. Smith, and M. L. Cleary.** 1990. Chromosomal translocation t(1;19) results in synthesis of a homeobox fusion mRNA that codes for a potential chimeric transcription factor. Cell **60:**535–545.
36. **Pai, C. Y., T. S. Kuo, T. J. Jaw, E. Kurant, C. T. Chen, D. A. Bessarab, A. Salzberg, and Y. H. Sun.** 1998. The Homothorax homeoprotein activates the nuclear localization of another homeoprotein, extradenticle, and suppresses eye development in Drosophila. Genes Dev. **12:**435–446.
37. **Patti, M. E., A. J. Butte, S. Crunkhorn, K. Cusi, R. Berria, S. Kashyap, Y. Miyazaki, I. Kohane, M. Costello, R. Saccone, E. J. Landaker, A. B. Goldfine, E. Mun, R. DeFronzo, J. Finlayson, C. R. Kahn, and L. J. Mandarino.** 2003. Coordinated reduction of genes of oxidative metabolism in humans with insulin resistance and diabetes: potential role of PGC-1 and NRF1. Proc. Natl. Acad. Sci. USA **100:**8466–8471.
38. **Penkov, D., P. Di Rosa, L. Fernandez Diaz, V. Basso, E. Ferretti, F. Grassi, A. Mondino, and F. Blasi.** 2005. Involvement of Prep1 in the αβ T-cell receptor T-lymphocytic potential of hematopoietic precursors. Mol. Cell. Biol. **25:**10768–10781.
39. **Rieckhof, G. E., F. Casares, H. D. Ryoo, M. Abu-Shaar, and R. S. Mann.** 1997. Nuclear translocation of extradenticle requires homothorax, which encodes an extradenticle-related homeodomain protein. Cell **91:**171–183.
40. **Rizzuto, G., M. Cappelletti, D. Maione, R. Savino, D. Lazzaro, P. Costa, I. Mathiesen, R. Cortese, G. Ciliberto, R. Laufer, N. La Monica, and E. Fattori.** 1999. Efficient and regulated erythropoietin production by naked DNA injection and muscle electroporation. Proc. Natl. Acad. Sci. USA **96:**6417–6422.
41. **Selleri, L., M. J. Depew, Y. Jacobs, S. K. Chanda, K. Y. Tsang, K. S. Cheah, J. L. Rubenstein, S. O'Gorman, and M. L. Cleary.** 2001. Requirement for Pbx1 in skeletal patterning and programming chondrocyte proliferation and differentiation. Development **128:**3543–3557.
42. **Somogyi, M.** 1945. Determination of blood sugar. J. Biol. Chem. **160:**69–73.
43. **Stoffers, D. A., J. Ferrer, W. L. Clarkem, and J. F. Habener.** 1997. Early-onset type-II diabetes mellitus (MODY4) linked to IPF1. Nat. Genet. **17:**138–139.
44. **Tavner, F. J., R. Simpson, S. Tashiro, D. Favier, N. A. Jenkins, D. J. Gilbert, N. J. Copeland, E. M. Macmillan, J. Lutwyche, R. A. Keough, S. Ishii, and T. J. Gonda.** 1998. Molecular cloning reveals that the p160 Myb-binding protein is a novel, predominantly nucleolar protein which may play a role in transactivation by Myb. Mol. Cell. Biol. **18:**989–1002.
45. **Vigliotta, G., C. Miele, S. Santopietro, G. Portella, A. Perfetti, M. A. Maitan, A. Cassese, F. Oriente, A. Trencia, F. Fiory, C. Romano, C. Tiveron, L. Tatangelo, G. Troncone, P. Formisano, and F. Beguinot.** 2004. Overexpression of the *ped*/*pea-15* gene causes diabetes by impairing glucose-stimulated insulin secretion in addition to insulin action. Mol. Cell. Biol. **24:**5005–5015.
46. **Waskiewicz, A. J., H. A. Rikhof, and C. B. Moens.** 2002. Eliminating zebrafish pbx proteins reveals a hindbrain ground state. Dev. Cell **3:**723–733.

Diabetologia (2009) 52:2642–2652
DOI 10.1007/s00125-009-1528-z

ARTICLE

Overproduction of phosphoprotein enriched in diabetes (PED) induces mesangial expansion and upregulates protein kinase C-β activity and *TGF-β1* expression

F. Oriente · S. Iovino · A. Cassese · C. Romano · C. Miele · G. Troncone · M. Balletta · A. Perfetti · G. Santulli · G. Iaccarino · R. Valentino · F. Beguinot · P. Formisano

Received: 18 May 2009 / Accepted: 5 August 2009 / Published online: 30 September 2009

Abstract
Aims/hypothesis Overproduction of phosphoprotein enriched in diabetes (PED, also known as phosphoprotein enriched in astrocytes-15 [PEA-15]) is a common feature of type 2 diabetes and impairs insulin action in cultured cells and in mice. Nevertheless, the potential role of PED in diabetic complications is still unknown.

Methods We studied the effect of PED overproduction and depletion on kidney function in animal and cellular models.
Results Transgenic mice overexpressing *PED* (PEDTg) featured age-dependent increases of plasma creatinine levels and urinary volume, accompanied by expansion of the mesangial area, compared with wild-type littermates. Serum and kidney levels of TGF-β1 were also higher in 6- and 9-month-old PEDTg. Overexpression of *PED* in human kidney 2 cells significantly increased TGF-β1 levels, SMAD family members (SMAD)2/3 phosphorylation and fibronectin production. Opposite results were obtained following genetic silencing of *PED* in human kidney 2 cells by antisense oligonucleotides. Inhibition of phospholipase D and protein kinase C-β by 2-butanol and LY373196 respectively reduced TGF-β1, SMAD2/3 phosphorylation and fibronectin production. Moreover, inhibition of TGF-β1 receptor activity and SMAD2/3 production by SB431542 and antisense oligonucleotides respectively reduced fibronectin secretion by about 50%. TGF-β1 circulating levels were significantly reduced in *Ped* knockout mice and positively correlated with PED content in peripheral blood leucocytes of type 2 diabetic patients.
Conclusions/interpretation These data indicate that PED regulates fibronectin production via phospholipase D/protein kinase C-β and TGF-β1/SMAD pathways in kidney cells. Raised PED levels may therefore contribute to the abnormal accumulation of extracellular matrix and renal dysfunction in diabetes.

Keywords Diabetic nephropathy · PEA-15 · PED · PKC · TGF-β1

Abbreviations

BIM	Bisindolylmaleimide
ECL	Enhanced chemiluminescence
ECM	Extracellular matrix

F. Oriente and S. Iovino contributed equally to this study.

Electronic supplementary material The online version of this article (doi:10.1007/s00125-009-1528-z) contains supplementary material, which is available to authorised users.

F. Oriente · S. Iovino · C. Romano · A. Perfetti · F. Beguinot · P. Formisano (✉)
Department of Cellular and Molecular Biology and Pathology,
Federico II University of Naples,
Via Pansini 5,
80131 Naples, Italy
e-mail: fpietro@unina.it

A. Cassese · C. Miele · R. Valentino · F. Beguinot · P. Formisano
Istituto di Endocrinologia ed Oncologia Sperimentale del C.N.R.,
Federico II University of Naples,
Naples, Italy

G. Troncone
Department of Biomorphological and Functional Sciences,
Federico II University of Naples,
Naples, Italy

M. Balletta
Department of Nephrology, Federico II University of Naples,
Naples, Italy

G. Santulli · G. Iaccarino
Department of Clinical Medicine,
Cardiovascular and Immunological Sciences,
Federico II University of Naples,
Naples, Italy

HK2 cells	Human kidney 2 cells
PBL	Peripheral blood leucocyte
PED	Phosphoprotein enriched in diabetes/ phosphoprotein enriched in astrocytes-15
Ped-KO	*Ped*/*Pea-15* knockout mice
PEDTg	Transgenic mice overexpressing *PED*
PKC	Protein kinase C
PLD	Phospholipase D
SMAD	SMAD family member

Introduction

Diabetic nephropathy is a frequent complication of type 1 and type 2 diabetes mellitus and is currently considered the leading cause of end-stage renal disease [1]. While thickening of the glomerular basement membrane, glomerular hypertrophy and mesangial expansion are well known features of diabetic nephropathy, the pathogenesis of these alterations is not very clear yet. The DCCT, UK Prospective Diabetes Study (UKPDS) and Action in Diabetes and Vascular Disease: Preterax and Diamicron MR Controlled Evaluation (ADVANCE) studies have shown the role of hyperglycaemia as a causative factor in the development and the progression of diabetic nephropathy [2–5]. Nevertheless, hyperglycaemia alone is clearly not sufficient to account for the heterogeneity and variability of the clinical appearance of the disorder. Indeed, accumulating evidence points to critical genetic factors predisposing only a subset of patients with diabetes to nephropathy [6–8].

Several studies have shown an important involvement of growth factors and cytokines [9, 10]. In particular, the TGF-β1 is a key factor in experimental models of diabetic kidney disease as well as in patients with diabetic nephropathy [11–15]. In fact, TGF-β1 levels are increased in diabetic patients and high glucose levels upregulate expression and bioactivity of TGF-β1 in almost all renal cell types [11, 12, 16, 17]. Upon binding to its receptor, TGF-β1 phosphorylates the receptor-regulated SMAD family members (SMAD)2 and 3, which form oligomeric complexes with the common SMAD (SMAD 4). These complexes then translocate into the nucleus, thereby regulating transcription of target genes, including those encoding type I and type IV collagen, laminin and fibronectin [14, 16, 18, 19].

Phosphoprotein enriched in diabetes (PED, also known as phosphoprotein enriched in astrocytes-15 [PEA-15]) is a scaffold cytosolic protein originally identified as a major astrocyte phosphoprotein and found to be widely present in different tissues [20, 21]. PED plays an important role in mitogenic and metabolic signalling [21–23]. Gene profiling studies have shown that *PED* (also known as *PEA15*) is commonly overexpressed in individuals with type 2 diabetes [21, 24]. In cultured muscle and adipose cells and in peripheral tissues from transgenic mice, forced production of PED impairs insulin-stimulated GLUT4 translocation and glucose transport, suggesting that PED may contribute to insulin resistance in type 2 diabetes [25]. Further studies have shown that PED stabilises phospholipase D (PLD) [26] and induces activation of classical protein kinase C (PKC) isoforms, including PKCα and PKCβ [23, 27]. The induction of classical PKCs, in turn, inhibits insulin signalling, at least in skeletal muscle, adipose and liver cells [28–31]. Nevertheless, the role of PED in diabetic complications is not known.

In the present work we addressed the question of whether PED overproduction determines abnormalities in kidney function and whether it may represent an initial defect in the progression toward diabetic nephropathy.

Methods

Materials Media, sera, antibiotics for cell culture and the lipofectamine reagent were from Invitrogen (Grand Island, NY, USA). The anti-PED polyclonal rabbit antibody and pcDNA3PED vector have been previously described [21]. pSMAD2/3 (Ser433/435), SMAD2, PKCα, PKCβ, fibronectin, laminin and collagen I and IV antibodies were from Santa Cruz Biotechnology (Santa Cruz, CA, USA). SMAD3 was purchased from Calbiochem (San Diego, CA, USA). Phosphorothioate oligonucleotides antisense sequences used were as follows: *SMAD2* AS: 5′-GCAC GATGGACGACAT-3′; *SMAD2* S: 5′-CAATGCGAGTACG CGA-3′; *SMAD3* AS: 5′-GCAGGATGGACGACAT-3′; *SMAD3* S: 5′-GGAGTCAGACTGACGA-3′; *PED* antisense oligonucleotides were as previously described [25]. Protein electrophoresis reagents were purchased from Bio-Rad (Richmond, VA, USA), and western blotting and enhanced chemiluminescence (ECL) reagents from Amersham Biosciences (Arlington Heights, IL, USA). All other chemicals were from Sigma Aldrich (St Louis, MO, USA).

Mouse phenotyping Generation of transgenic mice overexpressing *PED* (PEDTg) [25] and of *Ped*/*Pea-15* knockout mice (*Ped*-KO) bearing ubiquitous ablation of the gene [32] has been previously described. Homozygous *Ped*-KO were used for the study. Both PEDTg and *Ped*-KO mice were fertile. Body weight of PEDTg was comparable to that of wild-type littermates, while, as previously described [32], *Ped*-KO displayed a slightly lower body weight. All procedures described below were approved by the Institutional Animal Care and Utilisation Committee. Animals were kept in a 12-h dark–light cycle and had free access to standard diet. Mice chosen for experimentation were

randomly selected from each box of mice housed in groups of three to four. Mice were habituated in individual metabolism cages (Lenderking Caging Products, Millersville, MD, USA) for 24 h. Then, the following variables were analysed: food intake (g/24 h), water intake (ml/24 h), urine volume excretion (ml/24 h), urine specific gravity, urine pH, urine glucose (mg/24 h) and albumin excretion (μg/24 h). The measurements of blood pressure and heart rate were performed partially modifying previously described methods [33]. Briefly, a 1.0-Fr polyimide pressure catheter (SPR 1000/2; Millar Instruments, Houston, TX, USA) was inserted into the left carotid artery and advanced into the ascending aorta of anaesthetised mice (2% isoflurane, 98% oxygen). Blood pressure and heart rate were recorded for 15 min after suspending isoflurane administration with an 8 channel recorder (Gould Instruments Systems, Cleveland, OH, USA). Data were analysed using Powerlab and Chart 5 software (AD Instruments, Sydney, NSW, Australia).

Renal histology and morphometric analysis Kidney sections were fixed by immersion in Carnoy solution followed by 4% buffered formaldehyde (vol./vol.) and embedded in paraffin. The fixed, embedded kidneys were cut into 2 μm sections and stained with periodic acid–Schiff's reagent. To quantify mesangial expansion, sections were coded and examined by light microscopy by two observers unaware of the experimental protocol applied. According to previous reports [34, 35], measurement of the mesangial area of 30 glomeruli randomly selected in each mouse by scanning of the outer cortex was performed with a computer-aided manipulator (KS-400; Carl Zeiss Vision, Munich, Germany)

Measurement of serum TGF-β1 and urine albumin Blood samples of mice were collected from the orbital sinus under anaesthesia. After centrifugation (800×*g*) of the blood samples, TGF-β1 levels in the supernatant fractions were measured using ELISA kits (R&D System, Minneapolis, MN, USA). The same kits were used to measure TGF-β1 levels in the media of the cells. Samples of urine collected through metabolism cages (five samples for each animal; ten animals/group) were briefly centrifuged at 500×*g* and then albumin concentration was determined using ELISA kits (Bethyl Laboratories, Montgomery, TX, USA).

Tissue collection and primary mouse tubular kidney cell cultures Tissue samples (kidney) were collected rapidly after mice were killed by pentobarbitone overdose. Tissues were snap-frozen in liquid nitrogen and stored at −80°C for subsequent western blot analysis. Mouse tubular epithelial cells were isolated as previously described [36]. Cells were grown until confluent (8 to 12 days) in RPMI 1640 medium supplemented with 20% fetal calf serum, 2% (wt/vol.) L-glutamine, 20,000 units/ml penicillin, 20,000 μg/ml streptomycin at 37°C in 5% CO_2.

Cell culture procedures and transfection Human kidney 2 (HK2) proximal tubular cells were cultured in RPMI 1640 medium (Invitrogen), containing 11.2 mmol/l glucose supplemented with 10% fetal calf serum, 2% (wt/vol.) L-glutamine, 10,000 units/ml penicillin, 10,000 μg/ml streptomycin at 37°C in 5% (vol./vol.) CO_2. Stable transfection of *PED* cDNA and transient transfection of antisense oligonucleotides [37] were performed by the lipofectamine method according to the manufacturer's instructions (Invitrogen). For these studies, 60 to 80% confluent cells were washed twice with Optimem (Invitrogen) and incubated for 8 h with 5 μg of plasmid construct or antisense oligonucleotides and 45 to 60 μl of lipofectamine reagent. The medium was then replaced with DMEM with 10% (vol./vol.) fetal calf serum and cells further incubated for 15 h before being assayed. Transfection efficiency for antisense oligonucleotides was estimated as 45±10% by co-transfection with green fluorescent protein.

Tissue and cell lysates and immunoblotting Tissue samples were homogenised in a Polytron (Brinkman Instruments, Westbury, NY, USA) in 20 ml T-PER reagent (Pierce, Rockford, IL, USA) per gram of tissue according to manufacturer's instructions. After centrifugation at 5000×*g* for 5 min, supernatant fraction was collected. Cells were solubilised in lysis buffer (50 mmol/l HEPES, pH 7.5, 150 mmol/l NaCl, 10 mmol/l EDTA, 10 mmol/l $Na_4P_2O_7$, 2 mmol/l Na_3VO_4, 100 mmol/l NaF, 10% (vol./vol.) glycerol, 1% (vol./vol.) Triton X-100, 1 mmol/l PMSF, 10 mg/ml aprotinin) for 1 h at 4°C and lysates were centrifuged at 5,000×*g* for 20 min. Total homogenates were separated by SDS-PAGE and transferred on to 0.45 μm Immobilon-P membranes as previously described [38]. Upon incubation with primary and secondary antibodies, immunoreactive bands were detected by ECL according to the manufacturer's instructions.

For peripheral blood leucocyte (PBL) separation, EDTA-treated whole-blood samples were first centrifuged for 10 min at 300×*g* and the plasma removed. PBLs were separated using a 6% (vol./vol.) dextran gradient in filtered PBS, pH 7.4, as previously described [24], washed three times in PBS, counted and resuspended in 1 ml of PBS for subsequent use.

Real-time RT-PCR analysis Total cellular RNA was isolated from whole kidneys of wild-type and PEDTg mice using a kit (RNeasy; Qiagen, Hilden, Germany) according to manufacturer's instructions. Tissue or cell RNA (1 μg) was reverse-transcribed using Superscript II Reverse Transcriptase (Invitrogen). PCR reactions were analysed using

SYBR Green mix (Invitrogen). Reactions were performed using Platinum SYBR Green qPCR Super-UDG and a multicolour real-time PCR detection system (Cycler IQ; Bio-Rad). All reactions were performed in triplicate and β-actin was used as an internal standard. Primer sequences used were as follows: *TGF-β1* (forward) 5′-TGCGC TTGCAGAGATTAAAA-3′, (reverse) 5′-CTGCCGTACA ACTCCAGTGA-3′; β-actin (forward) 5′-GCGTGACATC AAAGAGAAG-3, (reverse) 5′-ACTGTGTTGGCATAG AGG-3′.

PKC assay For this assay, HK2 cells were deprived of serum and PKC activity then measured in immunoprecipitates with anti PKCα or PKCβ antibodies, as previously described [28].

Statistical methods Data were analysed with Statview software (Abacus Concepts, Piscataway, NJ, USA) by one-factor analysis of variance. *p* values of less than 0.05 were considered statistically significant.

Results

Kidney phenotype in PEDTg mice PED was present at comparable levels in renal cortex and medulla of C57/BL6 mice (Fig. 1a). A 4.5-fold overproduction was detected in PEDTg mice compared with their wild-type littermates. In 6- and 9-month-old PEDTg mice, urine volume was increased by about two- and threefold, respectively, compared with controls, accompanied by a similarly sized increase of daily urinary albumin excretion (Table 1). No significant differences were detected in younger animals (3 months). In addition, at 9 months, plasma creatinine levels were significantly elevated only in PEDTg. Specific gravity, urinary pH and glucose and kidney weight, as well as food and water intake, blood glucose, HbA_{1c}, systolic and diastolic blood pressure, and heart rate did not show significant differences at 3, 6 and 9 months of age. Moreover, consistent with previous reports [25], fasting insulin, NEFA and triacylglycerol were higher in PEDTg than in wild-type mice, independently of age. In 9-month-old PEDTg mice, histological examination of the kidney, followed by morphometrical analysis, revealed a 2.3-fold increase of mesangial area compared with their wild-type littermates (Fig. 1b). Again, no change was detected in 3- and 6-month-old mice (data not shown). Thus, as well as deranging glucose tolerance [25], overproduction of PED induces age-dependent mesangial expansion and affects renal function in transgenic mice.

TGF-β1 is a cytokine that has been extensively studied as a major mediator of kidney damage in diabetic

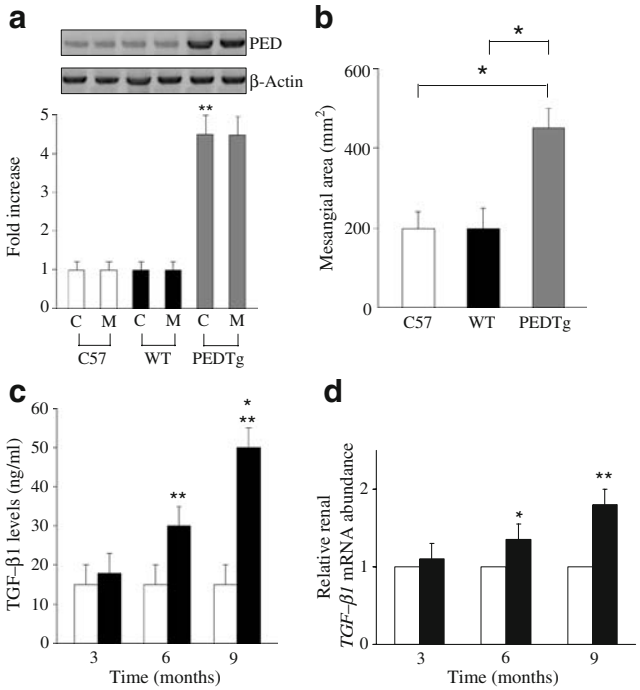

Fig. 1 PED levels, mesangial expansion and TGF-β1 levels/expression in PEDTg. **a** Cortex (C) and medulla (M) of the kidneys from wild-type (WT) and PEDTg were dissected, solubilised and western blotted with anti-PED antibodies. Blots were revealed by ECL and autoradiography, and quantified by laser densitometry, as shown in bar graph. Values were normalised for actin. Each bar represents the mean ± SD of duplicate determinations in ten mice per group. **b** Mesangial area from 9-month-old WT and PEDTg mice was measured as described. Bars represent mean ± SD of determinations in ten mice per group. **c** Serum TGF-β1 levels were determined by ELISA in PEDTg (black bars) and control mice (white bars) at 3, 6 and 9 months, n=15/group. **d** *Ped* mRNA was determined by real-time RT-PCR analysis of total RNA isolated from kidneys of the PEDTg (black bars) and control mice (white bars), using β-actin as internal standard. Each bar represents the mean ± SD of four independent experiments in each of which reactions were performed in triplicate using the pooled total RNAs obtained from seven mice per genotype. *p<0.05, **p<0.01, ***p<0.001

nephropathy [15]. We therefore measured plasma and renal TGF-β1 levels in PEDTg animals. In 9-month-old PEDTg mice we saw a greater than twofold increase of circulating TGF-β1 levels compared with wild-type littermates (Fig. 1c). Moreover, *Tgf-β1* (also known as *Tgfb1*) mRNA content was increased by about twofold in kidney extracts of PEDTg mice (Fig. 1d). Less evident, although significant, changes were detected in 6-month-old but not in 3-month-old PEDTg mice.

Effect of PED overexpression on TGF-β1 signalling in HK2 proximal tubular cells To address whether PED directly regulates *TGF-β1* expression in renal cells, HK2 proximal tubular cells were stably transfected with a *PED* full-length cDNA. Several clones were selected and characterised, of which two, namely those displaying lower (HK_{PED1}) and

Table 1 Characterisation of wild-type and PEDTg mice

Variable	At 3 months		At 6 months		At 9 months	
	Wild-type	PEDTg	Wild-type	PEDTg	Wild-type	PEDTg
Body weight (g)	26±1	25±2	28±1	28±3	30±2	31±2
Food intake (g/day)	2.8±1.1	2.7±1.1	3.0±0.8	3.1±0.4	3.3±0.6	3.5±0.2
Water intake (ml/day)	5.2±0.7	5.5±1.2	5.7±0.7	6.2±1.2	5.8±0.5	6.1±0.8
Urine excretion (ml/day)	1.0±0.05	1.5±0.5	1.1±0.7	2±0.7*	1.2±0.5	3.8±0.7**
Kidney weight (g)	0.23±0.2	0.24±0.2	0.32±0.4	0.31±0.3	0.38±0.2	0.37±0.2
Urine specific gravity	1030±3	1033±2	1032±3	1035±2	1030±3	1035±2
Urine pH	5±0.4	5±0.3	5±0.5	5±0.5	5±0.4	5±0.5
Urine glucose (mg/day)	0.5±0.2	0.5±0.1	0.5±0.4	0.5±0.2	0.5±0.1	0.5±0.3
Urinary albumin excretion (μg/day)	14±3	17±2	15±2	24±3*	14±3	33±3**
Plasma creatinine (μmol/l)	12.4±0.9	14.1±2.6	13.3±1.8	16.8±4.4	12.4±1.8	18.6±3.5***
Fasting blood glucose (mmol/l)	4.4±0.2	4.5±0.1	4.3±0.2	4.4±0.2	5.2±0.4	5.3±0.5
Fasting serum insulin (pmol/l)	63.7±6.8	191±13.8**	72.3±5.2	206.5±10.3**	122.2±8.6	309.8±5.5**
Systolic BP (mmHg)	116±1.4	112±2	118±5.3	117±4	119±3	116±1.7
Diastolic BP (mmHg)	80±0.6	80±0.5	81±1.3	82±0.8	80±1	81±1
Heart rate (beats/min)	384±17.7	377±11.6	361±9	358±14	370±13	374±10
HbA_{1c} (%)	4.5±0.2	4.5±0.3	4±0.4	4.2±0.2	5.2±0.4	5.5±0.3
NEFA (nmol/l)	0.58±0.08	0.82±0.02*	0.53±0.05	0.78±0.06*	0.61±0.05	0.93±0.09*
Triacylglycerol (mmol/l)	0.11±0.03	0.24±0.04*	0.15±0.02	0.26±0.03*	0.19±0.04	0.35±0.03*

Mice were analysed as described in the Methods

Data are the means ± SD of determinations in ten PEDTg and ten wild-type littermates

*$p<0.05$, **$p<0.01$, ***$p<0.001$

higher (HK_{PED2}) PED levels, were studied in detail (Fig. 2a). *TGF-β1* mRNA content was increased by 1.5- and 2.1-fold, respectively in HK_{PED1} and HK_{PED2} cells (Fig. 2b), while connective tissue growth factor levels did not change (data not shown). Moreover, TGF-β1 levels were increased by 2.6- and 3.2-fold in the culture media of HK_{PED1} and HK_{PED2}, respectively, compared with the parental HK2 cells (Fig. 2c). In addition, the amount of phosphorylated SMAD2/3 in the transfected clones was higher than in control cells, with no change in the cellular content of SMAD2 and SMAD3 proteins (Electronic supplementary material [ESM] Fig. 1), indicating functional

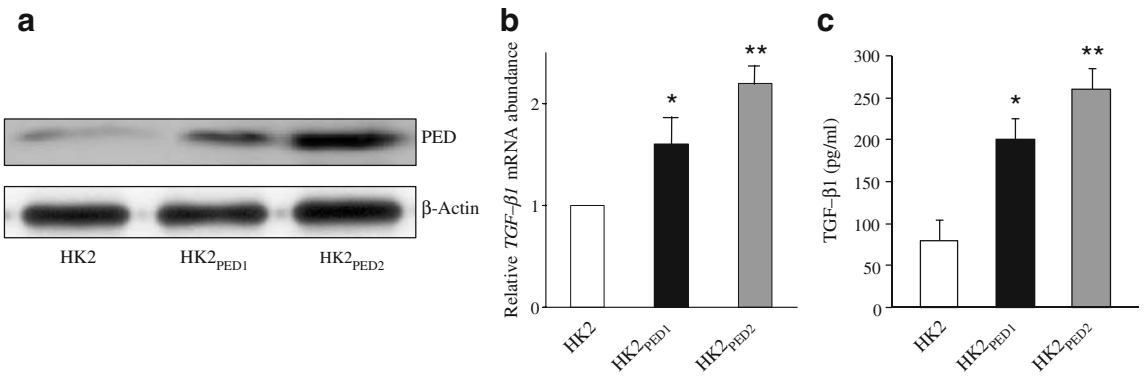

Fig. 2 Effect of *PED* overexpression on TGF-β1 in HK2 cells. HK2 cells were stably transfected with *PED* cDNA. HK_{PED1} and HK_{PED2} represent two different clones. Cell lysates were analysed by SDS-PAGE followed by blotting (**a**) with PED or actin antibodies. Alternatively (**b**), the abundance of *TGF-β1* mRNA was determined by real-time RT-PCR analysis, using β-actin as internal standard. **c** TGF-β1 levels were measured in the culture medium by ELISA assay. Bars represent the means ± SD of triplicate measurements in four independent experiments. *$p<0.05$, **$p<0.01$

activation of the TGF-β1 signalling pathway. Further supporting this hypothesis, treatment of HK2 cells with 0.1 μmol/l SB431542, a TGF-β1 receptor kinase inhibitor, reduced SMAD2 and SMAD3 phosphorylation by 40% (Fig. 3a). A 50% decrease was observed in HK_{PED2} cells. Total SMAD2 and SMAD3 levels were unchanged following exposure of both cell types to SB431542 (Fig. 3a). Results consistent with the above were obtained in HK_{PED1} cells (data not shown).

Effect of PED overexpression on fibronectin production in HK2 cells TGF-β1 regulates the synthesis of key extracellular matrix proteins, including fibronectin, laminin, and collagen I and IV [14, 16, 18, 19]. Thus, consistent with the augmented TGF-β1 production, 1.5- and 1.9-fold increased levels of fibronectin were detected, independently of glucose concentration (5.0, 11.2 and 30.0 mmol/l), in the media of HK_{PED1} and HK_{PED2}, respectively, compared with control cells (Fig. 3b). Slight, though not statistically significant, increases of laminin and both collagen I and IV were also observed (data not shown).

We have previously shown that overproduction of PED in cultured cells leads to activation of the PLD/PKC pathway [23, 27]. To study the possible involvement of PLD and PKC as potential mediators of PED-induced fibronectin production, wild-type and HK_{PED2} cells were incubated for 15 min with the PLD inhibitor 2-butanol (0.3% vol./vol.) and with the classical PKC inhibitor bisindolylmaleimide (BIM) (100 nmol/l) or the specific PKCβ inhibitor LY379196 (50 nmol/l). At the concen-

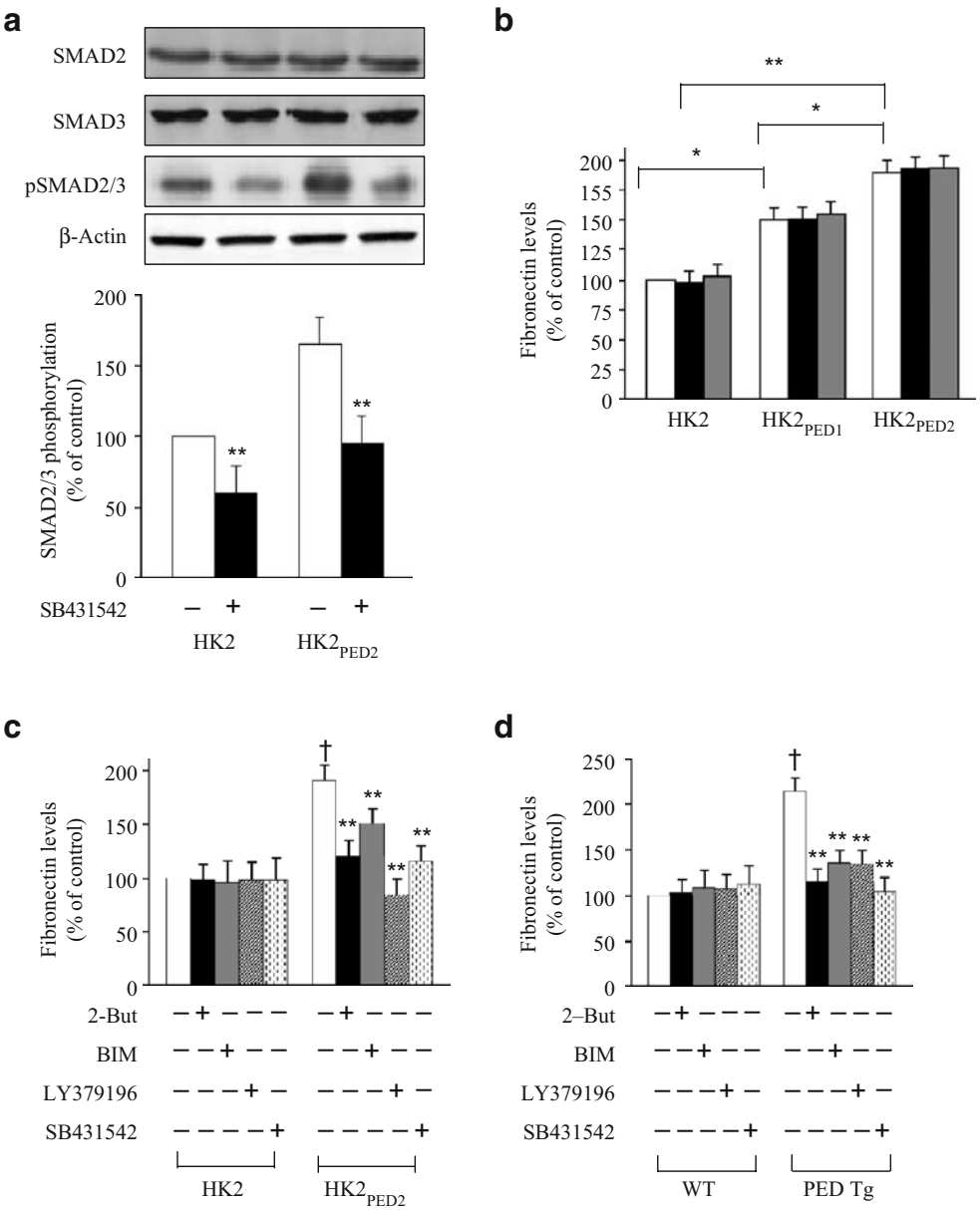

Fig. 3 Effect of *PED* overexpression and of PLD, PKC and TGF-β1 inhibition on fibronectin production in HK2 cells. **a** HK2 and $HK2_{PED2}$ cells were incubated with SB431542 (0.1 μmol/l). Total SMAD and actin levels, and SMAD2/3 phosphorylation were measured as described. A representative autoradiograph of four independent experiments is shown, with densitometric analysis of pSMAD2/3:SMAD2 ratio, normalised for actin levels, in bar graph. Values are mean ± SD, $^{**}p<0.01$. **b** Culture media with different glucose concentrations (white bars, 5 mmol/l; black bars 11.2 mmol/l; grey bars, 30 mmol/l) from control and *Ped* overexpressing cells were collected and subjected to western blot with fibronectin antibodies. Bands were quantified by laser densitometry and normalised for actin of the corresponding cultured cells. Bars represent means ± SD of three independent experiments in triplicate. $^{*}p<0.05$, $^{**}p<0.01$. **c** Culture media from HK2 and $HK2_{PED2}$ cells or (**d**) from murine tubular epithelial cells isolated from wild-type (WT) and PEDTg mice were collected, immunoblotted with fibronectin antibody. Bands were quantified by laser densitometry and normalised for actin of the corresponding cultured cells. Bars represent the mean ± SD of duplicate determinations in five independent experiments. $^{**}p<0.01$; $^{\dagger}p<0.01$ for differences between $HK2_{PED2}$ and HK2 cells

trations used, these compounds did not inhibit PKCα (ESM Fig. 2a) and PKCβ (ESM Fig. 2b) activity in parental HK2 cells. HK_{PED2} cells displayed higher levels of PLD (data not shown), PKCα (ESM Fig. 2a) and PKCβ (ESM Fig. 2b) activity. In these cells, PKCα activity was unchanged by LY379196 and reduced by 30% and 35% following exposure to 2-butanol and BIM, respectively. PKCβ activity was decreased by 30%, 32% and 60%

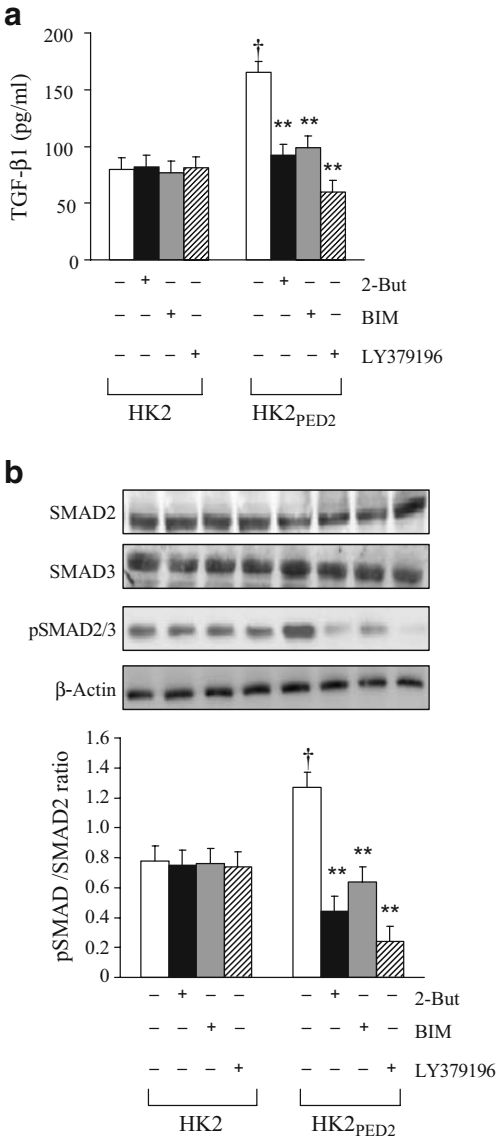

Fig. 4 Effect of PLD and PKC on TGF-β1 signalling in HK2 cells overexpressing *PED*. HK2 and $HK2_{PED2}$ cells were incubated with 2-butanol (But), BIM, LY379196 or SB431542 for 15 min. **a** TGF-β1 levels were measured in the culture media by ELISA assay. Bars represent means ± SD of triplicate measurements in four independent experiments. **b** Cells were solubilised and lysates analysed by SDS-PAGE and western blotted with total Smad2 or Smad3, p-Smad2/3 and actin antibodies. The autoradiograph shown is representative of four independent experiments. Densitometric analysis of pSMAD2/3:SMAD2 ratio is shown in bar graph, with values as mean ± SD. *$p<0.05$, **$p<0.01$; †$p<0.05$ for differences between $HK2_{PED2}$ and HK2

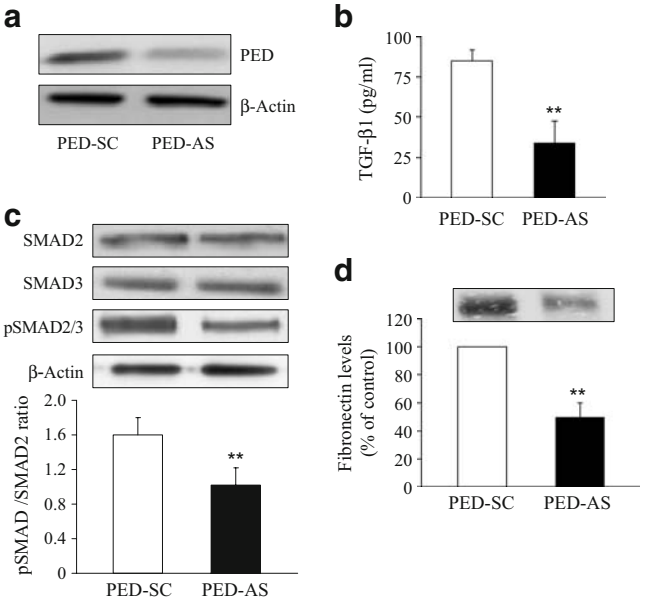

Fig. 5 Role of *PED* depletion in TGF-β1 signalling. HK2 cells were transiently transfected with *PED* antisense (PED-AS) or scrambled (PED-SC) oligonucleotides. **a** PED was detected by western blot, as previously described. The autoradiograph is representative of four independent experiments. **b** TGF-β1 was measured by ELISA. Bars represent means ± SD of duplicate measurements in four independent experiments. **c** Total SMAD2 and SMAD3 levels, and SMAD2/3 phosphorylation were detected by western blot, with densitometric analysis (bar graph) of pSMAD2/3:SMAD2 ratio. Values are mean ± SD. **d** Fibronectin from the culture media of the cells was analysed by western blot and quantified by bar graph, mean ± SD of duplicate determinations in four independent experiments. **$p<0.01$

following exposure to 2-butanol, BIM and LY379196 respectively. Finally, no change of PKCα (ESM Fig. 2a) and PKCβ (ESM Fig. 2b) activity was induced by treatment with SB431542, either in HK2 or in HK_{PED2} cells, indicating that TGF-β1 was not upstream to PKC activation.

In parallel with the unmodified PKC activity, neither PLD nor PKC inhibitors reduced fibronectin production by native HK2 cells (Fig. 3c). In contrast, exposure of HK_{PED2} cells for 15 min to 0.3% 2-butanol, 100 nmol/l BIM and 50 nmol/l LY379196 decreased fibronectin by 37%, 22% and 55%, respectively. A similar effect was also observed following treatment with SB431542 for 15 min, which reduced fibronectin levels by 40% in HK_{PED2} cells, without affecting control cells (Fig. 3c). To confirm these data, we also measured fibronectin production in primary cultures from the kidneys of wild-type and PEDTg mice. As shown in Fig. 3d, exposure to 2-butanol, BIM, LY379196 and SB431542, respectively reduced the levels of fibronectin by 47%, 38%, 38% and 50% in PEDTg-derived cells only. Thus, these data indicate that PLD, PKCβ and TGF-β1 signalling are required for regulation of fibronectin release by cells overexpressing *PED*.

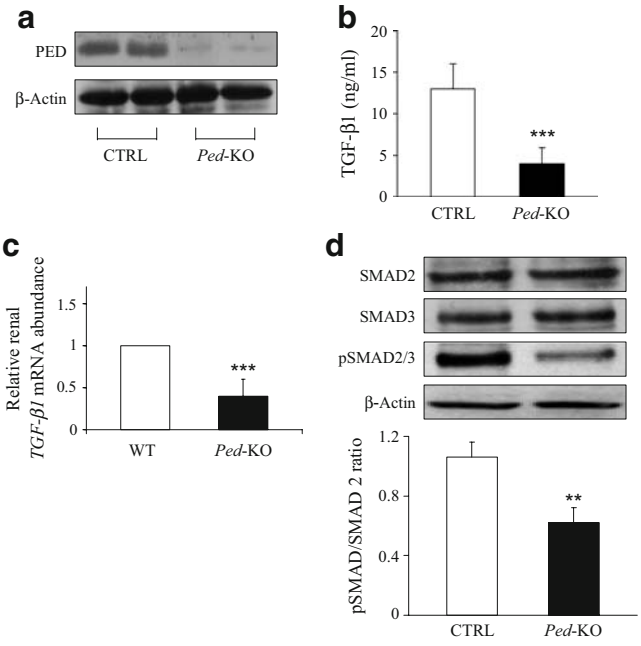

Fig. 6 Determination of serum and renal TGF-β1 levels, and SMAD2/3 phosphorylation in *Ped*-KO. **a** Kidneys from wild-type and *Ped*-KO were dissected, solubilised and western blotted with anti-PED or actin antibodies. Blots were revealed by ECL and autoradiography (representative autoradiograph of four independent experiments). **b** Serum TGF-β1 levels were determined in *Ped*-KO and control mice (n=11 per group) by ELISA assay. Bars are the mean ± SD of duplicate determinations. ***p<0.001. **c** The abundance of *Ped* mRNA was determined by real-time RT-PCR analysis of total RNA isolated from kidneys of the KO and control mice, using β-actin as internal standard. Bars represent the mean ± SD of four independent experiments in each of which reactions were performed in triplicate using the pooled total RNAs obtained from five mice per genotype. ***p<0.001. **d** Tissue lysates from kidneys of the KO and control mice (n=5 per group) were pooled and analysed by SDS-PAGE followed by blotting with total SMAD2 or SMAD3, p-SMAD2/3 and actin antibodies. The autoradiograph is representative of three independent experiments, with densitometric analysis of pSMAD2/3:SMAD2 ratio in bar graph, mean ± SD. **p<0.01

Effect of PLD and PKC inhibition on TGF-β1 signalling in HK2 cells We then measured TGF-β1 production and function in parental HK2 and in HK_{PED2} cells following PLD and PKC inhibition. 2-Butanol and BIM had no significant effect in the HK2 cells, but reduced TGF-β1 levels in HK_{PED2} cells by 45% and 40%, respectively (Fig. 4a). Interestingly, the selective block of PKCβ with LY379196 led to 65% reduction of TGF-β1 levels in HK_{PED2} cells, while being ineffective in HK2 cells. The effect of PKCβ inhibition was also well detectable in terms of reduction of SMAD2 phosphorylation, as well as of SMAD3 (data not shown), with an almost complete block following treatment with LY379196 of HK_{PED2} cells (Fig. 4b).

Role of TGF-β1 signalling in PED-mediated fibronectin production Next, HK2 cells were transiently transfected with *SMAD2*- or *SMAD3*- specific phosphorothioate antisense oligonucleotides (SMAD2 AS and SMAD3 AS) to block production of the two proteins. SMAD2 AS and SMAD3 AS caused a > 70% reduction of SMAD2 and -3 compared with scrambled oligonucleotides, both in wild-type and in HK_{PED2} cells (ESM Fig. 3a). Specific depletion of the SMAD2 and SMAD3 isoforms was followed by a 30% and 35% fibronectin reduction in HK2 cells and by 60% and 65% reductions in HK_{PED2} clones, compared with the respective cell clone treated with scrambled control oligonucleotides (ESM Fig. 3b). Similar results were obtained in HK_{PED1} cells (data not shown). Thus, overpro-

Table 2 Characterisation of wild-type and *Ped*-KO mice after streptozotocin treatment

Variables	Wild-type	*Ped*-KO
Fasting serum insulin (pmol/l)	70.6±5.2	39.6±8.6**
Fasting blood glucose (mmol/l)	4.0±0.4	4.5±0.5
Body weight (g)	30±2	28±2
Urine excretion (ml/day)	1.4±0.6	1.1±0.2
Urinary albumin excretion (μg/day)	13.4±4	13±2
Plasma creatinine (μmol/l)	11.5±4.4	9.7±4.4
Systolic BP (mmHg)	112±1.7	109±3.8
Diastolic BP (mmHg)	82±0.9	77±0.8
Heart rate (beats/min)	372±15	369±13.9
NEFA (nmol/l)	0.78±0.05	0.82±0.03
Triacylglycerol (mmol/l)	0.20±0.03	0.24±0.04

Mice were analysed as described in the Methods

Data are the means ± SD of determinations in seven wild-type and seven *Ped*-KO mice

**p<0.01

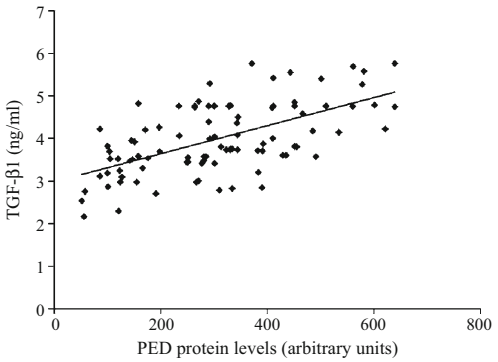

Fig. 7 Correlation between PED levels from PBLs and plasma TGF-β1 levels in type 2 diabetic patients. PED protein levels were analysed by western blot in PBLs from 95 type 2 diabetic patients and bands were quantified by laser densitometry as described. Plasma TGF-β1 levels were measured by ELISA. Linear regression analysis revealed a positive correlation between PED and TGF-β1 levels (r=0.593, p<0.001)

duction of PED upregulated fibronectin production through a TGF-β1/SMAD2/3-dependent pathway.

PED depletion decreases TGF-β1 signalling and fibronectin production To assess whether endogenous PED controls TGF-β1 and fibronectin production, HK2 cells were transiently transfected with a *PED*-specific phosphorothioate antisense oligonucleotide (PED-AS). PED-AS treatment induced a 65% PED depletion compared with a scrambled oligonucleotide (PED-SC) (Fig. 5a).

TGF-β1 levels were about 60% lower in PED-AS cells than in the controls (Fig. 5b) and, in parallel, SMAD2, as well as SMAD3 (data not shown) phosphorylation was decreased by about 50% in the presence of the antisense (Fig. 5c). However, total SMAD protein levels were unchanged. Consistently, fibronectin secretion was reduced by about 50% in cells treated with PED-AS compared with those treated with PED-SC (Fig. 5d). Consistent results were obtained in *Ped*-KO [32] (Fig. 6a). In spite of normal glucose levels (Table 2), *Ped* gene ablation coincided with a 65% and 60% decrease of TGF-β1 plasma levels and renal mRNA content, respectively, compared with control mice (Fig. 6b, c). SMAD2 phosphorylation was also reduced by 40% in kidney extracts of *Ped*-KO (Fig. 6d). SMAD3 phosphorylation also displayed a similar decrease (data not shown).

Correlation between individual levels of PED and plasma TGFβ in humans We had analysed plasma TGF-β1 levels and PED protein abundance in PBLs in 95 type 2 diabetic patients matched for age, BMI, waist circumference, systolic and diastolic BP, and fasting HDL-cholesterol [24]. As shown in Fig. 7, there was a positive correlation between the individual levels of PED and plasma TGF-β1.

Discussion

The molecular mechanisms responsible for the onset and/or progression of renal complications of diabetes mellitus are still poorly understood. While hyperglycaemia plays a crucial role [2–5], other environmental conditions as well as specific genetic backgrounds may strongly contribute to the clinical appearance of the disorder, either as protective or as predisposing factors [39]. A further complicating element for understanding the molecular determinants is the lack of animal models fully representative of human diabetic nephropathy [40]. We have previously generated a transgenic mouse ubiquitously expressing high levels of *PED*, a gene whose expression is elevated in a large proportion of individuals with type 2 diabetes and in their first-degree relatives [21, 24]. In mice, PED overproduction impairs glucose tolerance by affecting insulin action and secretion [25, 41], and the animals develop overt diabetes following administration of high-fat diets [25].

Here we show that PEDTg mice also displayed mesangial expansion, and mildly elevated plasma creatinine levels and urinary albumin excretion between 6 and 9 months of age, in the absence of frank hyperglycaemia. Indeed, blood glucose, systolic and diastolic blood pressure, heart rate and HbA_{1c} did not significantly change in wild-type and PEDTg mice, when early signs of renal disorder were found. The renal functional changes were paralleled by elevation of TGFβ1 levels, a cytokine which has been commonly found elevated in patients with diabetic nephropathy [11–15]. However, none of these abnormalities was detectable in younger littermates, suggesting that while PED overproduction represents an early defect, it may also play a role in the slow progression toward renal damage.

Since glucose tolerance of these animals is significantly reduced, and plasma triacylglycerol and NEFA are increased [25], we cannot exclude the possibility that the renal abnormalities observed in PEDTg mice could be linked to the metabolic phenotype. Consistent with this hypothesis, individuals with impaired glucose tolerance display a higher risk of developing nephropathy [42], and microalbuminuria often precedes the onset of diabetes [43]. Nevertheless, studies in HK2 human proximal tubular cells and in primary cultures from the kidneys have shown that selective overexpression of *PED* in kidney cells may, at least in part, be directly responsible for renal derangement. In this regard, forced expression of *PED* increased the production of extracellular matrix (ECM) proteins, whose accumulation is a hallmark of mesangial expansion [17]. In addition, these changes occurred independently of glucose concentration in the extracellular media (Fig. 3b) and of insulin treatment (data not shown), indicating that elevation of PED levels is sufficient to impair ECM production.

The potential mechanisms leading to hyperproduction of ECM proteins are likely to involve hyperactivation of PKCβ and the TGF-β1 signalling pathways. PED binds PLD, increasing its intracellular stability and leading to the accumulation of diacylglycerol [23, 27]. This, in turn, determines abnormal activation of conventional PKC isoforms, including PKCα and PKCβ. Increased PKCβ activity may account, at least in part, for the renal phenotype observed in PEDTg mice. In HK2 cells, inhibition of PKCβ largely reversed the effect of *PED* overexpression. In particular, the increase in *TGF-β1* mRNA levels and signalling caused by PED in HK2 cells was almost completely blocked by the PKCβ inhibitor. Interestingly, both PKCβ hyperactivity and elevated TGF-β1 levels are commonly found in diabetic nephropathy, both in vitro and in vivo [44–46]. In several experimental

and clinical studies, inhibition of PKC (LY333531) has been shown to delay or halt the progression of diabetic complications [47]. Part of the beneficial effect of PKC inhibition is due to the consequent downregulation of TGF-β1 [48]. Consistently, higher circulating levels of TGF-β1 have been detected in PEDTg mice and are paralleled by increased *Tgf-β1* mRNA content in kidney extracts. However, the question of whether other cell types contribute to the increase of TGF-β1 content in the bloodstream is currently not resolved and under investigation in our laboratory.

Inhibition of PLD and PKCβ, as well as of TGF-β1 receptor activity, or genetic silencing of *SMAD2* and *SMAD3* decreased production of fibronectin. Thus, *PED* overexpression may lead to increased PKCβ activity, which enhances expression of *TGF-β1*, which in turn upregulates fibronectin production. Further support of this hypothesis was seen in the fact that inhibition of *PED* by antisense oligonucleotides in HK2 cells was paralleled by reduced PKCβ activity and TGF-β1 expression and signalling, as well as by decreased fibronectin production. Similarly to PED-depleted cells, kidney and total TGF-β1 levels and PKCβ activity were reduced in animals bearing the complete ablation of *Ped* gene, indicating a cause–effect relationship.

It remains unknown whether PED overproduction is involved in diabetic nephropathy in humans. However, in a cohort of patients with type 2 diabetes [24], we found a positive correlation between levels of PED measured in PBLs and plasma TGFβ1 levels. It could therefore be inferred that high expression levels of PED deranges renal function in a subset of diabetic individuals, thereby facilitating the onset and/or progression of diabetic nephropathy.

The mechanism leading to the increase of PED cellular levels are only partially known and may be due to altered transcriptional control [49] or to post-translational modifications [50]. The contribution of genetic variations and epigenetic modifications is currently under investigation in our laboratory.

Thus, high expression levels of PED determine an increase of PKCβ activity and of TGF-β1 expression in cellular and animal models, as well as in humans. They therefore may represent an early abnormality, contributing to the derangement of ECM deposition and to progression toward nephropathy.

Acknowledgements This study was supported by the European Community's FP6 EUGENE2 (LSHM-CT-2004-512013) and PREPOBEDIA (201681) projects, the European Foundation for the Study of Diabetes and grants from the Associazione Italiana per la Ricerca sul Cancro (AIRC) and the Ministero dell'Università e della Ricerca Scientifica (PRIN and FIRB). The financial support of Telethon–Italy is also gratefully acknowledged.

Duality of interest The authors declare that there is no duality of interest associated with this manuscript.

References

1. Wolf G (2004) New insights into the pathophysiology of diabetic nephropathy: from haemodynamics to molecular pathology. Eur J Clin Invest 34:785–796
2. The Diabetes Control and Complications Trial Research Group (1993) The effect of intensive treatment of diabetes on the development and progression of long-term complications in insulin-dependent diabetes mellitus. The Diabetes Control and Complications Trial Research Group. N Engl J Med 329:977–986
3. UK Prospective Diabetes Study (UKPDS) Group (1998) Intensive blood-glucose control with sulphonylureas or insulin compared with conventional treatment and risk of complications in patients with type 2 diabetes (UKPDS 33). UK Prospective Diabetes Study (UKPDS) Group. Lancet 352:837–853
4. Members of the ADVANCE collaborative group (2008) Intensive blood glucose control and vascular outcomes in patients with type 2 diabetes. N Engl J Med 358:2560–2572
5. Bilous R (2008) Microvascular disease: what does the UKPDS tell us about diabetic nephropathy? Diabet Med 25(Suppl 2):25–29
6. Fogarty DG, Hanna LS, Wantman M, Warram JH, Krolewski AS, Rich SS (2000) Segregation analysis of urinary albumin excretion in families with type 2 diabetes. Diabetes 49:1057–1063
7. Imperatore G, Knowler WC, Pettitt DJ, Kobes S, Bennett PH, Hanson RL (2000) Segregation analysis of diabetic nephropathy in Pima Indians. Diabetes 49:1049–1056
8. Boright AP, Paterson AD, Mirea L et al (2005) Genetic variation at the ACE gene is associated with persistent microalbuminuria and severe nephropathy in type 1 diabetes: the DCCT/EDIC Genetics Study. Diabetes 54:1238–1244
9. Flyvbjerg A (2000) Putative pathophysiological role of growth factors and cytokines in experimental diabetic kidney disease. Diabetologia 43:1205–1223
10. Wolf G (2003) Growth factors and the development of diabetic nephropathy. Curr Diab Rep 3:485–490
11. Azar ST, Salti I, Zantout MS, Major S (2000) Alteration in plasma transforming growth factor β in normoalbuminuric type 1 and type 2 diabetic patients. J Clin Endocrinol Metab 85:4680–4682
12. Pfeiffer A, Middleberg-Bisping K, Drewes C, Schatz H (1996) Elevated plasma levels of transforming growth factor β-1 in NIDDM. Diabetes Care 18:1113–1117
13. Ziyadeh FN (2004) Mediators of diabetic renal disease the case for TGF-beta as the major mediator. J Am Soc Nephrol 15(Suppl 1):S55–S57
14. Wang W, Koka V, Lan HY (2005) Transforming growth factor-beta and Smad signalling in kidney diseases. Nephrology 10:48–56
15. Sharma K, Ziyadeh FN (1995) Hyperglycemia and diabetic kidney disease. The case for transforming growth factor-beta as a key mediator. Diabetes 44:1139–1146
16. Ha H, Yu MR, Lee HB (2001) High glucose-induced PKC activation mediates TGF-beta 1 and fibronectin synthesis by peritoneal mesothelial cells. Kidney Int 59:463–470
17. Bloomgarden ZT (2005) Diabetic nephropathy. Diabetes Care 28:745–751
18. Cheng J, Grande JP (2002) Transforming growth factor-beta signal transduction and progressive renal disease. Exp Biol Med 227:943–956
19. Ten Dijke P, Hill CS (2004) New insights into TGF-beta-Smad signalling. Trends Biochem Sci 29:265–273
20. Araujo H, Danziger N, Cordier J, Glowinski J, Chneiweiss H (1993) Characterization of PEA-15 a major substrate for protein kinase C in astrocytes. J Biol Chem 268:5911–5920

21. Condorelli G, Vigliotta G, Iavarone C et al (1998) PED/PEA-15 gene controls glucose transport and is overexpressed in type 2 diabetes mellitus. EMBO J 7:3858–3866
22. Condorelli G, Trencia A, Vigliotta G et al (2002) Multiple members of the mitogen-activated protein kinase family are necessary for PED/PEA-15 anti-apoptotic function. J Biol Chem 277:11013–11018
23. Condorelli G, Vigliotta G, Trencia A et al (2001) Protein kinase C (PKC)- α activation inhibits PKC- ζ and mediates the action of PED/PEA-15 on glucose transport in the L6 skeletal muscle cells. Diabetes 50:1244–1252
24. Valentino R, Lupoli G, Raciti GA et al (2006) The PEA15 gene is overexpressed and related to insulin resistance in healthy first-degree relatives of patients with type 2 diabetes. Diabetologia 49:3058–3066
25. Vigliotta G, Miele C, Santopietro S et al (2004) Overexpression of the ped/pea-15 gene causes diabetes by impairing glucose-stimulated insulin secretion in addition to insulin action. Mol Cell Biol 24:5005–5015
26. Zhang Y, Redina O, Altshuller YM et al (2000) Regulation of expression of phospholipase D1 and D2 by PEA-15, a novel protein that interacts with them. J Biol Chem 275:35224–35232
27. Viparelli F, Cassese A, Doti N et al (2008) Targeting of PED/PEA-15 molecular interaction with phospholipase D1 enhances insulin sensitivity in skeletal muscle cells. J Biol Chem 283:21769–21778
28. Caruso M, Miele C, Oriente F et al (1999) In L6 skeletal muscle cells, glucose induces cytosolic translocation of protein kinase C alfa and transactivates the insulin receptor kinase. J Biol Chem 274:28637–28644
29. Li Y, Soos TJ, Li X et al (2004) Protein kinase C theta inhibits insulin signaling by phosphorylating IRS1 at Ser(1101). J Biol Chem 27:45304–45307
30. Ishizuka T, Kajita K, Natsume Y et al (2004) Protein kinase C (PKC) beta modulates serine phosphorylation of insulin receptor substrate-1 (IRS-1)—effect of overexpression of PKCbeta on insulin signal transduction. Endocr Res 30:287–299
31. Nakajima K, Yamauchi K, Shigematsu S et al (2000) Selective attenuation of metabolic branch of insulin receptor down-signaling by high glucose in a hepatoma cell line HepG2 cells. J Biol Chem 275:20880–20886
32. Kitsberg D, Formstecher E, Fauquet M et al (1999) Knock-out of the neural death effector domain protein PEA-15 demonstrates that its expression protects astrocytes from TNFalpha-induced apoptosis. J Neurosci 19:8244–8251
33. Ciccarelli M, Santulli G, Campanile A et al (2008) Endothelial alpha1-adrenoreceptors regulate neoangiogenesis. Br J Pharmacol 153:936–946
34. Kasahara M, Mukoyama M, Sugawara A et al (2000) Ameliorated glomerular injury in mice overexpressing brain natriuretic peptide with renal ablation. J Am Soc Nephrol 11:1691–1701
35. Ziyadeh FN, Hoffman BB, Han DC et al (2000) Long-term prevention of renal insufficiency, excess matrix gene expression, and glomerular mesangial matrix expansion by treatment with monoclonal antitransforming growth factor-beta antibody in db/db diabetic mice. Proc Natl Acad Sci U S A 97:8015–8020
36. Terryn S, Jouret F, Vandenabeele F et al (2007) A primary culture of mouse proximal tubular cells, established on collagen-coated membranes. Am J Physiol Renal Physiol 293:F476–F485
37. Hao C, Beguinot F, Condorelli G et al (2001) Induction and intracellular regulation of tumor necrosis factor-related apoptosis-inducing ligand (TRAIL) mediated apoptosis in human malignant glioma cells. Cancer Res 61:1162–1170
38. Miele C, Caruso M, Calleja V et al (1999) Differential role of insulin receptor substrate (IRS)-1 and IRS-2 in L6 skeletal muscle cells expressing the Arg1152 → Gln insulin receptor. J Biol Chem 274:3094–3102
39. Granier C, Makni K, Molina L, Jardin-Watelet B, Ayadi H, Jarraya F (2008) Gene and protein markers of diabetic nephropathy. Nephrol Dial Transplant 23:792–799
40. Breyer MD, Böttinger E, Brosius FC 3rd et al (2004) AMDCC. Mouse models of diabetic nephropathy. J Am Soc Nephrol 16:27–45
41. Miele C, Raciti GA, Cassese A et al (2007) PED/PEA-15 regulates glucose-induced insulin secretion by restraining potassium channel expression in pancreatic beta-cells. Diabetes 56:622–633
42. Singleton JR, Smith AG, Russell JW, Feldman EL (2003) Microvascular complications of impaired glucose tolerance. Diabetes 52:2867–2873
43. Mykkanen L, Haffner SM, Kuusisto J, Pyorala K, Laakso M (1994) Microalbuminuria precedes the development of NIDDM. Diabetes 43:552–557
44. Koya D, Jirousek MR, Lin YW, Ishii H, Kuboki K, King GL (1997) Characterization of protein kinase C beta isoform activation on the gene expression of transforming growth factor-beta, extracellular matrix components, and prostanoids in the glomeruli of diabetic rats. J Clin Invest 100:115–126
45. Meier M, Park JK, Overheu D et al (2007) Deletion of protein kinase C-beta isoform in vivo reduces renal hypertrophy but not albuminuria in the streptozotocin-induced diabetic mouse model. Diabetes 56:346–354
46. Kelly DJ, Zhang Y, Hepper C et al (2003) Protein kinase C beta inhibition attenuates the progression of experimental diabetic nephropathy in the presence of continued hypertension. Diabetes 52:512–518
47. Das Evcimen N, King GL (2007) The role of protein kinase C activation and the vascular complications of diabetes. Pharmacol Res 55:498–510
48. Koya D, Haneda M, Nakagawa H et al (2000) Amelioration of accelerated diabetic mesangial expansion by treatment with a PKCbeta inhibitor in diabetic db/db mice, a rodent model for type 2 diabetes. FASEB J 14:439–447
49. Ungaro P, Teperino R, Mirra P et al (2008) Molecular cloning and characterization of the human PED/PEA-15 gene promoter reveal antagonistic regulation by hepatocyte nuclear factor 4alpha and chicken ovalbumin upstream promoter transcription factor II. J Biol Chem 283:30970–30979
50. Perfetti A, Oriente F, Iovino S et al (2007) Phorbol esters induce intracellular accumulation of the anti-apoptotic protein PED/PEA-15 by preventing ubiquitinylation and proteasomal degradation. J Biol Chem 282:8648–8657